NORTHWESTERN UNIVERSITY

Active Integration of Movement-Related Synaptic Inputs by Spinal Motoneurons

A DISSERTATION

SUBMITTED TO THE GRADUATE SCHOOL IN PARTIAL FULFILLMENT OF THE REQUIREMENTS

for the degree

DOCTOR OF PHILOSOPHY

Field of Neuroscience

By

Allison Suzanne Hyngstrom

EVANSTON, ILLINOIS

December 2007

Abstract

Active Integration of Movement Related Synaptic Inputs by Spinal Motoneurons

Allison Hyngstrom

During movement, the dendrites of spinal motoneurons receive steady excitatory and inhibitory synaptic input from supraspinal sources, interneurons, and sensory afferents. Motoneurons also have dendritic voltage sensitive ion channels. Most notable is a persistent inward current (PIC), which can enhance the amplitude of synaptic input by several fold. PICs are subject to the state dependent level of brainstem monoaminergic drive. Previously, studies of the PIC had focused on cellular mechanisms and the basics of integration of excitatory input. My goal was to determine how the PIC interacted with the mixture of excitation and inhibition required for generation of movement. Data from Chapter 1 showed that when synaptic inputs were applied separately, the PIC resulted in a dendritic amplification of excitatory and inhibitory inputs that occurred in different voltage ranges. The predicted algebraic summation of excitatory and inhibitory inputs would thus result in a large variability in effective synaptic current (I_n) amplitude as a function of voltage. However, non-linear summation during simultaneous activation of both inputs tended to compensate for this dual-range amplification, producing better balancing between excitation and inhibition as function of membrane potential. In addition to regulation by levels of monoaminergic drive, we found that the amplitude of the PICs of ankle extensor motoneurons could be modulated by as much as 50% as a

function of joint angle through reciprocal inhibitory pathways (Chapter 2). This evidence indicates how the modulation of PICs within a given motor pool can be shaped by the biomechanics of the limb. In Chapter 3, we demonstrated that PICs can amplify the movement related I_N of ankle extensor, knee extensor, and hip flexor MNs generated by passive flexion and extension rotations of the ankle, knee, and hip joints without altering the overall pattern of each cell's movement related receptive field. The presence and regulation of PICs optimize motor control by providing an intrinsic source of excitation that can be modulated by several mechanisms in order to match the motor requirement.

ACKNOWLEDGEMENTS

"Only I have left to say, More is thy due than more than all can pay."

(*Macbeth*, William Shakespeare)

I am truly grateful for all the help I have received from my thesis advisor, laboratory colleagues, thesis committee members, and family during graduate school. I do not think my thesis advisor, C.J., will ever know the profound influence he has had on the development of my scientific "compass." I could not have had a better example to follow, and his words and actions will continue to resonate and guide me as I begin the next phase of my career. I would also like to thank everyone in the Heckman laboratory who has given me help and advice: Bob Lee, Tom Sandercock, Mingchen Jiang, Roberta Anelli, Ted Ballou, Renee Theiss, Lei Cui, Lori Waltonen-Weaver, Aaron Daub, Jenna Schuster, and Huub Maas. Special thanks goes to Michael Johnson for doing all the surgical preparations necessary for the *in vivo* experiments, for helping with data collection and for always being willing to debate any point. Although more times than not we ended up agreeing to disagree, I have valued all your input and assistance you have provided. I wish to also thank Jack Miller for assisting with data collection and for always having an answer or reference for any question I have ever had for him. I thank the members of my thesis committee members, Zev Rymer, Lee Miller, Gianmaria Maccaferri, and George Hornby, for all their suggestions and advice that have been crucial in the development of my thesis. A special thanks to my dear friend Jena Pitman who has been my constant sounding board and cheerleader. I thank my family, Mom, Dad, John, Jennifer and the Nelsons. You have all been critical in the completion of my

graduate studies with my sanity intact. I thank my daughter Sophie for motivating and inspiring me to finish. Last but not least, I am forever indebted to my husband, Andy. His love and support has made all of this possible. I am so very lucky.

This is dedicated to my little angel.

TABLE OF CONTENTS

Figures and Tables

Introduction

Chapter 1

Chapter 2

Chapter 3

Introduction

Nearly a century ago, Sherrington described motoneurons as "*the final common pathway"* to movement (Sherrington 1906). Motoneurons (MNs) transform synaptic inputs from higher centers, local interneuronal circuits, and sensory afferents into precise commands to muscle cells to produce movement. However, the rules governing how MNs with active dendrites transform excitatory and inhibitory synaptic inputs into motor commands are not fully understood.

The Anatomy and Cell Morphology of Motoneurons Facilitate Synaptic Integration

The cellular structure and anatomy of MNs matches their function of integrating multiple synaptic inputs to create a movement signal. MN cell bodies are located in the ventral horn (lamina IX) of the spinal cord (Rexed 1952). Studies using retrograde tracers such as horseradish peroxidase have been useful in showing a columnar distribution of motor nuclei for a given muscle spanning several segments within the cord (Burke, Strick et al. 1977). Motoneuron pools are somatotopically arranged with more medially located cells innervating axial musculature and laterally located cells innervating limb musculature (Rekling, Funk et al. 2000).

Compared to other types of neurons, the alpha motoneuron soma is relatively large. Diameters can range from ~40 to 80 microns in the cat, a common model system for motor control (Burke, Strick et al. 1977). The dendritic tree of alpha motoneurons is extensive, estimated to constitute 95% of the cell's surface area. In general, the branches project radially such that the cell body is in the center of its receptive field (Cullheim, Fleshman et al. 1987; Cullheim, Fleshman et al. 1987). In the cat, lumbar motoneurons have 11-12 primary dendrites which can extend over 1 mm from the soma, which is well into the white matter (Rose and Richmond 1981; Kernell and Zwaagstra 1989). It is estimated that alpha motoneurons receive between 50 and 140,000 synaptic inputs, largely contacting dendritic regions (Brannstrom 1993; Ornung, Ottersen et al. 1998; Fyffe 2001). The far reaching and radial dendritic structure of MNs indicates that they have the potential to gather large amounts of synaptic inputs at any given time.

The Effect of Passive Motoneuron Membrane Properties on Synaptic Integration

A neuron's physical characteristics and resting conductances all contribute to its ability to spread changes in membrane potential after synaptic transmission has occurred. Since dendrites comprise most of a MN's surface area and a large percentage of synaptic contacts are located in the dendrites (Fyffe 2001), it is helpful to consider how the passive properties of MNs may influence synaptic integration.

The earliest intracellular recordings of neurons were of spinal motoneurons in the anesthetized cat using sharp electrodes. (Brock, Coombs et al. 1952; Woodbury and Patton 1952; Brock, Coombs et al. 1953; Coombs, Eccles et al. 1955; Eccles, Eccles et al. 1957). Basic electrical properties were described such as a resting membrane potential of ~-70 mV and action potential heights of 80-90 mVs with durations of 1-2 ms. These studies laid the groundwork for the direct measurement of the excitatory and inhibitory nature of various synaptic inputs as well as the integrative properties of MNs.

As a change in synaptic potential travels from the dendrites to the soma, it diminishes in size as a function of the specific membrane resistance of the cell (i.e. resistance per unit area) and dendrite geometry. This can be described mathematically by the length constant (λ) which is defined as the distance at which a steady state voltage change has diminished to ~0.37 of its original size (Hille 2001). The length constant in cat spinal motoneurons has been estimated to be between 1.1 and 1.6 (Barrett and Crill 1971; Barrett and Crill 1974; Barrett and Crill 1974). Excitatory postsynaptic potential (EPSP) size can diminish as a function of the specific membrane resistance as current is lost through non-voltage gated potassium channels (Hille 2001). Since the dendrites have a relatively high capacitance, and synaptic EPSPs have fast rise times, the membrane can act as a filter (Rekling, Funk et al. 2000). Due to the extensive dendritic tree of MNs, a small isolated EPSP in the distal dendrites might not have a large effect on somatic membrane potential. Decreases in electrotonic length due to active properties of the dendrites are considered in the next section.

The spatial distribution of EPSPs is also important when considering the integration of multiple inputs. If EPSPs occur close together on the cell membrane, summation would likely be sub-linear (i.e. less than the algebraic sum) due to shunting and changes in driving force. Conversely, if EPSPs occur in relatively isolated dendritic regions then summation would be linear, i.e. equal to the algebraic sum (Binder and Powers 1999; Reyes 2001). Studies where active dendritic properties were suppressed showed that MNs firing frequency in response to a given input could be predicted by the magnitude of synaptic current that reaches the soma multiplied by the slope of the cell's frequency –current (F-I) function (Powers and Binder 1995; Binder and Powers 1999). In summary, passive properties of MNs would predict sub-linear to linear summation of synaptic inputs as measured at the soma.

From a motor control standpoint, sub-linear summation could result in a loss of magnitude and timing signal resolution to the MN, but it would provide some low pass filtering of synaptic noise. Since motoneurons are involved in the precise control of muscles as a part of a voluntary command or reflex circuit, it would seem more important for the motoneuron to have an accurate history of the timing and amplitude of its inputs.

Fast Synaptic Transmission and Motoneurons

Like other neurons, MNs have ligand gated ionotropic or metabotropic ion channels. Ionotropic receptors are associated with fast synaptic transmission. The receptor is

physically associated with an ion channel, which opens when the neurotransmitter molecule is bound to the receptor. Many excitatory synaptic inputs to MNs release glutamate, including descending inputs and afferents (Matthews 1972; Jankowska 1992; Rekling, Funk et al. 2000). MNs express three types of ionotropic glutamatergic receptors: AMPA, NMDA, and Kainate (Mitchell and Anderson 1991; Furuyama, Kiyama et al. 1993; Tolle, Berthele et al. 1993). These channels primarily allow NA^{+} and K^{+} currents to pass and have a reversal potential of zero. If membrane potential is depolarized enough, NMDA channels also become permeable to Ca^{++}. AMPA receptors lacking a specific subunit (GLUR2) will also pass Ca^{++} and have been identified in MNs in the spinal cord (Mayer, Westbrook et al. 1984; Hollmann, Hartley et al. 1991). Both NMDA and AMPA receptors have been implicated in monosynaptic and polysynaptic afferent transmission to motoneurons, but it is believed that AMPA receptors primarily underlie monosynaptic transmission in the adult, such as from Ia afferents (Rekling, Funk et al. 2000).

The main inhibitory transmitters are GABA and glycine. They are believed to carry the Cl^{-} ion and have reversal potentials around -80mV. The Ia inhibitory interneuron is classically believed to release GABA and bind to ionotropic GABAa receptors located on the MN, but synaptic boutons in the ventral horn have been shown to co-release GABA and glycine (Jonas 1998). Furthermore, others have shown co-localization of GABAa and glycine receptors on the MN (Geiman 2002, Todd 1996). The Ia interneuron is believed to act via ionotropic receptors (Jankowska 1992), but there may be spill over to metabotropic receptors on the motoneuron (Curtis and

Lacey,1998,Stuart and Redman 1992,Svirskis and Hounsgaard 1998) and interneurons (Derjean, Bertrand et al. 2005). Transmission of information to MNs via ionotropic receptors would be most effective for precise and timely motor commands. Conversely, ionotropic receptors would be relatively inefficient in delivering motor commands that require sustained generation of force. One example might be motor commands to postural musculature, which would require constant synaptic drive.

Neuromodulation of Motoneurons

Motoneuron excitability can be affected on a longer time scale via metabotropic receptors. In addition to ionotropic receptors, glutamate also binds to a number of metabotropic receptors that open channels as a result of second messenger cascades within the cell. In general these pathways act to open channels on a slower time course than ionotropic receptors, but can have longer lasting effects on MN excitability. There are three classes of metabotropic glutamate receptors (mGluR): I, II, and III. Group I receptors are located post-synaptically while group II/III receptors are found presynaptically (Conn and Pin 1997; Pin and Acher 2002). Group I receptors activate second messenger systems which result in the intracellular release of Ca^{++} via PLC pathways and increase the excitability of MNs by inhibiting a K+ current and increasing an L-type Ca^{++} current (Delgado-Lezama, Perrier et al. 1997; Del Negro and Chandler 1998). Conversely, group II/III receptors act to diminish synaptic transmission to motoneurons, although the exact mechanism is not understood (Ishida, Saitoh et al. 1993; Cao, Evans et al. 1995). GABA can also have metabotropic effects through the

GABAb receptor and has been shown to inhibit MNs by increasing K^+ and decreasing Ca++ currents (Stuart and Redman 1992; Curtis and Lacey 1994; Li, Li et al. 2004). Other molecules known to bind to metabotropic receptors of spinal MNs include: thyroid releasing hormone (Cao, O'Donnell et al. 1998),adenosine (Reppert, Weaver et al. 1991), ATP (Collo, North et al. 1996), and ACh (Kurihara, Suzuki et al. 1993).

The monoamines serotonin (5-HT) and norepinephrine (NE) perform neuromodulatory functions on a variety of channels that contribute to motoneuron excitability within the spinal cord. Although a small number of serotonin and norepinephrine cell bodies exist in the spinal cord (Willis 1991), the majority of 5-HT and NE cell bodies reside in the raphe nuclei and the locus ceorulus of the brainstem respectively (Bjorklund and Skagerberg 1982).The raphe nuclei are tonically active in the waking state and activity increases with rise in motor activity, especially repetitive movements such as locomotion or chewing (Jacobs and Fornal 1993). Activity in the locus ceorulus has been correlated more generally to the state of arousal (Aston-Jones, Rajkowski et al. 2000). Neuroanatomical data has shown multiple serotonin contacts globally distributed over the MN soma and dendritic tree (Alvarez 1998) and strong norepinephrine input to the ventral horn (Fyffe 2001). Given the diffuse innervation of 5-HT and NE projections to the spinal cord and the relatively long acting effects on MN excitability, it is likely that these monoamines are involved in setting the overall state of excitability in the cord and adjust with changes in motor demands on longer time scales (Heckman, Gorassini et al. 2005).

5-HT and NE bind to g-protein coupled receptors which in turn activate second messenger pathways that alter cellular excitability (Hochman et al 2001, Reckling 2000). Both 5-HT and NE have a depolarizing effect on motoneurons. Specifically, 5-HT results in a decrease in the activity of calcium activated potassium channels, a decrease in resting or "leak" potassium conductances, and an enhancement of the hyperpolarizing activated cation current (I_h) (Larkman and Kelly 1992,1998; Hsiao 1997,1998; Takahashi and Berger 1990). Stimulation of the raphe obscurus nucleus results in motoneuron depolarization that can be blocked by a non-selective 5-HT antagonist (Roberts et al 1988). Similar to the function of 5-HT, NE excites motoneurons through a decrease in potassium conductances and an increase in an inward current (Larkman and Kelly 1992, Parkis 1995, Elliot and Wallis 1992).

In addition to effects on cell excitability described above, 5-HT and NE are critical for inducing plateau potentials (Hounsgaard et al 1988, Hounsgaard and Kiehn 1989). In current clamp, plateau potentials permit self sustained firing (Hounsgaard and Kiehn 1989; Bennett, Hultborn et al. 1998; Lee and Heckman 1998; Bennett, Li et al. 2001). Physiologically, this means that either a depolarizing current step or an excitatory synaptic input could initiate repetitive firing that continues for several seconds after the original stimulus has been removed. For motor control, self-sustained firing would be particularly useful for muscle tasks that require sustained force production over long periods of time.

Persistent Inward Currents of Spinal Motoneurons

A voltage dependent persistent inward current (PIC) is required for the plateau potential to develop in MNs. Schwindt and Crill were the first to describe the PIC (Schwindt and Crill 1980; Lee and Heckman 1998). In voltage clamp, the PIC manifests as a downward deflection in current during a slow voltage ramp (Figure 1) creating a negative slope region. As the voltage reaches more depolarized levels voltage gated outward currents are activated resulting in a return to a positive slope conductance. Electrophysiological studies have demonstrated that the MN PIC is primarily composed of L-type Ca++ currents (Carlin 2000b; Hounsgaard and Kiehn 1989; Perrier and Hounsgaard 2003), but, in mammals, also has a significant persistent sodium component (NaP) (Lee and Heckman 1999c, Li and Bennett 2003). Cav1.3 subtype of L type Ca^{++} channels are believed to carry the Ca^{++} component of the PIC due to their relatively hyperpolarized activation levels and an insensitivity to dihydropyridines (Carlin, Jiang et al. 2000; Li and Bennett 2003). A persistent sodium current has been documented in a variety of neuron types besides MNs (Alzheimer, Schwindt et al. 1993; Raman and Bean 1997; Maurice, Tkatch et al. 2001). The general consensus is that the channel is the same as the transient Na^{+} involved in the generation of the action potential in a non-inactivating mode. (Brown, Schwindt et al. 1994; Crill 1996; Heckman, Gorassini et al. 2005). For motoneurons, it is not known which molecular subtype is

involved, but Nav 1.6 and 1.1 are current candidates since they both can generate persistent currents (Goldin 2001). The PIC in mammals is thus composed of both relatively fast activating NaP and a more slowly activating Ca^{++} channels(Heckman, Lee et al. 2003; Jones and Lee 2006). Because the synaptic inputs applied in this thesis are slow and steady, the amplification probably includes both NaPIC and CaPIC.

The Dendritic Origin of Persistent Inward Currents

Although Schwindt and Crill were the first to describe the PIC, a study by Iansek and Redman had previously demonstrated active dendritic properties in MNs (1973). Iansek and Redman showed that EPSPs from different dendritic origins had similar amplitudes. If dendrites were completely passive with no voltage dependent conductances, it would be predicted that the more distally generated EPSP would have a smaller amplitude as compared to the more proximally located EPSP when measured at the soma. It was suggested that active dendrites act to compensate for attenuation of EPSP size due to passive membrane properties, although the alternative of greater postsynaptic receptor density distally was also considered. They then went on to show that blocking K+ channels intracellularly increased the amplitude of EPSPs (Clements, Nelson et al. 1986).

Electrophysiological (Hounsgaard and Kiehn 1993; Lee and Heckman 1996; Bennett, Hultborn et al. 1998) and computational (Gutman 1991; Elbasiouny, Bennett et al. 2005; Elbasiouny, Bennett et al. 2006; Grande, Bui et al. 2007) evidence indicates that MN

PICs originate primarily in the dendritic tree (but see also (Moritz, Newkirk et al. 2007). A strong indirect indicator of dendritic PICs is hysteresis in the frequency-current (F/I) relationship of motoneurons that generate plateau potentials(Bennett, Hultborn et al. 1998; Lee and Heckman 1998; Svirskis and Hounsgaard 1998; Carlin, Jiang et al. 2000; Carlin, Jones et al. 2000). Additionally, in the Bennett study, PICs were elicited more easily by synaptic input as compared to injected current (1998). Hounsgaard and Kiehn provided more direct evidence of a dendritic PIC by using an electrical field to depolarize the dendrites while hyperpolarizing the soma (Hounsgaard and Kiehn 1993).

Extremely relevant to the methods of this thesis, is the use of *in vivo* , discontinuous single electrode voltage clamp recording techniques, developed by Lee and Heckman, to show the dendritic origin of PICs (Lee and Heckman 1996; Heckman and Lee 2001). Due to the large size of the dendritic tree, voltage clamp of regions beyond the soma and proximal dendrites is likely not very effective, resulting in poor “space clamp”. A steady synaptic input, similar to those employed in this thesis, is applied while the soma is voltage clamped (see actual recorded voltage traces in lower panel of Chapter 2, Fig.2). Because the voltage is effectively clamped at the soma, the synaptic input activates primarily dendritic PICs (Lee and Heckman 1996; Heckman and Lee 2001). However, as indicated in the 1996 study by Lee and Heckman, sufficient hyperpolarization of the soma during voltage clamp can hyperpolarize the dendrites enough to prevent activation of the PIC by synaptic excitation. Estimates based on *in vivo* voltage clamp recordings predict as much as 70% of the PIC is dendritic (Lee and Heckman 2000).

Anatomical data reveals the presence of Cav1.3 and 1.2 channels in the MN dendrites (Carlin, Jones et al. 2000; Zhang, Sukiasyan et al. 2006; Anelli, Sanelli et al. 2007). Analogous anatomical studies showing NaP channels have yet to be done, but nucleated patch studies of spinal dorsal horn cells by Safronov and colleagues provide evidence for a dendritic or axonal location of NaP channels (Safronov, Wolff et al. 1997; Safronov 1999).

Several lines of evidence support the presence of voltage sensitive conductances in the dendrites of motoneurons and the idea that steady excitatory synaptic inputs are able to sufficiently depolarize the membrane enough to cause activation. Advances in measuring PICs using *in vivo* voltage clamp techniques permit the study of interactions between steady excitatory and inhibitory synaptic inputs and active conductances and the resulting effective synaptic current measured at the soma.

Relationship Between Motoneuron Type and Function of the PIC

A motor unit is defined as a MN and all the muscle fibers it innervates. MN electrical properties are matched to the contractile properties of the muscles that the MN innervates (Kernell 2006). For example, the relatively small MNs with higher input resistances require less excitatory current to generate action potentials and tend to innervate muscles that are relatively fatigue resistant and weak (S motor units). Likewise the larger MNs with lower input resistance require more excitatory current to

generate an action potential and innervate more fatigue sensitive and powerful muscle fibers (FR, F motor units). In this way, the S motor units are recruited first followed by the F and FR units, a biological phenomenon referred to as the “size principle” (Henneman and Mendell 1981).

Studies by Heckman and colleagues have demonstrated that the promotion of plateau potentials and self-sustained firing by PICs mainly occurs in type S or fatigue resistant motoneurons (Lee and Heckman 1998; Lee and Heckman 1998). In F and FR units, the PIC is well maintained during the input, but fades once the input is removed. In this way PICs would facilitate prolonged muscle contraction which requires S motor units and reduce the need for constant command signals to drive these MNs during relatively static tasks such as posture (Heckman, Lee et al. 2003).

One important function of the PIC is common to all MN types. Lee and Heckman showed that in all MN cell types, the PIC enhances the amplitude of excitatory synaptic input by as much as 6 fold (Lee and Heckman 1996). In this intracellular voltage clamp study, ionotropic excitatory synaptic input was produced by selectively activating the Ia muscle fibers via tendon vibration. As the dendritic tree became depolarized, the PIC was activated and contributed significantly to the effective synaptic current measured at the soma. Since it has been shown that the excitatory effective synaptic currents of various synaptic inputs are relatively small when PICs are not present (Binder, Robinson et al. 1998; Binder and Powers 1999; Binder, Heckman et al. 2002), the authors concluded that the PIC could thus be used to drive MNs at their maximum firing

rate with little synaptic current. The enhancement of MN synaptic input by PICs has been shown by others as well (Bennett, Hultborn et al. 1998; Delgado-Lezama, Perrier et al. 1999; Prather, Powers et al. 2001; Hultborn, Denton et al. 2003). In animal models, there is evidence for the involvement of PICs in whole limb reflexes and locomotor circuits (Brownstone, Gossard et al. 1994; Perrier and Tresch 2005) and plateau behavior has been measured via motor unit and force recordings in humans (Collins, Burke et al. 2001; Collins, Burke et al. 2002; Gorassini, Yang et al. 2002).

Modulation of the PIC

As described above, the PIC can have a significant impact on cell excitability and firing properties. Regulation of the PIC is necessary to promote precise control of MN firing. Recent work has shown that the excitability of dendrites, and thus the PIC, can be controlled by altering the overall neuromodulatory state of the cord as well as more specific modulation of the PIC from stimulation of sensory afferents (Lee and Heckman 2000; Hultborn, Denton et al. 2003; Kuo, Lee et al. 2003).

As described previously, the work of Hounsgaard and colleagues showed that plateau potentials require the presence of the monoamines (Conway, Hultborn et al. 1988; Hounsgaard, Hultborn et al. 1988). But these important studies did not indicate whether the relative levels of monoamines had a systematic effect on MN excitability, specifically the amplitude of the PIC. Lee and Heckman were able to show that the degree of enhancement of excitatory synaptic current by PICs depended on the relative level of

monoaminergic drive present in the cord (Lee and Heckman 2000). PIC amplitude and degree of synaptic enhancement was largest when a NE agonist was administered and least when the animal was anesthetized. Anesthesia is believed to depress monoaminergic centers. The authors concluded that the relative magnitude of monoaminergic tonic drive to the cord could alter the firing gain of the MN to an excitatory input. The neuromodulatory state of the cord is thus important when considering sensory integration.

The diffuse monoaminergic projections to the cord and globally distributed synaptic contacts to the MN's dendritic tree are qualities which contribute to setting the overall neuromodulatory state of the cord. However, local modulation of the PIC would seem necessary for rapidly controlling the PIC of specific motoneurons and avoiding excessive co-contraction of muscles around a single joint. Kuo et al., showed that the amplitude of the PIC varies as a function of the magnitude of synaptic inhibition (Kuo, Lee et al. 2003). In this study, strong inhibition was produced by stimulating the mixed nerve innervating the antagonist muscle, thereby utilizing Ia inhibitory pathways. In current clamp, Hultborn and colleagues have also shown modulation of the PIC related firing properties by synaptic inhibition by either stimulating recurrent inhibitory pathways, pyramidal inhibition, or crossed extension-flexion reflex pathways (Hultborn, Denton et al. 2003). Although these studies indicate that isolated sources of inhibition can effectively control PICs, presently it is unknown how effective more physiological inputs, such as those generated by limb movement, are in regulating the PIC.

Spatial Distribution of Synaptic Inputs to MNs

As described in the morphology section, the MN dendritic tree is extensive and radial in shape. The physical arrangement of synaptic inputs is important when considering the integration of several inputs. The spike generating center of the MN is believed to be the axon-hillock. Assuming passive membrane conditions and equal probability of transmitter release, receptors and their associated ion channels located proximally on the dendritic tree would have a greater effect on MN excitability than those located on the distal dendritic tree. Alternatively, active conductances clustered around a particular receptor could give an additional "boost" to a particular synaptic input (Kernel 2006). Globally distributed active conductances, however, might enhance all inputs equally. In this way, the organization of synaptic inputs onto MNs could help shape its movement related receptive field (MRRF).

Synaptic organization for several types of sensory and brainstem inputs likely to be involved in a MN's MRRF has been well characterized. One of the most intensively studied is the Ia input. It is estimated that there are 1000 to 2000 globally distributed Ia bouton contacts with the MN , almost entirely on dendritic surfaces (Burke, Fedina et al. 1971; Brown and Fyffe 1978; Burke, Walmsley et al. 1979; Brown and Fyffe 1981; Burke and Glenn 1996; Fyffe 2001). The Ia inhibitory interneurons make contacts

primarily on proximal dendrites and somatic regions while inhibitory inputs from Renshaw cells make contacts relatively more distal on the dendritic tree (Burke, Fedina et al. 1971; Fyffe 1991; Fyffe 2001). Anatomical data of synaptic contacts from group II inputs or group II interneurons onto MNs is limited, but a recent study by Maxwell and colleagues provides evidence for inhibitory group II interneurons on the soma and dendrites of a lumbar MN (Bannatyne, Edgley et al. 2006). Although studied more extensively in the serotonergic system, both 5-HT and NE afferents appear to be widely distributed on MN dendritic surfaces (Pilowsky, de Castro et al. 1990; Alvarez, Pearson et al. 1998; Gladden, Maxwell et al. 2000).

Organization of Sensory Pathways Likely to be Stimulated During Movement

Ia afferents from muscle spindles signal changes in muscle length and are especially sensitive to velocity of stretch (Matthews 1964). Studies using either transient electrical shocks or force responses to stretch have shown that this system is highly focused, resulting in monosynaptic excitation of the homonymous and, to a lesser extent, synergist muscles and inhibition of the antagonist muscle via an inhibitory interneuron (Eccles, Eccles et al. 1957; Eccles and Lundberg 1958; Nichols, Cope et al. 1999).

From this system, MNs primarily receive information about muscle length that is, in general, limited to agonist/antagonist muscle pairs- focused around one or two joints. Functionally, the stretch reflex circuitry promotes reciprocal activation of agonist-antagonist pairs necessary for movement transitions, for instance the transition from

ankle extension to flexion as the foot moves from stance to swing. The presence of the PIC introduces a potential problem for this scenario. If the net excitatory effective synaptic current from both the Ia afferents and the PIC is too large and cannot be modulated, co-contraction of muscles around the joint might impede smooth movement.

Wider patterns of convergence onto motoneurons via polysynaptic pathways are seen in all other afferent pathways including: Ib fibers of golgi tendon organs, group II, III, and IV muscle afferents, and both low and high threshold cutaneous afferents (Jankowska 1992). Like Ia afferents, group II muscle afferents are also sensitive to changes in muscle length (Matthews 1972) but studies using electrical stimulation have shown group II afferents affect a broader range of motoneurons through polysynaptic pathways (Edgley and Jankowska 1987; Lundberg, Malmgren et al. 1987). It is thought that the group II pathway is involved in whole limb movements (Jankowska 1992) since the reflex action associated with stimulation of this pathway is excitation of limb flexors and inhibition of limb extensors (Edgley and Jankowska 1987; Lundberg, Malmgren et al. 1987; Riddell and Hadian 2000). A similarly wide pattern of effects is seen in the Ib system where Golgi tendon organs, which signal muscle force (Houk and Henneman 1967), synapse on interneurons that inhibit extensor motoneurons throughout the hindlimb (Eccles, Eccles et al. 1957; Nichols, Cope et al. 1999). Transient stimulation of low threshold cutaneous afferent*s* in the anesthetized cat preparation has revealed excitatory convergence from cutaneous nerves throughout the hindlimb on ankle extensor motoneurons (LaBella and McCrea 1990).

The flexor reflex afferent pathway (FRA) includes interneurons that receive input from a variety of sources including group II, III, and IV muscle afferents, as well as cutaneous and joint afferents. The FRA pathway is associated with the widespread actions resulting in excitation of limb flexors ipsilaterally and limb extensors contralaterally. High threshold muscle afferents are activated during stretch and active contraction of the muscle (Cleland and Rymer 1990). These afferents trigger the “clasp knife reflex” characterized by a stereotypical short depolarization followed by inhibition of motoneurons whose associated muscles have been stretched to end ranges (Cleland and Rymer 1990; Cleland and Rymer 1993).

Information from these systems provides a picture to the MN of what is happening throughout the whole limb and direct the MN to cooperatively participate in a whole limb movement. This would allow coupling of several joints throughout the hindlimb, depending on the movement task. For instance, during the swing phase of locomotion flexors throughout the limb are active in order to advance the limb and clear the ground. As with the Ia system, it would be important for coordinated inhibitory input to modulate the PICs of the various extensor musculature in a timely manner to allow MNs throughout the whole limb to participate in the movement

Neuromodulatory Effects of the Monoamines on Sensory Afferents and Spinal Interneurons

Both 5-HT and NE have been shown to suppress high and low threshold cutaneous afferents stimulated by electrical shocks (Hochman, Garraway et al. 2001; Jankowska 2001). Group Ia and Ib interneurons are facilitated by both 5-HT and NE (Miller, Paul et al. 1996; Jankowska, Hammar et al. 2000; Hammar and Jankowska 2003). Interestingly, the effect of 5-HT and NE on group II interneurons depends on the location of the interneuron. Interneurons that are dominated by group II input in the dorsal horn are primarily inhibited by 5-HT and facilitated by NE. This pattern is reversed for more ventrally located group II interneurons (Jankowska, Hammar et al. 2000; Jankowska 2001). Both 5-HT and NE enhance the monosynaptic stretch reflex and suppress the flexion withdrawal/crossed extension reflex and clasp knife reflex (Tremblay and Bedard 1986; Miller, Paul et al. 1995; Miller, Paul et al. 1996). Moreover, Chen et al, showed that removal of descending monoaminergic input via dorsal cold block led to a suppression of Ia interneuron activity and a facilitation of interneurons that had not responded to Ia afferent stimulation (Chen, Theiss et al. 2001).

Monoaminergic Receptor Subtypes Involved in Spinal Cord Neuromodulation

Recent evidence suggests that monoaminergic excitatory effects on motoneurons are primarily mediated through 5-HT2c (Perrier and Hounsgaard 2003) and NEα1 receptor subtypes (Lee and Heckman 1999; Lee and Heckman 2000). The 5-HT1a and NEα2 receptor subtypes are thought to mediate inhibition of high and low threshold afferents, while 5-HT1b/D subtypes are involved in suppressing the flexor reflex pathway (Chen,

Bianchetti et al. 1987; Miller, Paul et al. 1995; Chau, Barbeau et al. 1998). NE$\alpha 1_{a-c}$ and 5-HT 2_{a-c} receptors signal through the Gα_q family that activates PLC and PKC (Rekling, Funk et al. 2000). NE$\alpha 2$ and 5-HT1_{a-e} receptors signal through the G$_{\alpha i}$ pathway resulting in inhibition of adenylyl cyclase (AC) and downstream inhibition of PKA.

The Decerebrate Cat as a Model to Study Sensory Integration by Spinal Motoneurons with Active Dendrites

The decerebrate cat preparation has long been important in demonstrating how brainstem and spinal centers of the CNS can autonomously generate simple movements. In the late 19th century, Sherrington and others began examining spinal reflexes in the decerebrate cat (Sherrington 1898). In particular, Sherrington described *decerebrate rigidity.* Following transection between the superior and inferior colliculi, tonic activity in the antigravity extensors is produced resulting in a standing posture. Important to understanding spinal cord circuitry in man, over the last century it has been shown that the cat shares many of the same interneuronal pathways and pathway functions including that of the group Ia, group Ib and group II systems (Jankowska and Hammar 2002). Pertinent to the work in this laboratory, a pre-collicular decerebration causes tonic activity in the brainstem monoaminergic centers and increased transmission of 5-HT and NE to the spinal cord (Baldissera F 1981; Jankowska 1992). *In vitro* work in turtle motoneurons has shown the monoamines induce plateau potentials (Hounsgaard and Kiehn 1985). In the cat, in a decerebrate preparation with

an intact cord, motoneurons exhibit bistable behavior (Conway, Hultborn et al. 1988; Hounsgaard, Hultborn et al. 1988; Bennett, Hultborn et al. 1998; Lee and Heckman 1998; Lee and Heckman 1998). If the cord is acutely transected, disrupting transmission from the monoaminergic centers in the brainstem, bistable behavior is lost but can be reinstated by applying NE or 5-HT precursors (Conway, Hultborn et al. 1988; Hounsgaard, Hultborn et al. 1988). In this way, we can examine how motoneurons with active dendrites as well as relatively passive dendrites (through spinalization) process sensory information related to movement.

Summary

During movement, single motoneurons receive whole limb multimodal sensory input via interneurons and sensory afferents that could either inhibit or excite them. Monoaminergic drive sets the neuromodulatory tone of the cord by setting both the relative level of intrinsic excitability of MNs and the excitability of sensory pathways. A number of previous studies have examined the convergence of specific pathways onto motoneurons using electrical stimulation or unnatural manipulation of a limited number of muscles or joints. Although some groups have examined extracellular interneuronal responses to voluntary limb movement (Perlmutter 1998, Fetz 2002) *in vivo*, the net effect of multimodal input due to whole limb movements on α-motoneuron current in response to whole limb movements in MNs with active dendrites has not been investigated. Further understanding of sensory integration as a function of MN intrinsic excitability is critical for understanding the full register of the cell's input-output function.

Chapter 1

Summation of Excitatory and Inhibitory Synaptic Inputs by Motoneurons with Highly Active Dendrites

Summary

In vivo, neurons that operate in a balanced mode receive simultaneous excitatory and inhibitory input. We investigated how summation of steady excitation and inhibition interacts with neuromodulatory input, using an *in vivo* preparation in which neuromodulatory input induces strong amplification of dendritic synaptic inputs to spinal motoneurons. This dendritic amplification, however, interacted with excitation and inhibition in different voltage ranges. Excitation was amplified at voltages near threshold for spike initiation whereas inhibition was amplified at more depolarized levels. Nonlinear summation during simultaneous activation of both inputs tended to compensate for this dual-range amplification, producing better balancing between excitation and inhibition as function of membrane potential. Nonlinear summation in the balanced state also allowed removal of inhibition to induce a net excitatory change in synaptic current that was amplified as much as excitation applied alone. The interactions between excitatory, inhibitory and neuromodulatory input may allow flexible control of synaptic integration during different motor behaviors.

Introduction

Many types of neurons have voltage-sensitive conductances distributed throughout their dendritic trees (Hausser, Spruston et al. 2000; Migliore and Shepherd 2002; Heckman, Lee et al. 2003; Gulledge, Kampa et al. 2005; Magee and Johnston 2005). Hence,

dendrites are active participants in synaptic integration, providing the potential not only for strong input amplification but also for highly nonlinear input interactions. *In vivo*, synaptic integration often involves spatial and temporal summation of both excitatory and inhibitory inputs, resulting in a high conductance state (Steriade 2001; Destexhe, Rudolph et al. 2003). In the "balanced" mode, excitation and inhibition are closely matched (Shadlen and Newsome 1998; Salinas and Sejnowski 2000; Chance, Abbott et al. 2002; Haider, Duque et al. 2006). This balancing can be dynamic, with excitation and inhibition waxing and waning in phase (Berg, Alaburda et al. 2007). Excitatory and inhibitory synaptic inputs located in dendritic regions necessarily interact with dendritic voltage-sensitive channels before reaching the soma and generating spikes. The question of whether summation of excitatory and inhibitory currents is linear in active dendrites is thus critical to understanding normal neuron function.

Neuromodulatory inputs are also very likely to be tonically active *in vivo* (Aston-Jones, Rajkowski et al. 2000; Steriade 2001; Jacobs, Martin-Cora et al. 2002). The impact of neuromodulators on voltage sensitive conductances is not limited to the soma but extends to the dendrites (Heckman, Lee et al. 2003; Frick and Johnston 2005). Thus normal synaptic integration *in vivo* depends on the interaction of neuromodulatory input with both excitation and inhibition.

In this study, we investigate the linearity of summation of excitatory and inhibitory synaptic inputs to the dendrites of adult spinal motoneurons subject to strong neuromodulation. We use a preparation of the feline spinal cord that provides two

important advantages: selective activation of ionotropic synaptic inputs via afferents from muscles, and tonic activity in a major neuromodulatory input from the brainstem, via axons releasing the monoamines serotonin and norepinephrine (Hounsgaard et al., 1988). Our voltage clamp technique eliminates contributions from voltage-sensitive channels at the soma, forcing the interactions between excitation and inhibition to occur in the relatively unclamped dendritic tree (Heckman and Lee, 2001). Previous studies using these methods have shown that monoaminergic input facilitates persistent inward currents (PICs) in motoneuron dendrites (Hounsgaard and Kiehn 1993; Lee and Heckman 1996; Carlin, Jones et al. 2000). Dendritic PICs amplify excitatory synaptic currents by as much as 5 -10 fold (Lee and Heckman 2000; Prather, Powers et al. 2001; Hultborn, Denton et al. 2003). Once the cell is depolarized sufficiently to achieve full PIC amplification, further excitatory input faces a saturating effect that severely limits its amplitude (Lee and Heckman, 2000) (see Figure 1B). Inhibition effectively suppresses the dendritic PIC in a voltage range more depolarized than the voltage range of peak amplification of excitatory input, overlapping with the range for saturation of excitation (Kuo, Lee et al. 2003; Hyngstrom, Johnson et al. 2007). If summation of inputs were strictly linear, excitatory and inhibitory inputs that produce equal effects on membrane potential at one level of membrane potential could nonetheless produce very unbalanced behavior as membrane potential changes. Excitation would dominate at voltage levels near threshold for firing and inhibition at more depolarized levels and higher firing rates. Instead, our results show that excitation and inhibition sum in a nonlinear fashion that compensates for the tendency of the dendritic PIC to unbalance

these inputs, resulting in a more consistent relation between summed input and membrane potential.

Results

Synaptic and Intrinsic Dendritic Conductances Shape the Current-Voltage Function.

Synaptic integration in spinal motoneurons was studied under two states of monoaminergic drive to the cord. In the standard state, the cord was intact and thus subject to the full tonic activity of monoaminergic drive present in the decerebrate preparation (Hounsgaard et al., 1988; Lee and Heckman, 2000). In the minimal state, the cord was fully transected at the thoracic level to eliminate descending monoaminergic input (Hounsgaard et al., 1988). All studies were carried out in quasi-steady state conditions, with both excitatory and inhibitory inputs applied as steady backgrounds. The basic protocol for all cells is illustrated in Figure 1A. The inputs illustrated are naturally balanced: monosynaptic excitation from muscle spindle Ia afferents in the parent muscle of the motoneurons (ankle extensors) and di-synaptic inhibition from the Ia afferents in the antagonist muscles (ankle flexors) (Matthews, 1972). Ia afferents are highly sensitive to changes in muscle length and were thus activated by high-frequency, low-amplitude tendon vibration (Matthews, 1972). The current voltage (I-V) function of the cell was assessed in control conditions (black), with

steady backgrounds of Ia excitation (lower thin trace), and Ia inhibition (upper thin trace). Results for simultaneous activation of both inputs are considered later.

The PIC is evident in the control I-V function as a strong downward deflection, producing a negative slope region (Fig. 1A) (Schwindt and Crill 1980; Lee and Heckman 1996; Delgado-Lezama, Perrier et al. 1997; Lee and Heckman 1998). The large changes in the I-V function during the synaptic background conditions are due to interactions between the PIC and these synaptic inputs in dendritic regions, outside of the good voltage clamp control applied at the soma (Heckman and Lee, 2001). The asymmetry of the PIC interaction with excitation and inhibition noted in the Introduction is evident in Fig. 1A: excitation hyperpolarizes and broadens the activation of the PIC (lower trace) (Lee and Heckman, 2000) while inhibition suppresses the PIC amplitude without altering is activation voltage (Kuo et al., 2003).

All subsequent results are derived from these basic I-V function protocols. In addition to Ia excitation and Ia inhibition generated through tendon vibration (in 14 cells), we also used stimulation of the common cutaneous sural nerve alone (n=3) and in combination with Ia excitation (n=3). No significant differences were found for Ia vs. sural excitation and these results were combined. We also studied Ia excitation combined with inhibition from electrical stimulation of a mixed nerve, the common peroneal (CP; n = 11). Both types of inhibitory inputs significantly increased input conductance ($p < 0.001$ in both cases, paired t-tests) but the average percent change in conductance for CP inhibition was significantly larger (Ia: 9 ± 10%; CP: 35 ± 25%; $p < 0.02$, t-test). It

should be emphasized that all sources of excitation and inhibition used in this study produce steady currents for several seconds (see Methods).

Amplification of Excitatory and Inhibitory Inputs Occurs in Different Voltage Ranges

The effective synaptic currents (I_N's) generated by these inputs are shown in Fig. 1B. I_N is the net current generated at the soma by a synaptic input (Heckman and Binder, 1988; Heckman and Binder, 1991) and can be calculated by subtracting the control I-V function in Fig. 1A from each of the steady synaptic background I-V functions (Lee and Heckman, 2000). Because the ramps were applied slowly, this subtraction process closely approximates what would occur if the membrane potential was stepped to a steady holding potential, synaptic input applied and the change in current measured (Lee and Heckman, 1996; Lee and Heckman, 2000). I_N was inverted in this study to make excitation positive and inhibition negative, simplifying presentation of summation results. Applying both excitation and inhibition in the same cell produced results consistent with previous work in which these inputs were studied in different cell samples. The cell in Fig. 1B displays very marked amplification of excitation (+Ia I_N; Fig. 1B, upper trace), with a peak around -55 mV, followed by strong reduction (saturation) above -45 mV (cf. Lee and Heckman, 2000). This saturation in excitatory synaptic efficacy may be due to both strong dendritic depolarization from PIC activation as well as activation of dendritic voltage-sensitive outward currents (Lee, Kuo et al. 2003). The suppression of the PIC by Ia reciprocal inhibition also provides net input amplification

(cf. Kuo et al., 2003), so that inhibitory Ia current (-Ia I_N) also exhibits a peak but at a more depolarized level (-48 mV compared to -55 mV for +Ia I_N; on average for the 31 cell sample this difference was 5.3 mV. ± 3.23 mV, $p < 0.0001$, paired t-test). The overall degree of amplification was also similar to our previous work (i.e. about a 3 fold amplification of excitatory Ia I_N and inhibitory Ia I_N in the standard compared to minimal monoaminergic states (Kuo et al., 2003; Lee and Heckman, 2000).

Is Summation of Excitation and Inhibition Linear When Neuromodulatory Input is also Present?

In a cell with perfect voltage and space clamp, ionotropic synaptic inputs not only generate linear I-V functions (hypothetically illustrated by the thin dotted lines in Fig. 1B), but also undergo linear or proportional summation of their currents. Here, only the soma is well clamped. Therefore, the amplification and saturation of synaptic input due to the dendritic PIC (Fig. 1B) may also induce nonlinear input summation in dendritic regions. In other words, the good voltage clamp at the soma (see Methods) forces any nonlinear interactions between inputs and the PICs observed in the following results to occur in dendritic regions.

Linearity of summation in the standard monoaminergic state was assessed by comparing the actual I_N generated by simultaneous activation of both excitation and inhibition to the predicted I_N based on the algebraic sum of the I_N generated by each input on its own (e.g. Powers and Binder 2000). Examples of this calculation are shown

in Figure 2. For the same cell as in Fig. 1, peak excitatory I_N was larger than peak inhibitory I_N (Fig. 2A; ~ 16 nA versus ~ -10 nA). Fig. 2B shows a cell where peak excitation was about equal to peak inhibition (~10 nA) and Fig. 2C shows a cell with peak inhibition larger (~ 10 nA versus ~ -18 nA). In each case, the predicted summed I_N (dashed traces) exhibits a strong variation with voltage, with inhibition reducing the peak of amplification but increasing the subsequent saturation. This predicted summation behavior is inherently unbalanced: even when excitation and inhibition are approximately equal (Fig. 2B), excitation strongly dominates at first and then the combination of saturation and inhibition transforms summed I_N to net inhibition. This unbalanced behavior could also be manifest during repetitive firing in unclamped conditions, because amplification and saturation behaviors occur in the voltage range traversed by the membrane potential between spikes (Lee and Heckman, 1998a; Lee and Heckman 1998, and see Discussion).

During the actual simultaneous application of both excitation and inhibition, however, the variation with voltage level is markedly reduced (Fig. 2, thick traces). Amplification of excitation is suppressed to a greater degree than predicted (actual summed I_N at the peak of excitatory I_N is reduced compared to linear summation). Yet, saturation is also reduced (actual summed I_N is more positive than the predicted linear sum). To quantify this difference between the actual and predicted I_N, we calculated the difference in summed I_N at the voltage for peak amplification of excitation and peak amplification of inhibition (ΔSum, see arrows in Fig. 2A). In the data set as a whole, summation tended to be nonlinear by an average of -1.5 ± 2.7 nA within a voltage window centered at the

peak of excitatory I_N ($p < 0.003$, paired t-test) and nonlinear by +1.9 ± 3.4 nA within the voltage window center at peak of inhibitory I_N ($p < 0.003$, paired t-test). As a result, ΔSum was reduced from about 7.7 ± 4.9 nA for the predicted case to 4.1 nA ± 2.9 in the actual case ($p = 0.0001$; and examples in Fig. 2). Thus, nonlinear summation tended to reduce the variation in I_N as a function of voltage and promote better balancing of the relative contributions of excitation and inhibition.

In the region subthreshold to PIC activation, we expected sublinear summation due to inhibitory shunting, but this result fell short of being statistically significant ($p = 0.1$; paired t-test). The relatively linear summation may have been due to activation of I_H conductances in this relatively hyperpolarized range. Thus, activation of a voltage-sensitive current appears to compensate for nonlinear behavior potentially induced by synaptic inhibition (see Discussion).

Are Deviations from Linearity Functionally Meaningful?

These results show that the nonlinear summation of inputs reduced the variation in the summed I_N as a function of voltage compared to what pure linear summation would produce. How functionally significant is this difference? In the context of the overall range of input amplitudes applied to the motoneurons in this study, the degree of nonlinear summation appears modest, as shown in Figure 3. For cells to the left of zero, inhibition was greater than the excitation (summed I_N of up to -20 nA or more in some cells); on the right excitation dominated (reaching as much as +10 nA in some

cells). The line of 1.0 with zero y-intercept (Fig. 3, thick line) indicates perfect linear summation and the deviations between the data points and this line quantify nonlinear summation. The deviations from linear summation (vertical distance from each point to the 1.0 line) across this range are relatively modest – typically 2 nA or less. For comparison, gain of the frequency-current function in this preparation is about 2 spikes/s/nA (Lee et al., 2003). An additional notable feature of Fig. 3 is that linear regression analysis provided good fits to each data set and the slope of each regression line falls within the 95% confidence intervals for a slope of 1.0. Thus, linearity of summation was similar regardless of the relative mixture of excitation and inhibition across the cells in this sample.

Some data points in Fig.3, however, diverge substantially from linearity. To determine if there was a systematic source of these deviations, we further analyzed our results for the reduction in ΔSum. We found that the larger the predicted ΔSum, the greater the reduction due to nonlinear summation – i.e. the smaller the actual ΔSum (Figure 4; $r = 0.81$; $r^2 = 0.65$; $p < 0.001$). This trend is evident in the examples in Fig. 2 (the cell in B has a larger predicted ΔSum and a smaller actual ΔSum than the cells in A and C). For large values of predicted ΔSum, the reduction in actual ΔSum reached as large as 10 to 15 nA (Fig. 4). A change of this amplitude is functionally important, being equivalent to changes in firing of 20 to 30 spike/s. Overall, the greater the predicted variation in I_N with voltage, representing an increase in saturation from adding inhibition to excitation, the greater the nonlinear summation to reduce this effect. Thus, nonlinear summation

appears to substantially compensate for the tendency of the dendritic PIC to un-balance the contributions of excitation and inhibition.

Input Summation in the Minimal Monoaminergic State

As in previous work (Lee and Heckman 2000, Kuo et al 2003), PICs in motoneurons in the minimal monoaminergic state (decerebrate, acute spinal transection; see Methods) were small (mean PIC amplitude = 3.6 nA ± 3.1, n = 18). As a result, I-V relations were much more linear than in the standard state, as illustrated by the example in Figure 5A, and neither excitatory nor inhibitory I_N showed strong deviations due to amplification (Fig. 5B). Thus, the minimal monoaminergic state provided an assessment of synaptic input summation in dendrites lacking the strong activation properties generated by the large PIC in the standard state. Because of the general lack of clear peaks in the excitatory and inhibitory I_N's, summation behavior was only calculated in the window where the small PIC in the control window reached its peak value following leak subtraction (similar to the peak inhibitory window in the standard state; see Methods) and in the subthreshold region (similar to the same region in the standard state).

Excitatory Ia I_N remained small at all voltages, due to the lack of PIC amplification (mean Sub-PIC I_N = 2.8 nA ± 2.2; mean peak PIC window I_N = 4 nA ± 3 , and was not significantly different than the mean excitatory I_N measured in the sub PIC voltage window in the intact condition ($p > 0.24$) . Both sources of inhibition, Ia reciprocal and CP stimulation, remained similar in intensity compared to the standard monoaminergic

state as percent changes in input conductance in the two states were not significantly different from each other (t-test, $p > 0.05$). We expected the dendrites to behave in a near passive manner with inhibitory shunting dominating**.** Instead, summation of excitatory Ia and inhibitory Ia I_N transitioned from near linear or supralinear to sublinear as the amplitude of excitatory input increased relative to inhibitory input (filled symbols, Figure 6; each data point is a separate cell). As a result, y=x line did not fall within the confidence bands for the regression relation (upper and lower thin black lines) for this data set (Fig. 6). This trend occurred in both voltage windows (see Discussion). In contrast, the sum of excitatory Ia I_N and CP inhibitory I_N was approximately linear in both windows (open symbols and corresponding dashed lines), though there was substantial scatter. The absence of shunting when CP inhibition was strong suggests that the dendrites were not completely passive but may have active properties that were sufficient to compensate for the inhibitory shunting (see Discussion).

Discussion

Our results show that nonlinear summation of excitation and inhibition in the standard monoaminergic state provides compensation for the tendency of the dendritic PIC to amplify excitation and inhibition within different voltage ranges. This compensation provides a more consistent relation between excitation and inhibition as a function of voltage, allowing motoneurons to operate in a reasonably balanced mode even when strong neuromodulatory input is present. To what degree motoneurons normally function in this mode in various motor behaviors is uncertain, but the balanced mode

does occur during the scratch reflex, which is driven by a central pattern generator (Berg et al., 2007). Functionally, Berg et al have argued that balanced input allows the pattern generator to control motoneuron output while reducing the impact of neuromodulatory input. The present results support their concept. In a sense, in the balanced mode, the motoneuron in the standard neuromodulatory state behaves as if it was in the low neuromodulatory state (note the qualitative similarity between summed I_N's in Figs. 2 and 5). Our results are also consistent with previous studies showing that the dendritic PIC is highly sensitive to inhibition (Hultborn et al., 2003; Hyngstrom et al., 2007). Why then have the neuromodulatory input only to suppress it? We believe there are two reasons.

First, neuromodulatory effects can be recovered either by removing inhibition or by adding more input to the cell in a push-pull configuration (i.e. coupling decreased inhibition to increased excitation) (Destexhe et al., 2003). Consider the net excitation generated by simply decreasing inhibition without changing excitation. A change in current is generated, which is defined by the difference (dotted trace in Figure 7) between the actual summed I_N and the excitatory I_N on its own. Because of the nonlinear summation near the peak of the excitatory I_N (compare arrow #1 to #2), this difference current undergoes nearly as much amplification as when excitation is applied alone (upper thin trace). This result was consistent across the full sample of cells in the intact condition: just as illustrated in Fig. 7, the peak of the difference current was not significantly different than the peak of the excitatory current on its own ($p > 0.48$). At more depolarized levels, the difference current is less than it would have been with pure

linear summation (compare arrow #3 to #4), but saturation of the difference current still tends to be less than for excitation on its own. This trend did not quite hold up across all cells, as the average current at saturation in excitation by itself was not significantly different than for the difference current ($p = 0.07$). This means, however, that the saturation in the difference current was no worse than for excitation alone. A push-pull change in input would be expected to produce a still greater difference current, because the amplification of both excitation and inhibition may sum together and produce a broad voltage range for amplification. Direct experimental test of this expectation is required, however, as increases in excitation required for push-pull may exceed the limit of the dendritic PIC for input amplification (cf. Kuo et al., 2003). The behavior of transient inputs also requires further study (cf. Jones and Lee 2006).

We have also postulated another role for the inhibitory suppression of the PIC. The descending monoaminergic systems are very diffuse, affecting many motor pools throughout a limb simultaneously (Heckman et al., 2003). Reciprocal Ia inhibition however is tightly focused between strict agonist-antagonist pairs operating at a single joint. We have shown that even small joint rotations strongly suppress the dendritic PIC via reciprocal inhibition, providing a mechanism to “sculpt” specific movement patterns out of a diffuse neuromodulatory background of high motoneuron excitability (Hyngstrom et al., 2007). Using this mechanism, motoneurons in motor pools not required for a particular movement pattern could be placed in either a high conductance mode (with inhibition dominating) or balanced mode, so that they would be activated only if needed for small but precise corrective adjustments.

Overall, the interaction between excitation, inhibition and neuromodulation provides a high degree of flexibility in controlling synaptic integration in spinal motoneurons and matching their excitability to different motor patterns. Such flexibility is a hallmark of invertebrate neural circuits (Harris-Warrick 2002; Marder and Bucher 2007) and may thus also be a fundamental in many mammalian circuits.

Possible Mechanisms for Nonlinear Summation in the Standard Monoaminergic State

An important concern with any study of summation of synaptic inputs is that the input interactions may occur partially by presynaptic mechanisms. For motoneurons, presynaptic interactions could occur among pre-motor interneurons, which are activated by the sensory afferents, or by presynaptic inhibition of afferent terminals, which is a fundamental feature of cord circuitry (Rudomin 2002). The inputs we used were selected to minimize these problems. The Ia excitation is primarily monosynaptic. A small multi-synaptic component may exist, but experiments in our lab have yet to detect any effects not due to ionotropic, monosynaptic excitation (Kuo et al., 2003; Lee and Heckman, 2000). Note also that the lack of amplification in the low monoaminergic state of Ia I_N indicates that this input does not significantly influence dendritic PICs by either metabotropic or NMDA glutamate receptors (see also Heckman et al., 2000). Presynaptic inhibition remains a possibility but would have been manifest as sublinear summation in the most hyperpolarized voltage window. Summation in this window did

not significantly deviate from linear, suggesting that the combined effects of post-synaptic inhibitory shunting and any presynaptic inhibition were small. Consequently, it is likely that the dominant interactions determining linearity of summation occurred post-synaptically. Moritz et al (2007) recently showed that PICs in the somatic region of motoneurons are strong and could thus amplify input (cf. Stuart and Sakmann 1995). The secure voltage clamp of the soma in the present studies, however, restricts amplification, saturation and nonlinear interactions to regions of poor voltage control, i.e. the dendrites.

Inhibition tends to suppress the dendritic PIC (Kuo et al., 2003 and Fig. 1) and thus should reduce the amplification of excitatory input. This suppression would account for sublinear summation in the voltage range for the peak excitatory I_N in the intact condition. In contrast, further depolarization brings on saturation of the Ia excitation when applied on its own (Fig. 1B), presumably due to dendritic depolarization or perhaps activation of voltage-sensitive outward currents. Simultaneous dendritic inhibition could provide hyperpolarization to reduce this saturation (Fig. 2). In the sub-PIC voltage window, inhibition may interact with the hyperpolarization activated cationic current I_H, which is responsible for the “sag” to hyperpolarizing steps in motoneurons and often imparts a substantial curvature to subthresold I-V functions (Powers and Binder 2001). Activation of I_H might offset the shunting effect of inhibition and account for the nearly linear summation in this hyperpolarized voltage window. This interpretation would imply that motoneurons have substantial I_H in dendritic regions.

Mechanisms Underlying Summation in the Low Monoaminergic State

When excitation is larger than inhibition in cells in the spinalized state, where monoaminergic drive is low, sublinear summation occurs (Fig. 6, triangles on right). This sublinearity is consistent with a shunting effect of inhibition on the excitatory I_N, as dendritic PICs appear to be small. However, in cells where inhibition was large compared to excitation, summation tends to become linear – though scatter in the results is fairly large (Fig. 6, left portion). As in the standard monoaminergic state, this near linearity may be due to activation of I_H compensating for the inhibitory shunt. I_H may not, however, fully explain this result, as the Ia inhibitory input exhibited a transition from sublinear to linear or (or perhaps slightly supralinear) summation in both the sub-PIC and PIC voltage windows – the latter being more depolarized than the former by 10 to 15 mV. Another possibility, entirely speculative at this point, is that acute spinalization uncovers an as yet unidentified local neuromodulatory circuits activated by sensory inputs.

Input Summation During Repetitive Firing in Unclamped Conditions

The voltage clamp method utilized in this study had the advantage of restricting nonlinear interactions between the inputs to unclamped dendritic regions (Heckman and Lee, 2001). To what degree will this effect also occur during repetitive firing in unclamped conditions? Prather et al (2002; 2001) demonstrated linear summation of two excitatory inputs during repetitive firing in the same preparation used here, though

the neurons were probably not driven strongly enough to enter the saturation range (cf. Lee et al., 2003). Our results in the minimal monoaminergic state showing sub-linear to linear summation during voltage clamp are consistent with those of Powers and Binder (2000) during repetitive firing in a deeply anesthetized preparation likely to have similarly low levels of monoaminergic drive. These similarities between firing and voltage clamp behaviors are reasonable in that the AHP that follows each spike limits the average membrane depolarization between spikes (Powers and Binder, 2001). The average voltage level during firing does depolarize substantially as firing rate increases, reaching the levels where excitatory saturation and inhibitory amplification occur (Lee and Heckman, 1998a; Lee and Heckman, 1998b; Lee and Heckman, 2000). Thus it is probable that the nonlinear summation seen here in voltage clamp would also produce a more consistent balance between excitation and inhibition as baseline firing rate increases from threshold levels. Direct experiments along these lines are needed however, as synaptic noise can have strong interactions with spike generation during repetitive firing (e.g. Chance et al., 2002).

Firing patterns during balanced input are in fact highly variable due to synaptic noise (Destexhe et al., 2003), a phenomenon that is also present during the scratch reflex in motoneurons (Berg et al., 2007). Motoneuron firing variability is typically quite low compared to cortical neurons and to spinal interneurons during voluntary movements (Prut and Perlmutter 2003). The large AHP in motoneurons, however, acts to stabilize firing rate (Manuel, Meunier et al. 2005; Manuel, Meunier et al. 2006) and may reduce the effect of balanced inputs in at least some motor outputs. Alternatively, behaviors

driven by central pattern generators exhibit greater firing variability than during voluntary movements.

Our results may also be relevant to firing patterns of motoneurons measured in human subjects via their one-to-one driving of muscle fibers. One striking aspect of these patterns is that during motor unit recordings an initial brief but steep period of rate modulation is followed by a sustained modulation at a much lower slope (Binder, Heckman et al. 1993), sometimes referred to as the “preferred” firing range (Hornby, McDonagh et al. 2002). The initial phase may be due to the activation of the PIC and its amplification effects, while the later more sustained phase may occur when voltage has increased to a range that saturation occurs (Fig. 1, 2). Our results predict that modulation of an inhibitory background would reduce both effects, i.e. lower the initial slope and increase the sustained slope.

EXPERIMENTAL PROCEDURES

SURGICAL PREPARATION

All surgical procedures were approved by the Northwestern University Institutional Animal Use and Care Committee. All experiments (total = 21) utilized the decerebrate cat preparation (for details see (Lee and Heckman, 1998b). The surgical preparation was completed under deep anesthesia (1.5-3% isofluorane in a 1:3 mixture of NO_2 andO_2). Carotid arteries were cannulated to monitor blood pressure and for delivery of drugs. The

mixed nerves to the medial gastrocnemius, lateral gastrocnemius and soleus (MG and LGS) muscles were located and cuff electrodes were applied for antidromic identification of MG and LGS motoneurons (all experiments). Additionally, the common cutaneous sural nerve (5 experiments) and common peroneal nerve (12 experiments) were isolated and cuff electrodes applied for excitatory and inhibitory synaptic input to MG and LGS motoneurons. The MG and LGS (all experiments) and tibialis anterior/extensor digitorum longus tendons (TA/EDL, 11 experiments) were cut distally and secured to a tendon vibrator. A bilateral pneumothorax was performed to promote stable recordings by lessening movement of the chest wall. A laminectomy was completed from L_1 to L_7 vertebrae to expose the spinal cord and the cord was then bathed in mineral oil. Motor thresholds were determined for MG and LGS nerves. The animal was then paralyzed with Flaxedil (120 mg initial dose, then supplemented as needed) and artificially respirated. In 6 of the experiments, to diminish descending monoaminergic drive from brainstem centers, the cord was spinalized at T_{10} prior to decerebration. A laminectomy was done at $T_{9,10}$ and two sutures were placed under the cord. The cord was then transected between the sutures. A precollicular decerebration was performed and all forebrain anterior to the lesion was aspirated. The anesthesia was discontinued and recordings began at least 45 minutes after decerebration.

Electrophysiology

Intracellular recordings were done using sharp electrodes with resistances of 3-5 MΩ. Electrodes were filled with 2 M potassium citrate. Voltage clamp recordings are

performed using the Axoclamp 2a amplifier (Axon Instruments) in single electrode discontinuous mode (9-10.5 kHz switching frequency). Due to the large current necessary to voltage clamp the motoneurons, an external feedback loop was added to increase the gain by a factor of 10 (with a total of 11x) for 10-40 nA/mV (Heckman and Lee, 2001). This gain factor resulted in excellent clamp control, with deviations of < 0.5 mV in voltage ramps. Voltage clamp data was smoothed by digital filtering (-3 db point of 0.3 KHz).

Synaptic Input

Ia monosynaptic excitatory synaptic input to MG and LGS motoneurons was achieved by vibration of the Achilles tendon (180 Hz, 80 µM peak to peak). In 6 experiments, polysynaptic excitatory synaptic input to MG motoneurons was generated by electrical stimulation of the common cutaneous sural nerve (100 Hz). Reciprocal Ia inhibition to MG and LGS motoneurons was produced by 100 Hz electrical stimulation of the common peroneal nerve at 1.2-2 x motor threshold or by vibration of the common TA/EDL tendon (180 Hz, 80 µM peak to peak). The protocol used to assess these inputs (next section) assumes that they are constant for about 5 s. Although both Ia and sural excitation exhibit a slight decay in the first 1 s of steady stimulation, current thereafter is steady for many seconds (e.g. Lee and Heckman, 2000; Prather et al., 2001). Many types of inhibition to motoneurons fade rapidly to repetitive stimulation (Lafleur, Zytnicki et al. 1992; Lafleur, Zytnicki et al. 1993; Heckman, Miller et al. 1994),

this is not true of the inputs used here and thus meet the 5s criterion (Kuo et al., 2003; Lee and Heckman, 2000).

Protocol and Data Analysis

MG and LGS motoneurons were first identified by antidromic stimulation of peripheral nerves. In discontinuous voltage clamp mode, a slow (6-8 mV/s) voltage ramp was applied in the absence of synaptic input. The same ramp was repeated in the presence of excitatory and inhibitory synaptic input alone and simultaneously. A second voltage ramp with no additional synaptic input was repeated to assure cell health was maintained. Order of synaptic inputs was varied to prevent biased effects. Effective synaptic current (I_N) was calculated by subtracting synaptic trials from an average of control trials. Input conductance was determined by fitting a line to the linear hyperpolarized portion of the cell's I-V function. By subtracting the cell's I-V function from the line fitted to the hyperpolarized region we were able to determine PIC amplitude. Criteria for cell acceptance included: 1) antidromic spike height of 60 mV or greater; 2) membrane potential did not change more than 20% of baseline; 3) control input conductance did not change more than 20%; 4) the peak amplitude of the persistent inward current did not decline by more than 20%; 5) inadequate settling of the electrode during the recording. Student's T-Test and paired T-Test were used to make significance comparisons ($p < 0.05$) and ANCOVAs were used to compare differences in the slopes and intercepts between regression lines ($p < 0.05$). Excel and SPSS programs were used for data processing and data analysis.

Chapter 2

Intrinsic Electrical Properties of Spinal Motoneurons Vary with Joint Angle

Foreword:

This chapter has been published (Hyngstrom, Johnson et al. 2007).

Summary

The dendrites of spinal motoneurons amplify synaptic inputs to a remarkable degree, via persistent inward currents (PICs). Dendritic amplification is subject to neuromodulatory control from the brainstem by axons releasing the monoamines serotonin and norepinephrine. Yet the monoaminergic projection to the cord is diffusely organized and does not allow independent adjustment of amplification in different motor pools. Using *in vivo* voltage clamp techniques, we show that dendritic PICs in ankle extensor motoneurons in the cat are reduced about 50% by small rotations ($\pm 10^0$) of the ankle joint. This reduction was primarily due to reciprocal inhibition, a tightly focused input shared only between strict muscle antagonists. These results demonstrate how a specific change in limb position can regulate intrinsic cellular properties set by a background of diffuse descending neuromodulation.

Introduction

Studying the spinal motoneuron provides a unique opportunity to investigate the relations between neuromodulation, synaptic integration and system function. This cell has the potential to generate a large persistent inward current (PIC) in its extensive dendritic tree (Lee, 1996; Hounsgaard, 1993; Bennett, 1998; Carlin, 2000). The amplitude of this dendritic PIC is, however, directly proportional to the intensity of descending neuromodulatory drive mediated by axons releasing the monoamines serotonin or norepinephrine (Alaburda, Perrier et al. 2002; Heckman, Lee et al. 2003;Hultborn, Brownstone et al. 2004). As this neuromodulatory drive

increases, dendritic synaptic integration is progressively switched from passive to highly active, with synaptic current amplified by the dendritic PIC as much as 5 to 10 fold (Lee and Heckman 2000; Hultborn, Denton et al. 2003; Cushing, Bui et al. 2005). The monoaminergic systems are highly state dependent, with the serotonergic system being especially active during tonic motor output (Jacobs, Martin-Cora et al. 2002) and the noradrenergic system varying with state of arousal (Aston-Jones, Rajkowski et al. 2000). As a result, the degree of synaptic amplification may vary widely during normal motor behavior (Heckman, Lee et al. 2003; Hultborn, Brownstone et al. 2004), potentially allowing the input-output properties of motoneurons to be tuned to match the demands of different motor tasks.

The descending monoaminergic projection is, however, diffuse, simultaneously affecting motor pools for muscles throughout a limb (Bjorklund and Skagerberg 1982). Moreover, when activated by an excitatory input that is then withdrawn, the dendritic PIC remains active and can generate repetitive firing of action potentials for many seconds – this is the so-called “bistable” behavior of motoneurons (Heckman, Lee et al. 2003; Hultborn, Brownstone et al. 2004). Thus, at medium to high levels of monoaminergic input to the cord, the dendritic PIC strongly biases motor output toward prolonged co-activation of antagonists. Co-activation enhances joint stiffness, which improves stability, but movements like locomotion require more compliance and rely on reciprocal patterns of agonist-antagonist activation. Ideally, a mechanism for independent adjustment of dendritic amplification for motoneurons innervating antagonist muscles would exist.

The dendritic PIC has been shown to be highly sensitive to synaptic inhibition, which, depending on its strength, can reduce PIC amplitude or fully deactivate the PIC (Hultborn, Denton et al. 2003; Kuo, Lee et al. 2003). One important source of this inhibition is from sensory inputs

activated by limb movements (Fyffe 2001). It is thus possible that sensory inhibition could link the amplitude of the dendritic PIC to rotation of limb joints, thereby providing a reciprocally organized, inhibitory control system for the dendritic PIC to oppose the diffuse facilitation mediated by the descending monoaminergic system.

We evaluated this concept by testing the specific hypothesis that the sensory inflow evoked by sustained changes in ankle joint angle alters the dendritic PICs in ankle extensor motoneurons. Experiments were carried out using voltage clamp in adult motoneurons using an *in vivo* preparation with high levels of monoaminergic drive to the cord, the decerebrate cat (Hounsgaard, Hultborn et al. 1988; Lee and Heckman 2000). We also investigated whether the primary source of joint angle - PIC interaction was due to antagonist muscle afferents or cutaneous afferents.

RESULTS

PIC amplitude varies with changes in joint angle

All data in this study were obtained from triceps surae motoneurons in the adult cat. These motoneurons innervate muscles (medial gastrocnemius, lateral gastrocnemius, and soleus) which extend the ankle via the Achilles tendon (Fig. 1). Ankle angle was controlled by a six degree of freedom robotic arm (see Supplementary Methods). Ankle extension shortens the triceps surae and lengthens the antagonist flexor muscles (tibialis anterior and extensor digitorum longus). Ankle flexion has the opposite effect. As in our previous studies (Lee and Heckman 2000; Kuo, Lee et al. 2003; Lee, Kuo et al. 2003), the voltage clamp applied at the

soma was highly effective and thus all changes in PIC amplitude in this study occurred outside the region of good space clamp – i.e., in the dendrites (see METHODS). It should also be emphasized that only inhibitory synaptic input changes PIC amplitude; excitatory synaptic input only has the capacity to activate a PIC whose amplitude is set by the level of descending monoaminergic input (see Supplementary Fig. 1). In the preparation used here (the decerebrate cat), relative monoaminergic levels remain approximately constant during the course of each experiment, as indicated by the consistency of their effects on motoneuronal intrinsic excitability (e.g. Hounsgaard, Hultborn et al. 1988; Lee and Heckman 1998; Lee and Heckman 1998).

In the first set of experiments, the hindlimb was left as intact as possible to preserve normal sensory inflow (see METHODS). The dendritic PIC was assessed by linearly increasing voltage ramps applied as the ankle was held steady at three different joint angles, as illustrated in Fig. 2 where the PIC is evident as a downward deflection. Joint rotation to the next position was done as voltage was linearly decreased to prepare for each measurement of the PIC. The ankle was first held at a midpoint angle (approximately 90^0) and then extended 10^0, flexed 10^0 and returned to midpoint (top row). The resulting current traces are superimposed in Fig. 3a (upper panel) and shown after leak subtraction in Fig. 3b. PIC amplitude in this extensor motoneuron was the least when the ankle was extended and greatest when the ankle was flexed. Voltage control remained excellent during all movements in this cell (Fig. 3a, lower panel) and in all other cells in this study (see METHODS).

PICs were measured for $\pm 10^0$ differences in joint angle in 18 cells (Fig. 4). In 17 cells, extension decreased and flexion increased PIC amplitude relative to the midpoints (Fig. 4a). The midpoint values were not significantly different from each other ($p = 0.23$, paired t-test),

demonstrating the consistency of PIC behavior with repeated trials. The two midpoint PIC amplitudes were thus averaged together. Extension and flexion generated PIC amplitudes that were significantly different from each other and from the midpoint ($p < 0.0167$; paired t-tests; Bonferroni's correction for 3 repeats; see Table 1 for all statistical results). Extension decreased PIC amplitude by an average of about 29% while flexion increased it by about 31%, for a net change greater than 50%. Given the potent impact of the PIC on dendritic excitability (Heckman 2003; Hultborn, Denton et al. 2003), this PIC-joint rotation interaction provides a mechanism for postural adjustments to markedly alter dendritic integration of synaptic input.

To study the scaling between joint angle and PIC amplitude, we also applied larger rotations ($\pm 30^0$ with respect to the midpoint). Strong modulation of the PIC was again observed, with extension decreasing and flexion increasing PIC amplitude in 8 of 11 cells (Fig. 4b). Midpoint values matched each other and the flexion increased PIC amplitude compared to extension ($p = 0.0003$) (Table 1). The extension and flexion vs. midpoint comparisons, however, did not quite reach statistical significance (Table 1; $p = 0.0167$, Bonferroni's correction for 3 repeated tests). Although we anticipated that larger rotations would produce larger PIC effects, this was not the case. The increase in PIC amplitude for flexion (normalized by the average of the midpoint values) was not significantly different when compared across the two data sets for the two movement amplitudes ($p = 0.54$, unpaired t-test). Similar results were obtained on a within cell basis in 3 cells, where extensions of 10^0 and 30^0 were compared. In two of these three cells, the relative reduction in PIC amplitude was smaller for the larger rotation (in cell 1, PIC amplitude was reduced to 41% of the midpoint value at 10^0 and to 34% at 30^0; cell 2: 53% vs. 43%; cell 3: 45% vs. 45%).

Reciprocal inhibition is critical for PIC modulation

What component of the synaptic input produces the joint-angle induced modulation in PIC amplitude? Several types of sensory afferent could be involved, but muscle spindle Ia afferents are likely to be especially important, as they are very sensitive to changes in muscle length and evoke disynaptic reciprocal inhibition between antagonists (Jankowska 1992). The joint angle modulation of PICs demonstrated in Fig. 4a,b is exactly what would be expected from Ia reciprocal inhibition evoked by the stretching and shortening of the antagonist flexor muscles. Note that the Ia monosynaptic excitation to agonists is probably not a significant factor because this input has little impact on PIC amplitude (Lee and Heckman 2000 and see Supplementary Fig. 1).

Thus, a second series of experiments was performed in which reciprocal inhibition was markedly reduced by cutting the tendons of tibialis anterior and extensor digitorum (TA/EDL), thereby eliminating the contribution of the antagonist muscles that are the main source of Ia reciprocal inhibition of the triceps surae (Nichols 1999). The ankle joint was again rotated $\pm 10^0$ with respect to midpoint and the PIC measured ($n = 16$ cells). The results for the cell shown in Fig. 5 show that the PIC assessed during extension actually increased instead of decreased (in contrast to Fig. 3b). Moreover, this increase was maintained during flexion and the return to midpoint (Fig. 5). In 11 of 16 cells, PIC amplitude was larger at all subsequent positions compared to the initial midpoint. In 13 of 16 cells, PIC amplitude was greater at the return to the midpoint than at the initial midpoint (Fig. 4c). Across trials, the mean PIC amplitude for the first mid position (10.0 nA $\pm$ 7.0) was significantly smaller than the mean PIC amplitude measured for each subsequent position (Table 1). The mean PIC amplitudes for these subsequent

positions (extension, flexion and return to midpoint) were not significantly different from each other (paired t-test; $p > 0.013$; Bonferroni's correction; Table 1).

The lack of co-variation of the PIC with joint rotation with antagonist tendons cut supports a fundamental role for reciprocal inhibition in PIC modulation with movement. The consistent increase in PIC amplitude across trials likely reflects the phenomenon of warm up (Svirskis and Hounsgaard 1997; Bennett, Hultborn et al. 1998). It is especially notable that PIC increased by ~20% during extension whereas the same movement with the antagonist tendons intact decreased PIC by ~30% (see Table 1). If reciprocal inhibition limits warm up, then warm up should also be absent when reciprocal inhibition is present as a steady background in the absence of joint rotations. In four of the cells from the tendon intact condition, we repeated the voltage ramp four times while maintaining the mid position. On average, PIC amplitude did not significantly vary between trials (midpoint 1 = 17.0 nA $\pm$ 5.9, midpoint 2 = 16.2 nA $\pm$ 4.9, midpoint 3 = 14.4 nA $\pm$ 6.1, midpoint 4 = 15.51 nA $\pm$ 6.5; $p > 0.56$, Mann-Whitney Test). The overall lack of warm up in the tendon-intact condition implies that reciprocal inhibition may act to prevent warm up from occurring during normal movements (see DISCUSSION).

Further support for reciprocal inhibition as the dominant source of joint position effects on the dendritic PIC was obtained by comparing the influence of hip joint position to that of ankle position in 6 of the 18 ankle extensor motoneurons for the intact, $\pm 10^0$ condition. Because muscles crossing the hip joint are unlikely to mediate significant reciprocal inhibition of ankle extensors (Nichols, Cope et al. 1999), we predicted that hip position would not have a strong impact on ankle extensor PICs. The results showed that hip position ($\pm 10^0$ flexion and extension) had a small effect but this was not statistically significant (mean PIC amplitude measured from triceps surae motoneurons: hip flexion = 5.8 nA $\pm$ 1.1, hip extension 7.3 nA $\pm$

2.5, p = 0.13, matched t-test). Normalized with respect to PIC amplitude at midpoint, this difference represented a total PIC modulation of 19%. In contrast, the $\pm 10^0$ changes in ankle position generated substantial PIC modulation in these same 6 cells (extension = 5.7 nA $\pm$ 1.9 and flexion = 9.6 nA $\pm$ 4.1). Despite the restricted sample size, ankle flexion and extension PICs were significantly different for this sub-sample of the $\pm 10^0$ ankle positions (p = 0.013, paired t-test) and the net modulation was about 56% of the PIC amplitude at midpoint (consistent with the 50% average for the full sample noted above). Moreover, the average %PIC modulation with ankle position was significantly larger than with hip position ($p < 0.01$, paired t-test).

Reciprocal inhibition usually generates a substantial change in input conductance as measured at the soma. Note that the input conductance of adult cat spinal motoneurons is unusually high, typically around 1 μS (Powers and Binder 2001), due to their exceptionally large size with 10 or more major dendritic branches extended for more than 1 mm from the soma (Rose, Keirstead et al. 1985; Cullheim, Fleshman et al. 1987). In the reciprocal inhibition intact condition ($\pm$ 10 degree sample, $n = 18$), input conductance was not significantly different across joint angles (midpoints = 1.07 μS $\pm$ 0.35, extension = 1.03 μS $\pm$ 0.43, flexion = 1.08 μS $\pm$ 0.36, $p \geq 0.17$, paired t-test). Moreover, changes in baseline holding currents between voltage ramps, which reflect the amplitude of the effective synaptic currents with minimal impact of the dendritic PIC, were also virtually unchanged ($p > 0.05$ in most cases; paired t-test). A small shift in baseline current was detected only during flexion, perhaps due to an increase in Ia excitation due to stretch of the triceps surae (flexion = 15.1 nA $\pm$ 8.8; initial mid = 12.2 nA $\pm$ 8.01 nA, p = 0.001, paired t-test). Thus the net synaptic inhibition due to changes in joint angle was small, but nonetheless had a remarkably large impact on the PIC in unclamped dendritic regions.

Lack of cutaneous input does not affect PIC modulation

Cutaneous afferents excite or inhibit ankle extensors, depending on their receptive fields (LaBella and McCrea 1990). The net effect of cutaneous afferents during stretch of skin during ankle rotation is unknown but could contribute net inhibition to PIC modulation. In the final series of experiments (n = 8 cells), we diminished cutaneous synaptic input by denervating cutaneous nerves (see METHODS). Denervation was done early in the surgical procedures, > 2 hours before the data collection, to prevent confounding effects from injury discharge. Tendons to antagonists were left intact to allow normal reciprocal inhibition.

Results were similar to control conditions, with good modulation of PIC amplitude. Mean PIC amplitude during ankle flexion (11.5 nA ± 4.2) was significantly greater than in the mid position (9.2 nA ± 4.9) and extended position (8.1 nA, ± 5.4) (Table 1). The mean PIC amplitude for extension was less than that for the mid position but the p value of 0.026 did not meet the alpha criteria of $p = 0.016$ (paired t-tests, Bonferroni's correction). These results suggest that cutaneous input is not a dominant source of PIC regulation during change in joint angle.

Modulation of the PIC is not limited to the ankle joint

The full pattern of reciprocal inhibition between the motor pools innervating all of the more than 30 muscles in the hindlimb has not yet been established. It is known, however, that knee extensors and knee flexors exchange reciprocal inhibition (Nichols, Cope et al. 1999). Therefore, to verify that the joint angle actions on the PIC were not confined to the ankle, we

investigated the effect of knee flexion and extension on hamstring motoneuron PICs ($n = 7$, see METHODS).

The results were analogous to those at the ankle, though of course opposite in sign as the hamstrings motoneurons innervate flexors instead of extensors. Knee extension, which shortened the antagonist quadriceps, on average doubled the PIC as compared to knee flexion (mean amplitudes 8.7 nA $\pm$ 2.2; 3.8 nA $\pm$ 3.2 respectively) resulting in significant differences in the PIC ($p < 0.0005$, matched t-test). These results show that PIC modulation with joint position is not limited to the ankle and moreover occurs in flexor motoneurons as well as extensors.

DISCUSSION

The foregoing results show that small changes in joint angle have a potent effect on the amplitude of the dendritic PIC. These effects occurred in dendritic regions because voltage at the soma was effectively clamped to repeat the same voltage trajectory throughout the sequence of different joint positions. Because PIC amplitude determines the magnitude of synaptic amplification (Lee and Heckman 2000), the degree to which synaptic integration is active versus passive in the dendrites of motoneurons depends on limb configuration.

Descending monoaminergic systems have wide spread effects on many motor pools (Bjorklund and Skagerberg) and thus tend to mediate an increased excitability throughout the motor system. In contrast, the control system for the PIC evoked by changes in joint angle is dominated by Ia reciprocal inhibition. This sensory input is tightly focused, being strong only between strict antagonists operating at single joints (Nichols, Cope et al. 1999). Reciprocal

inhibition was highly potent in its actions on the dendritic PIC, suppressing it markedly without significantly altering input conductance measured at the soma.

Depending on the task required, the motor system needs to either stabilize itself against perturbation via co-activation of antagonist muscle groups or produce movements by reciprocal activation. The wide spread of the monoaminergic systems would strongly predispose the motor system toward co-activation, especially when monoaminergic drive is high and even small inputs can produce strong motoneuron activation. The potency of the tightly focused reciprocal inhibitory system in suppressing the dendritic PIC would, however, allow reciprocal movements to be readily "sculpted" from this overall high excitability state, maintaining the organism's ability to combine stability and movement as needed at any state of arousal. It seems likely that reciprocal inhibition from muscle stretch is particularly important for the transition from agonist to antagonist activation: as the agonist shortens, it would receive reciprocal inhibition from the antagonist; while the antagonist reciprocal inhibition from the agonist would be reduced. These interactions provide a remarkable example of a how normal motor system function arises from the interaction between diffuse neuromodulation (the monoaminergic system), specific sensory inhibition (Ia reciprocal inhibition) and active dendritic integration (the dendritic PIC).

Comparison of Ia reciprocal inhibition to other types of inhibition

The hindlimb of the cat contains multiple joints and more than 30 muscles, so we did not systematically evaluate joint angle - PICs relations throughout the limb. Nonetheless our results provide considerable support for the specificity of joint angle modulation of the PIC that would be expected for Ia reciprocal inhibitory connections. There are 10 muscles that cross the ankle joint. Cutting the tendons of only the two muscles that have the strongest reciprocal inhibitory

effects on the triceps surae, the tibialis anterior and extensor digitorum longus (Nichols, Cope et al. 1999), eliminated PIC changes with ankle flexion-extension. Thus, the peroneal group, the deep tibial flexors beneath the triceps surae and the triceps surae themselves, all of which undergo changes in length during ankle flexion-extension (Nichols 1999; Nichols, Cope et al. 1999), had no influence on PIC amplitude. We also demonstrated that changes in hip angle did not significantly modulate triceps surae PICs.

Further support for Ia reciprocal inhibition as the dominant source of PIC modulation with joint angle was demonstrated by our results showing a lack of effect of cutaneous denervation. Important roles for other muscle afferents appear to be unlikely. We discount the contribution of tendon organ Ib afferents in TA/EDL because our preparation was paralyzed and Ib afferents are relatively insensitive to passive changes in muscle length over the midrange of movement applied here (Stephens, Reinking et al. 1975). Free nerve endings are also unlikely to contribute as they respond most strongly at extremes, generate widespread inhibition of extensors and excitation of flexors as part of the flexion reflex, and connect to interneurons that tend to be inhibited by descending monoaminergic systems (Cleland and Rymer 1990; Jankowska 1992). In contrast, monoaminergic systems tend to facilitate transmission in group I pathways (Hammar and Jankowska 2003). This facilitation does not appear to broaden the actions of Ia reciprocal inhibition, as the pattern of reciprocal inhibition studied by reflex actions in the decerebrate preparation is tightly focused (Nichols, Cope et al. 1999). Muscle spindle group II afferents are highly length sensitive (Matthews 1972) and some group II interneurons are facilitated by descending monoaminergic systems (Jankowska 2001). The known pathways of these afferents, however, do not match the simple reciprocal patterns demonstrated here for PIC modulation with joint angle (Jankowska 1992; Jankowska 2001).

An alternative explanation of our results might be that sensory input from changes in joint position alters firing patterns of brainstem monoaminergic neurons that project to the cord. This explanation does not appear likely for several reasons. Raphe spinal neurons are not sensitive to passive limb rotations (Jacobs, Martin-Cora et al. 2002) , while the locus coeruleus appears to be largely involved in arousal, not specific sensory stimuli (Aston-Jones, Chen et al. 2001). Moreover, the descending monoaminergic system has diffuse effects on motoneurons both temporally, in that motoneuron excitability is raised for many minutes after drug administration and washout (Lee and Heckman 1998; Lee and Heckman 1998; Machacek, Garraway et al. 2001) and spatially, due to the divergence of the descending axons (Bjorklund and Skagerberg). These characteristics are not consistent with the specificity of our results noted above.

Descending systems also inhibit motoneurons. Both the cortico- and rubrospinal systems powerfully suppress low threshold, type S extensor motoneurons (Powers, Robinson et al. 1993; Binder, Robinson et al. 1998). Presumably this inhibition will also suppress the PIC. One speculation is that these systems have the capacity to suppress PICs in type S motoneurons so that gain of these motoneurons can be reduced during very precise movements (Heckman and Binder 1988). This would allow errors in motor commands to have minimal impact on motor output, whereas a large amplitude PIC would magnify such errors.

During the swing phase of locomotion, extensors are not just deactivated but undergo active inhibition (Shefchyk and Jordan 1985). PICs may be a major component of the depolarization of extensor motoneurons during the stance phase (Brownstone, Gossard et al. 1994; Heckman, Lee et al. 2003). The extension of the ankle at the end of the stance phase may generate significant reciprocal inhibition, which could play an important role in deactivating these

motoneurons for the swing phase. Dynamics of the PIC activation and deactivation are likely to be very important in locomotion and future studies need to be directed at this issue.

Other monoaminergic actions on motoneurons

Monoaminergic effects on motoneurons are not restricted to dendritic PICs. Substantial hyperpolarization of spike voltage threshold occurs (Krawitz, Fedirchuk et al. 2001; Fedirchuk and Dai 2004) coupled with a depolarization of resting membrane potential, an increase in input resistance and significant shortening of the spike after-hyperpolarization (Powers and Binder 2001). All these effects act in concert to increase motoneuron excitability. Reciprocal inhibition naturally opposes most of these effects by hyperpolarizing membrane potential and increasing conductance.

The PIC, however, appears to be especially sensitive to reciprocal inhibition, perhaps due to its dendritic location. Changes in hyperpolarization and input conductance as measured at the soma mediated by changes in joint angle were almost undetectable, yet the PIC was modulated by nearly 50% and warm up was eliminated. This potency suggests that reciprocal inhibition may have a significant neuromodulatory action via GABAb receptors (e.g. (Svirskis and Hounsgaard 1998) in addition to its classic glycinergic actions (Baldissera, Hultborn et al. 1981; Curtis and Lacey 1998). This issue cannot be resolved experimentally at present because drugs that influence GABAb receptors are not selective for pre- versus postsynaptic sites of action (Bowery, Bettler et al. 2002).

Nonlinear scaling of the PIC with joint angle amplitude

Increasing the change in joint angle did not produce larger PIC suppression. The stretch reflex generated in agonist muscles by Ia afferents scales well with amplitude of applied length changes in the midrange of movement (Matthews 1972), so perhaps processing of Ia afferent information in the network of Ia inhibitory interneurons limits amplitude scaling. This possibility is supported by previous studies showing increasing inhibition via increasing the strength of electrical stimulation of a large nerve with both muscle and cutaneous afferents does in fact produce a proportional reduction in PIC amplitude (Kuo, Lee et al. 2003).

Functionally, the amplitude limitation within the Ia interneuron circuitry may provide an effective compromise between PIC suppression through a reasonable movement range and avoiding such strong suppression that the PIC could not be activated at extreme joint angles. It should be kept in mind, however, that Ia afferents have a strong dynamic sensitivity (Matthews 1972). Consequently, dynamic movements may produce larger inhibitory inputs that allow better scaling of PICs with movement amplitude.

Organization and plasticity of reciprocal inhibition

Skeletal joints are complex mechanical structures with multiple muscles influencing their actions. Thus, it seems likely that reciprocal inhibition varies in its organization at different joints and in different species. Studies in human subjects have demonstrated that reciprocal inhibition is clearly evident –for example, the linkage studied here between triceps surae and TA/EDL is present in humans (Crone, Hultborn et al. 1987). The elbow of human subjects also exhibits clear agonist-antagonist reciprocal inhibition yet the wrist does not (Wargon, Lamy et al. 2006).

Ia inhibitory interneurons receive strong input from descending systems like the corticospinal tract (Jankowska 1992) and descending control of reciprocal inhibition has been detected in human subjects (Nielsen, Crone et al. 1995). In addition, Ia reciprocal inhibition has recently been shown to be subject to operant conditioning (Chen, Chen et al. 2006), much like Ia excitation (e.g. Chen, Chen et al. 2005). Thus it appears likely that reciprocal inhibition is a flexible system that differs from joint to joint and can be adapted by descending input both on short and long time scales. Our results suggest that this same flexibility could be extended to control of the dendritic PIC, presumably allowing motoneuron excitability to be precisely matched to the demands of different motor tasks.

METHODS

Surgical Procedures

All animal procedures were fully approved by the Northwestern University Institutional Animal Use and Care Committee. Details of the surgical preparation can be found in our previous work (Lee and Heckman 1998; Lee and Heckman 2000). All 31 experiments were done in the decerebrate cat preparation. Surgical preparations were done under gaseous anesthesia (1.5–3.5% isoflurane in a 3:1 mix of N_2O and O_2). The nerves to medial gastrocnemius, lateral gastrocnemius/soleus and hamstring (semi-membranosus, semi-tendinosus, and biceps-femoris) muscles were isolated and placed in cuff electrodes for antidromic stimulation. The foot was attached to a six degree of freedom robotic arm (Fig. 1.) Staubli AG Robotics. The hip was set at 105 degrees and the knee at 130 degrees. The ankle was positioned at 88 degrees

relative to the tibia. In 11 experiments, to decrease reciprocal inhibition, the common tendon to the tibialis anterior and extensor digitorum muscles was cut, with the muscle left at resting length. In 4 experiments, to diminish cutaneous input from the skin, the hindlimb musculature was left intact, but the skin and superficial fat was separated from the musculature using blunt dissection, with all cutaneous nerve branches severed. This was done from the thigh up to the pad of the paw. A laminectomy from L_2 to S_1 was performed to expose the spinal cord. A pre-collicular decerebration was then performed, and the preparation was then paralyzed with Flaxedil.

Intracellular recordings

Sharp electrode intracellular recordings were obtained from motoneurons in the lumbar region of the spinal cord (total $n = 60$). Microelectrode tips were broken back under microscope observation and control and had resistances between 3 to 5 MΩ in saline before entering the cord. Electrodes were filled with 2M potassium citrate. Voltage clamp was applied using the single electrode discontinuous mode (Axoclamp 2a amplifier, Axon Instruments; switching frequency of 8–10 kHz; data with inadequate settling of the electrode were rejected). Low frequency gain of the feedback loop (–3 dB of 30 Hz) was enhanced 11 fold by an external circuit, resulting in gains that ranged from 100 to 300 nA per mV (Heckman and Lee 2001). This high gain provided excellent voltage control, with deviations less than 0.5 mV in voltage ramps within each cell despite the large differences in PIC amplitude due to changes in joint angle.

Robotic control of joint rotations

Software provided by Staubli AG allows the endpoint of the robotic arm to produce rotations about any nearby axis. In all cases, this axis was aligned to precisely match to the center of rotation of a hindlimb joint. To accomplish this, centers of joint rotation for the ankle, knee and hip for sagittal plane movements were measured with respect to the robot endpoint and this information put into the control software. Rotations were then tested to confirm that these movements were free and smooth. No constraints were placed on the leg whatsoever except for the attachment of the foot to the robotic arm and fixing of the pelvis. Thus, hip, knee and ankle joints were free to rotate, subject only to the constraints of the passive musculoskeletal system. We found that small errors in specifying the center of joint rotation, which likely produced aberrant compression or twisting forces, were readily manifest by the induction of clear compensatory movements at the other two joints, i.e., errors in specifying ankle joint rotation produced significant rotations at the hip and knee. With the correct specification, movement at the desired joint was virtually friction free, so that even the largest movements at the ankle were not accompanied by significant hip and knee rotations. Hip and knee rotations were similarly adjusted to be specific.

Experimental protocols and data analysis

Starting with the ankle at 88 degrees (Mid 1), the computer controlled robotic arm rotated the ankle into either 10 or 30 degrees of extension or flexion. This position was then held during the

following intracellular voltage clamp protocols (see the Supplemental material online for details of robotic control and efforts taken to assure smooth joint rotations). Motoneurons were identified by antidromic stimulation of triceps surae, or hamstring mixed nerves. Spike height and overshoot were assessed in current clamp mode and cells with spike heights less than 60 mV were rejected. We then switched to voltage clamp mode. A slow voltage ramp was applied (6–9 mV s^{-1} for a total of 30–45 mV) with the ankle in the starting Mid 1 position. The PIC is manifest as a strong downwards deflection in the resulting I-V relation (see Fig. 2, dashed arrows). This voltage ramp was repeated three more times with the ankle rotated into in extension and then flexion (Fig. 2). The ankle was then returned to the midpoint (Mid 2). All ankle rotations were performed during the descending, hyperpolarizing phase of the voltage command. The ankle remained in its new position for at least one second prior to the onset of the next voltage ramp (Fig. 2). Current-voltage (I-V) relationships were constructed for each voltage ramp. Input conductance was calculated as the slope of a regression line fit to this I-V function within a 5–10 mV range, 10–15 mV sub-threshold to the onset of the negative slope region of the PIC. This regression line was extended throughout the voltage range and used for leak subtraction to calculate the peak amplitude of the PIC in each I-V function. Cells in which peak PIC amplitude calculated from the Mid 2 decreased more than 30% as compared to that from the Mid 1 trial were rejected. Baseline currents were obtained by averaging the measured current 0.5 s period just before the onset of each depolarizing phase of the voltage command. Statistics relied mainly on paired t-tests to evaluate differences at different positions within each cell. When multiple tests were performed, the Bonferroni correction was applied to the p value of 0.05 (i.e., 0.05 divided by the total number of tests to prevent Type I errors). Where the sample size was five or less, the Mann-Whitney U-test was used.

Chapter 3

The Active Integration of Movement Related Synaptic Inputs by Spinal Motoneurons

Introduction

In vivo, neuronal output depends on the integration of the cell's electrical processes as well as synaptic inputs. Spinal motoneurons are an excellent cell type for studying this process as they have voltage dependent conductances, and they receive synaptic inputs from higher centers in the brainstem and cortex, interneurons, as well as multimodal sensory afferents (Jankowska 1992; Binder 1996; Rekling, Funk et al. 2000). In addition to the many synaptic inputs, an important source of motoneuronal excitability is the voltage dependent persistent inward current (PIC) that in mammals is carried by sodium and calcium currents (Hounsgaard and Kiehn 1989; Lee and Heckman 1999; Carlin, Jones et al. 2000; Li and Bennett 2003; Perrier, Alaburda et al. 2003). Functionally relevant, PICs amplify excitatory synaptic current as much as 5 fold (Lee and Heckman 2000). Monoaminergic drive, primarily originating from the brainstem, permits the activation of these channels in motoneurons and the level of monoaminergic drive sets the PIC amplitude (Lee and Heckman 2000). In this way, changes in brainstem drive could affect the intrinsic electrical properties of motoneurons and the net excitatory effect of synaptic inputs. At this time, it is not well understood how active dendrites as well as supraspinal inputs affect the integration of movement related synaptic input to create a cell's movement related receptive field (MRRF).

As a function of synaptic input, a motoneuron's MRRF could be either relatively focused or include whole limb information depending on the sensory pathway. If dominated by the group Ia muscle afferent system, motoneurons would largely receive information

regarding changes in muscle length and velocity, primarily from homonymous and synergist muscles or antagonists via inhibitory interneurons (Eccles, Eccles et al. 1957; Eccles and Lundberg 1958; Matthews 1972; Edgley, Jankowska et al. 1986). In this way, the motoneuron receives information restricted to muscles around a single joint, decoupling it from the rest of the limb. In contrast, other muscle afferents (Ib, II, III, and IV) as well as the cutaneous and joint pathways tend to utilize polysynaptic pathways with wider patterns of convergence on to motoneurons spanning multiple spinal segments and promote coordinated whole limb responses (Matthews 1972; Jankowska 1992).

From a motor control standpoint, it would be inefficient for a given motoneuron's excitability to be driven by all of its inputs all of the time. Evidence for flexible MRRF patterns can be found in experiments which altered the electrical state of the cord via interruption of brainstem and other supraspinal inputs to the cord (Eccles and Lundberg 1959; Holmqvist and Lundberg 1961). Pharmacologically, this could also be achieved as the monoamines are known to enhance Ia pathways and inhibit polysynaptic inputs (Jankowska, Riddell et al. 1993; Miller, Paul et al. 1995; Miller, Paul et al. 1996; Jankowska, Hammar et al. 2000; Chen, Theiss et al. 2001; Hammar and Jankowska 2003). Supraspinal input could simplify a motoneuron's output profile by shaping its MRRF. In this study, we are the first to examine the intracellular response of spinal motoneurons to whole limb movements in the sagittal plane as a function of intrinsic excitability and supraspinal control. We hypothesized that PICs would enhance all movement related I_N. Furthermore, we predicted that in the standard monoaminergic

state, the motoneuron's MRRF would be focused, following patterns of Ia connectivity and in the spinalized state the MRRF would be comparatively wider.

Results

PICs Enhance Multi-joint Movement Related Synaptic Input to Spinal Motoneurons

Data for this study were collected from spinal motoneurons innervating muscles generating either ankle extension (medial and lateral gastrocnemius and soleus, note: these muscles also have a flexion moment at the knee), knee extension (vastus medialus and rectus femoris) or hip flexion (rectus femoris). To examine each cell's movement related receptive field (MRRF) in the sagittal plane, a six degree of freedom computer controlled robotic (Staubli, A.G. Robotics) arm flexed and extended the ankle, knee, and hip joint separately and then simultaneously for a whole limb movement (Figure1 and also see Methods). In this way, we were able to stretch and shorten agonist and antagonists muscle pairs which excite (stretch of agonist) and inhibit (stretch of antagonist) motoneurons via the stretch reflex and reciprocal inhibition. For example, ankle flexion would excite ankle extensor motoneurons and ankle extension would inhibit them.

Previously, we have shown that reciprocal inhibition generated by moderate changes in joint position modulates PIC amplitude by ~50% (Hyngstrom, Johnson et al. 2007). In

this study, we rotated joints throughout the hindlimb to examine the convergence of polysynaptic multimodal pathways (e.g. group II and cutaneous afferents) on to motoneurons during joint movements. Cells were voltage clamped and movement related changes in the net synaptic current generated at the soma (i.e. the effective synaptic current or I_N :(Heckman and Binder 1988) was measured as the robot manipulated the hindlimb. In the preparation used here (decerebrate cat), there is tonic monoaminergic drive from the brainstem resulting in relatively constant levels of monoamines to the spinal cord throughout the experiment (Baldissera, Hultborn et al. 1981).

In the first set of experiments, except for the application of small nerve cuffs applied for antidromic identification of motoneurons (see Methods), the hindlimb was left intact, leaving movement related sensory input as undisturbed as possible. To determine the effects of the PIC on the MRRF, we first assessed the voltage onset of the PIC by applying a slow linear voltage ramp (30-40 mVs/5 s). The PIC manifests as a downward deflection in the current trace with a negative slope region (see Figure 2). Since we have previously shown that this intracellular recording method is extremely effective at voltage clamping the soma, (Lee and Heckman 2000; Kuo, Lee et al. 2003; Lee, Kuo et al. 2003; Hyngstrom, Johnson et al. 2007), any amplification of the MRRF by the PIC occurs in the dendritic regions of the cell (outside of the clamp). The PIC voltage onset was estimated to coincide with the onset of the negative slope region apparent in the current trace (Fig. 2, arrow). Holding the cell 5-10 mVs hyperpolarized to the resting membrane potential, we then applied a depolarizing voltage step

corresponding to the approximate voltage onset of the PIC. From a mid-point position, the robot then flexed (Fl) and extended (Ext) the ankle (+/- 15°'s), knee (+/- 15°'s), and hip (+/- 10°'s), (see Figure 3; note 2 repetitions per movement and also see Methods). For the whole limb movement, each joint was rotated the same amount as in the single joint movements and moved from the starting position to ankle extension, knee flexion and hip extension and then to ankle flexion, knee extension, and hip flexion. The joint excursion during the whole limb movement is within the range seen during functional activities such as ambulation and crouching, and is not large enough to significantly activate group III and IV afferents (Goslow, Stauffer et al. 1973). We then repeated the same movements while holding the cell at a hyperpolarized voltage (equal to the voltage level before application of the step) to prevent PIC activation by the input (Heckman and Lee 2001).

Figure 3 shows the modulation of I_N by hindlimb movement for an ankle extensor motoneuron (MG) in the depolarized (top panel, dark trace) and hyperpolarized (top panel, thin trace) voltage conditions as a series of peaks and troughs. In the depolarized condition, return of the current to baseline levels was often slow and could be a slow decay of a PIC tail current. Differences between the peak and trough amplitudes (ΔPT) for each voltage command condition were then calculated (Fig. 3). Note that ΔPT is larger for each movement in the depolarized condition, where PICs are present, as compared to the hyperpolarized condition. Note, however, that the pattern of the movement related I_N modulation is the same for both voltage conditions. For this

cell, ΔPT was largest during the whole leg movement and ankle ΔPT was greater than knee and hip.

The ΔPT due to ankle, knee and hip movement was calculated for 15 ankle extensor motoneurons in both the depolarized (Fig. 4, Fig. 5a) and hyperpolarized voltage conditions (Figure 4, not shown in Fig. 5). For 12 of these cells, whole limb movement data was collected as well (Fig. 5a, solid lines). For this sample of cells, mean PIC amplitude was 15.5 nA ± 9.2. As predicted, mean ΔPT amplitudes were significantly larger (paired student's t-test, $p \leq 0.0005$) in the depolarized condition as compared to the hyperpolarized condition for each respective movement (mean ΔPT depolarized ± STD, hyperpolarized ± STD, Ankle: 6.9 nA ± 2.9, 3.7 nA ± 1.8; Knee 3.9 nA ± 2.4, 2. 0 nA ± 1.85, Hip 2.6 nA ± 1.5, 0.9 ± 0.9; WL 8.7 nA ± 3.5, 3.5 nA ± 1.9, see Figure 4). Thus, dendritic PICs can enhance the I_N from movement related input from the whole limb. This could be explained by the generally global distribution of synaptic inputs to motoneurons (Fyffe 2001) and recent computational work showing the highest density of Ca^{++} channels to occur midway out on the dendrites (Elbasiouny, Bennett et al. 2005; Grande, Bui et al. 2007).

PICs Enhance Both Excitatory and Inhibitory Movement Related I_N

PICs amplify excitatory synaptic current and when PIC conductances are reduced by inhibition, the resulting inhibitory I_N is also enhanced due to the PIC suppression (Kuo, Lee et al. 2003). With respect to our study, this would mean that the total ΔPT would be

larger in the depolarized condition due to an increase in both excitation and inhibition. To evaluate this prediction, we compared the relative contribution of inhibition versus excitation to the total ΔPT amplitude for both the depolarized (PICs present) and hyperpolarized (diminished PICs) voltage conditions in the MG/LGS sample. The inhibitory contribution to the ΔPT (IΔPT) for each voltage condition was determined by averaging the peak amplitudes for each movement and subtracting the average steady state I_N (I_N averaged over 0.2 s where no movement was occurring). In the next section, we consider whether IΔPT is inhibition or disfacilitation. Likewise, the excitatory contribution to the ΔPT (EΔPT) was calculated by averaging the trough amplitudes for each movements and subtracting the same steady state I_N used in the IΔPT calculation. On average, both the IΔPT and EΔPT for each respective joint movement were significantly larger in the depolarized condition as compared to the hyperpolarized condition (see Table 2 for IΔPT and EΔPT values, paired t-test between voltage conditions for each movement, $p \leq 0.04$). The only exception was for the knee EΔPT comparison (paired t-test, $p = 0.13$). These data indicate that both excitation and inhibition are important in the voltage dependent enhancement of the movement related current modulation and predict a decrease in movement related current modulation with the removal of inhibition.

Reciprocal Inhibition Shapes the Movement Related I_N Modulation

It is possible that the I∆PT could be a result of either an increase in inhibition or a relative decrease in excitation (disfacilitation). To examine this we recorded intracellularly from 9 ankle extensor cells using the same movement and voltage clamp protocols and diminished Ia inhibition by cutting the distal tendon insertion of tibialis anterior and extensor digitorum longus (TA/EDL). Since Ia inhibition is important in modulating PIC amplitude in static conditions (Hyngstrom, Johnson et al. 2007), we expected to find a reduction in the I∆PT as compared to the tendon intact sample, especially in the depolarized voltage clamp conditions where the PIC likely to be active.

The lower panel in Fig. 6 shows a comparison of the movement related I_N for two cells: one with reciprocal inhibition present (tendon intact, black trace) and one without (tendon cut, gray trace). With Ia inhibition present, the current modulation closely follows the triangular robot trajectory. In comparison, with the tendon cut, the current trace exhibits a smaller ∆PT amplitude with limited I∆PT and a square shape. This pattern of current modulation more closely matches what would be predicted by just the Ia afferent response to the stretch. The mean I∆PT during ankle extension/flexion was calculated for both the depolarized (0.59 nA $\pm$ 0.5) and hyperpolarized voltage conditions (0.23 $\pm$ 0.28). Although both values were on average smaller than measured in the tendon intact sample, only the depolarized I∆PT for the tendon cut sample was significantly smaller (for tendon intact values see Table 2, ANOVA,

Bonferroni Post Hoc, $p < 0.03$). In order to examine the relative IΔPT contribution to the total ΔPT, the IΔPT was normalized to the total ΔPT. For the depolarized condition, the IΔPT contribution was significantly smaller (mean = 0.2 ± 0.1) in the tendon cut sample as compared to the tendon intact sample (mean = 0.34 ± 0.1, ANOVA, Bonferroni Post Hoc, $p \leq 0.01$). This evidence suggests that inhibition is an active process that is enhanced by the presence of the PIC and promotes the shaping of the cells MRRF.

Ia Connectivity Dominates the MRRF Pattern of Ankle Extensor Motoneurons in the Intact Cord

Within each voltage condition, we used the ΔPT for each movement to determine each cell's MRRF. All MG/LGS cells in this sample were excited by ankle flexion, knee extension and hip flexion and inhibited by ankle extension, knee flexion, and hip extension (see Fig. 3 for cell example). On average, WL ΔPT was the largest followed by ankle, knee, and hip ΔPT respectively (see Fig.4 and paragraph above for means, Fig. 5a for ΔPT amplitudes for each cell). For both voltage conditions, ankle ΔPT was significantly larger than knee and hip ΔPT's (ANOVA, Bonferroni Post Hoc, $p \leq 0.003$). Although knee ΔPT was on average larger than hip ΔPT, it did not reach statistical significance (ANOVA, Bonferroni Post Hoc, $p > 0.05$). In the depolarized condition, knee ΔPT was 56% of ankle ΔPT and 54% of the ankle ΔPT in the hyperpolarized condition. Hip ΔPT was an even smaller proportion of the ankle ΔPT for the depolarized and

hyperpolarized voltage conditions (37% and 24% respectively). Since the gastrocnemius muscle complex crosses the knee joint, it was not surprising that knee FL/Ext created larger ΔPT's as compared to the hip. Although significantly different than zero (t-test, $p \leq 0.0001$) the small total I_N modulation seen during hip movement is likely from group II or cutaneous afferents, which are known in both the cat and humans to project across multiple spinal segments and can contribute to the coordination of whole limb movements (Lundberg, Malmgren et al. 1987; Jankowska 1992). I_N modulations from ankle and knee movements can readily be explained by previous studies of Ia connectivity using individual muscle stretch and electrical stimulation of muscle nerves studies (Eccles, Eccles et al. 1957; Eccles and Lundberg 1958; Nichols 1999).

A Focused MRRF is not Limited to Ankle Extensor Motoneurons

In a separate set of experiments, the MRRF was evaluated in 7 vastus medialus (VM) and 5 rectus femoris (RF) motoneurons. Although both types of motoneurons innervate muscles which extend the knee, RF is bi-articular and also flexes the hip. VM is a uni-articular knee extensor. As with the ankle extensors, the ΔPT's from ankle, knee, hip and WL movements was evaluated for each cell (Fig. 5b, c). The MRRF for both samples closely followed what would be predicted from known Ia connectivity (Eccles and Lundberg 1958).

For VM cells, the ΔPT was largest during knee and WL movements followed by hip and ankle movements (Fig. 5b). The mean ΔPT for knee flexion (depolarized condition: 5.1 nA ± 1.3, hyperpolarized 2.6 nA ± 0.8) was significantly larger (paired t-test, p = 0.00006) than average ΔPT's for ankle (mean depolarized 0.1 nA ± .37; hyperpolarized 0.0 nA ± 0.15) and hip movements (mean depolarized 0.8 nA ± 0.02, hyperpolarized 0.3 nA ± 0.02).

The average PIC amplitude for the VM sample was 8 nA ± 6.7. As with the ankle extensor motoneurons, the ΔPT's were significantly greater from the depolarized condition as compared to the hyperpolarized condition for the knee, hip, and whole limb movements (paired student's t-test, $p \leq 0.03$). For the ankle movements, the average ΔPT's for the depolarized and hyperpolarized conditions were not significantly different than zero (student's t-test, p = 0.35). This MRRF agrees with Eccles 1957 paper which details Ia connectivity for ankle and knee motoneurons, where the vasto-crureus complex (VC) was shown to monosynaptically excite LGS, but with no reciprocal excitation of LGS onto VC.

Since RF has effects at both the knee and the hip, it was predicted that the ΔPT's would be largest for knee and hip movements with minimal ΔPT's from the ankle movements. The average PIC amplitude from this sample was low (2.6 nA ± 4.1). Consequently, mean ΔPT's for all movements were not significantly different between voltage conditions (paired t-test, $p \geq 0.06$). Since cell inclusion criteria were met (see Methods)

and data from the VM and MG/LGS samples showed that the presence of the PIC does not alter the overall MRRF pattern, ΔPT's for the both voltage conditions were averaged together. Even from a small sample size, the MRRF pattern was evident (Fig. 5c). The mean ΔPT for knee (4.3 nA ± 2.6) and hip movements (4.1 nA ± 2.6) were not significantly different (ANOVA, Bonferroni Post Hoc, p = 0.6), but were both larger (ANOVA, Bonferroni Post Hoc, p = 0.0006) than the mean ankle ΔPT (1.2 nA ± 1.7).

Biomechanics of Pre-tibial Flexors and Triceps Surae Muscles Contribute to the MRRF of Ankle Extensor Motoneurons

If Ia excitation and reciprocal inhibition dominate MRRFs then the differences in ΔPT seen during movement at different joints (Fig. 5) should be consistent with the relative changes in agonist and antagonist muscle lengths induced by the joint rotations. Using a muscle length model developed by Nichols and colleagues , we compared normalized ΔPT of ankle extensor motoneurons during knee flexion/extension to normalized changes in muscle lengths of MG and LG (ΔPT for knee FL/Ext normalization = ΔPT knee / ΔPT ankle and MG and LG Δmuscle length normalization = Δmuscle length knee / Δmuscle length ankle (Burkholder and Nichols 2004). During knee Fl/Ext, the normalized MG length was 0.77 and LGS was 0.67. The normalized ΔPTs of MG/LGS for knee Fl/Ext for both the depolarized and hyperpolarized voltage conditions were smaller: 0.56 and 0.53 respectively. This suggests muscle length and its effect on Ia excitation of MG and LGS is not sufficient to account for the MRRF of MG/LGS

motoneurons. The explanation may, however, lie with Ia reciprocal inhibition from antagonists. MG/LGS motoneurons primarily receive Ia inhibition from TA and EDL (Nichols, Cope et al. 1999). TA does not cross the knee, and although EDL does have an insertion on the femur in the cat, the model did not predict significant changes in muscle length for EDL during knee movements. Thus, knee rotation markedly changed the lengths of MG and LGS but not their antagonists TA and EDL. In other words, ankle rotation combined Ia excitation and reciprocal inhibition; knee rotation lacked significant modulation from reciprocal inhibition. These results are consistent with effects primarily from muscle spindle Ia afferents and their monosynaptic and disynaptic connections to ankle extensors.

Unlike MG and LG, the bi-articular motoneurons of RF received approximately equal currents from both knee and hip rotations (compare 5a and 5c). RF primarily extends the knee, but also flexes the hip. Rotations around the knee produced larger changes in muscle length than rotations at the hip. The change in muscle length during hip rotations was 0.82 when normalized to change in muscle length during knee Fl/Ext. The hip ΔPT normalized to knee ΔPT was slightly higher (0.94). Qualitatively, expectations based on muscle length and Ia excitation and inhibition would predict equal effects for knee and hip on RF motoneurons. Unlike the antagonists to MG and LG at the ankle, antagonists to RF (the hamstrings) cross the same joints that RF does, i.e. the knee and hip. Perhaps the slightly larger relative effect for synaptic current relative to change in length of RF for the hip compared to the knee is due to Ia excitation from synergists. RF, in addition to its own homonymous Ia input, receives Ia excitation from both

monoarticular knee extensors (the vasti) and from hip flexors (e.g. iliospoas) (Eccles and Lundberg 1958).

For VM, a MRRF dominated by knee movement is also consistent with muscle length changes activating primarily Ia afferents in agonists and antagonists. The slight modulation from the hip may reflect Ia reciprocal inhibition from the antagonist knee flexors, which also cross the hip joint. Thus, when the spinal cord is intact, the MRRFs of MG, LGS, VM and VL are reasonably consistent with the known patterns of Ia excitation and reciprocal inhibition.

Movement Related Current Modulations of this Magnitude are Large Enough to Shape Motor Output

It has previously been determined that in the decerebrate preparation the current frequency gain of function is 2 spike/nA/s (Lee et al, 2003). Certainly in the depolarized condition, where ankle ΔPT's were ~7 nA and whole limb ΔPT were ~ 9 nA a functionally significant change in firing would be predicted (25-30% of a motoneuron's firing range). Although smaller in amplitude, the ankle motoneuron ΔPT's for the hip and knee in the depolarized condition (representing ~ 5-10% of the cells firing range), could contribute to the cells total rate modulation when combined with ankle movement. Even though the PIC did not alter the general pattern of I_N modulation seen between the two voltage conditions, it is possible at least for the ankle and whole limb movements that the additional current provided by the PIC could have significant effects on firing

rate. This evidence suggests that the PIC could simplify motor control at the spinal level, not by altering the underlying synaptic message to motoneurons from peripheral or descending inputs, but instead regulating the output of the cell by enhancing the cell's probability of repetitively firing in response to functionally relevant inputs (see Discussion).

Spinalization Eliminates Voltage Dependent Enhancement of Movement Related I_N

Acute spinalization, following decerebration, interrupts descending brainstem inputs to the cord. Along with other effects on the cord, tonic monoaminergic drive is eliminated and the PIC generating capacity of motoneurons is dramatically reduced (Conway, Hultborn et al. 1988; Hounsgaard, Hultborn et al. 1988). To examine the effects of diminished PICs, movement related I_N modulation was evaluated in MG/LGS (n= 15), VM (n= 9), and RF (n = 5) motoneurons following acute spinalization and decerebration. These experiments were separate from the intact cord experiments.

As in the intact cord experiments, the cell was held 5-10 mV hyperpolarized to the resting membrane potential and a slow voltage ramp was applied to assess the voltage onset of any apparent PIC. On average, the PIC amplitude was very small (3.5 nA $\pm$ 3.5). In most cases, no negative slope region was apparent and the voltage was stepped 10-15 mV depolarized from the resting membrane potential. Depolarizing step sizes of this magnitude approximates the average onset of the PIC (Heckman 2003). The ΔPT's were then calculated for each movement in both voltage conditions (Table

1). With limited PICs present, the ΔPT's were not significantly different between voltage conditions (paired t-test, $p \geq 0.06$, Fig. 5) for each motoneuron sample. Consequently, ΔPT's were averaged together to quantify the MRRF for each motoneuron pool sample (see next section). This suggests that the modulation of a motoneuron's movement related I_N following acute spinalization is not voltage dependent.

Spinalization Has Mixed Effects on Movement Related Receptive Fields

With the cord intact and tonic monoaminergic drive, data from this study show that the MRRF of ankle extensor, knee extensor and hip flexor motoneurons reflects the relatively focused Ia patterns of connectivity. The movement related synaptic input of agonist/antagonist pairs clearly dominates the cells MRRF. However, electrical connectivity studies have demonstrated polysynaptic pathways that cross multiple spinal segments from both muscle and cutaneous afferents and contribute to whole limb coordination (Eccles and Lundberg 1959; Lundberg, Malmgren et al. 1987). Human and animal studies show that often following cord injury, local muscle stretch or cutaneous stimulation will result in a whole limb reflex response suggesting alterations in motoneuronal receptive field (Roby-Brami and Bussel 1987; Schmit, McKenna-Cole et al. 2000; Schmit and Benz 2002; Bennett, Sanelli et al. 2004).

As with the cord intact sample, each cell's MRRF was assessed from ΔPT amplitudes for each movement. Figure 7 shows the averaged ΔPT amplitudes for all cells for each

motoneuron sample in the spinalized condition. For the MG/LGS cells in the intact cord experiments, ankle ΔPT amplitudes were significantly larger than knee and hip ΔPT. However, following acute spinalization, the mean hip ΔPT (5.0 nA ± 2.6) was larger than the mean ankle ΔPT (3.7 nA ± 2.5), but the difference did not reach statistical significance (ANOVA, Bonferroni Post Hoc, $p = 0.06$). Both ankle and hip ΔPTs were significantly larger than knee ΔPT (ANOVA, Bonferroni Post Hoc, $p = 0.04$ and 0.003 respectively). The lower panel in Fig. 7 shows the large movement related I_N modulation of an MG/LGS motoneuron to hip movements. Overall, the spinalized hip ΔPT was found to be significantly greater than the intact cord hip ΔPT measured in the hyperpolarized voltage condition (ANOVA, Bonferroni Post Hoc, $p = 0.0001$), but less than the hip ΔPT from the depolarized voltage condition (ANOVA, Bonferroni Post Hoc $p = 0.02$). It appears that following spinalization, ankle motoneurons broaden their receptive field through an increase in hip ΔPT.

With a diminishment of PIC amplitude following spinalization, it might be expected that the movement related IΔPTs and EΔPTs I_N would be similar to the intact cord, hyperpolarized condition. However, important differences between the composition of the intact and spinalized IΔPTs and EΔPTs were found that help to describe the spinalized MRRF. Just as in the intact condition, the IΔPTs and EΔPTs amplitudes were evaluated for each movement for both voltage conditions. Since the IΔPTs and EΔPTs amplitudes were not significantly different between voltage conditions for all movements (paired t-test, $p > 0.05$), the hyperpolarized and depolarized amplitudes

were averaged together (means IΔPTs, EΔPTs ± STD: Ankle 1.8 nA ± 2.1 , 2.3 nA ± 1.8 ;knee 1.2 nA ± 1.7 ,1.7 nA ± 2.1;Hip 2.2 nA ± 2.5 , 3.8 nA ± 2.6). Although spinalized ankle IΔPT was not significantly different than the intact state (t-test, $p \geq 0.23$), the spinalized EΔPT was less than the intact depolarized EΔPT (t-test, $p = 0.001$). Knee IΔPTs and EΔPTs were not significantly different between cord conditions.

The greatest differences between the spinalized and intact conditions were found in the analysis of the hip IΔPTs and EΔPTs. Here the spinalized IΔPT was greater as compared to the intact hyperpolarized IΔPT (t-test, $p = 0.015$) and the EΔPT was larger compared to the intact depolarized and hyperpolarized EΔPTs (t-test, $p \leq 0.002$). These results suggest that the increase in movement related hip I_N in the spinalized condition is due to an increase in both IΔPT and EΔPT, with a greater overall contribution from EΔPT. Since the increased EΔPT is not likely due to PICs or from excitatory brainstem drive, the additional EΔPT may be due to a decrease in tonic inhibition of excitatory polysynaptic pathways from the hip onto ankle MNs.

To examine if the widening of receptive fields is limited to ankle extensor motoneurons, the movement protocol was also repeated in VM and RF cells following acute spinalization. Similar to the adaptations in MG/LGS MRRF following spinalization, VM cells also showed an increase in hip ΔPT (Fig. 6b, Fig. 7 middle panel) as compared to intact condition (T-test, $p < 0.002$). Mean knee ΔPT was larger than hip ΔPT (3.2 nA ± 1 and 2.5 nA ± 1.5 respectively), but this did not reach statistical significance (ANOVA,

Bonferroni Post Hoc, $p = 0.13$). Both the knee and hip ΔPTs were larger than the ankle ΔPT (ANOVA, Bonferroni Post Hoc, $p \leq 0.001$).

In contrast to the MG/LGS cells, the RF cells did not show any changes to their overall MRRF (Fig. 6c, Fig. 7 top panel). The average ankle ΔPT was smaller than knee and hip ΔPT (ANOVA, Bonferroni Post Hoc, $p \leq 0.006$) and while average knee and hip ΔPTs were not different (ANOVA, Bonferroni Post Hoc, $p = 0.76$). Furthermore, intact and spinalized average ΔPT's for all movements were not significantly different from each other (ANOVA, Bonferroni Post Hoc, $p \geq 0.37$). The widening of a motoneurons receptive field could be a result of an increased intrinsic excitability (post-synaptically more sensitive to inputs) or an increase in the total synaptic input to the cell. Since in all three motoneuron cell samples the average PIC amplitudes were small and the movement input was the same, it is possible that following spinalization there is a relative increase in interneuronal input to motoneurons (i.e. interneuronal receptive fields widen or interneurons are disinhibited). Possible mechanisms for adaptations in MRRF seen in the MG/LGS and VM motoneurons and not for RF are considered in the discussion.

Cutaneous Afferents Have a Limited Contribution to the MRRF Following Acute Spinalization

Both muscle and cutaneous afferents which utilize polysynaptic pathways could be responsible for the significant changes in hip ΔPT in the VM and MG/LGS cells seen

after acute spinalization (Eccles and Lundberg 1959). However, it was shown previously that in the decerebrate, intact cord preparation the PIC amplitude of ankle extensors varied with static joint position and cutaneous denervation did not alter the modulation pattern (Hyngstrom et al, 2007). In the present study, however, it is possible that cutaneous input might have a larger effect on motoneuronal I_N due to changes in the levels of excitability in interneuronal circuitry secondary to both spinalization as well as the comparatively more dynamic movement protocol. If this hypothesis is true, then diminishing cutaneous input might result in MRRFs that resemble the cord intact condition, i.e. focused.

To examine this hypothesis, the same movement protocols were repeated in 5 MG/LGS cells and 5 VM cells with the cord spinalized and the lower limb denervated (skin separated from the muscle, see Methods). It was found that the overall MRRF pattern was not different than the spinalized, cutaneous intact condition. Like in the spinalized cutaneous intact condition, MG/LGS cells ankle and hip flexion ΔPT were greater than knee ΔPT (ANOVA, Bonferroni Post Hoc, $p \leq 0.01$), but not from each other (ANOVA, Bonferroni Post Hoc, $p = 0.52$). VM cells also maintained the spinalized cutaneous intact MRRF pattern with knee and hip ΔPT being significantly greater than ankle ΔPT (ANOVA, Bonferroni Post Hoc, $p \leq 0.01$), but not from each other (ANOVA, Bonferroni Post Hoc, $p = 0.44$). This indicates that the change in the MRRF for VM and MG/LGS cells is related to muscle afferents with polysynaptic connections within the cord such as the group II's. This is supported by an early study by Eccles and Lundberg which

showed that polysynaptic pathways were enhanced following spinalization but group Ia pathways were relatively unaffected (1959).

Discussion

Our results demonstrate how active dendrites and varying levels of supraspinal drive can shape the integration of synaptic inputs by spinal motoneurons. Moreover, since the voltage was effectively clamped at the soma, the cell's MRRF was predominately determined by events in the dendrites. The primary role of the PIC was to enhance all movement related synaptic input, as much as three fold. This enhancement occurred due to an increase in both excitatory and inhibitory components of the movement related I_N. Interestingly, the PIC does not seem to have a role in shaping the overall pattern of the MRRF as both hyperpolarized and depolarized patterns matched for all cells (i.e. there were no cases where a modulation existed in one voltage condition and not the other). Instead, our data suggests that the PIC does not change the overall synaptic message to the motoneuron, which would complicate motor commands, but regulates the gain of firing as a function of the state of the cord. In this way, cells with active dendrites increase their register of firing gains in a voltage dependent manner.

Our results indicate that in the presence of tonic monoaminergic drive to the cord, motoneurons have MRRFs that are relatively focused and can be explained largely by patterns of Ia connectivity. In this way, motoneurons listen primarily to agonist and antagonist muscle afferents, and less to inputs from distal joints. Presumably, this is due

to the facilitation of the Ia inhibitory system by the monoamines (Jankowska 1992). When descending drive was removed, the MRRF for ankle extensors and uni-articular knee extensors included increased synaptic input from hip movements that equaled the movement related I_N that could be explained by Ia inputs. Others have shown the facilitation of group II pathways and changes in FRA pathway excitability following spinalization (Eccles and Lundberg 1959; Matthews 1972) and attribute it to a release of extensor excitability. By interrupting monoaminergic transmission, which is known to suppress high threshold input, synaptic information from convergent sources may be released. Although acute spinalization is known to depress motoneuron excitability, it is not known to suppress interneuronal or direct afferent input. It is therefore likely that following spinalization the motoneuron is receiving both focused inputs from Ia pathways and more convergent synaptic information from the whole limb. Motoneurons with wider MRRFs would thus be more likely to participate in a whole limb response.

It is probable that monoaminergic centers are not totally responsible for determining the MRRF. For instance, activity in the monoaminergic centers in the brainstem are known to increase during repetitive movements such as locomotion (Jacobs and Fornal 1993). During locomotion it is likely that the motoneuron would also require whole limb information to coordinate limb movement. Sources of convergent input originating higher than the brainstem may provide this information and therefore contribute to the MRRF by adding another layer of control parallel to the focused pathways. In this way MRRF could match the demands of the motor task. The contribution of other descending inputs and task dependency on a motoneuron's MRRF needs further study.

Reciprocal Inhibition Shapes the Movement Related I_N Modulation

To perform a new movement, continue with a current one, or correct a movement error, it is critical that a motoneuron receives a movement signal that reflects the ongoing state of the limb. Here we show, during passive movements, the MRRFs of motoneurons are largely shaped by muscle receptor activity. In the decerebrate, cord intact state we showed that group Ia connectivity dominated the overall pattern of the MRRF and PICs enhanced both excitatory and inhibitory input. Diminishment of reciprocal inhibition, by cutting of the antagonist tendon, revealed that inhibition not only increased the relative amplitude of the total ΔPT but also contributed to the shaping of the movement related I_N by acting possibly through "push, pull" mechanisms (Berg, Alaburda et al. 2007). With the hindlimb relatively intact, ankle flexion resulted in maximal excitation via an increase in Ia afferent firing coupled with a decrease in Ia inhibitory drive. Conversely, ankle extension resulted in a decrease in Ia afferent input and an increase in reciprocal inhibition. This results in a movement signal that closely followed the triangular limb trajectory. Future studies will be necessary to see how well inhibition can shape other movement trajectory patterns such as locomotion.

Widening of Movement Related Receptive Fields Following Spinalization

In MG/LGS and VM cells, we were able to show a widening of MRRFs following acute spinalization. Specifically, both cell groups saw an increase in ΔPT from hip

flexion/extension that was not primarily due to cutaneous afferents. In the case of MG/LGS, there was a relative increase in the excitatory I_N caused by hip flexion. It is not likely to originate from group Ia connections as monosynaptic connections between the hip extensors and ankle extensors were not documented by either connectivity studies done by Eccles and colleagues (1958, 1959) and Nichols (1999), but these experiments were done under anesthesia which could have suppressed pathways. It is more likely to originate from group II or FRA pathways which have whole limb connectivity through polysynaptic pathways and have been shown to excite extensors, especially following spinalization (Eccles and Lundberg 1959; Matthews 1972).

Interestingly, spinalization did not result in a change in the RF sample's MRRF. This may in part be related to differences in muscle function or distal/proximal locations. Although RF, VM, and MG/LGS samples share the function of being extensors, RF differs in that it also flexes the hip. Because of its dual extensor/flexor functions, in the decerebrate cord intact state RF already receives a relatively broad range of heteronymous Ia inputs from other knee extensors and hip flexors (Eccles and Lundberg 1958). Although we did not examine movements out of the sagittal plane, it is possible that following spinalization RF may have an increased sensitivity to limb abduction or adduction or rotations at the hip. Work examining pathways associated with locomotion has shown the importance of stretch of hip musculature (Kriellaars, Brownstone et al. 1994; Hiebert, Whelan et al. 1996) and may indicate a general flow of information from proximal to distal motoneurons. Our results support this by revealing hip onto knee and ankle pathways. Although these pathways were strongly evident

following spinalization, they could be utilized in the intact cord state by either a decrease in monoaminergic drive or a facilitation of these convergent pathways via cortical commands.

Implications for Pathology Seen after Spinal Cord Injury

Following spinal cord injury, motoneurons may lose supraspinal control over converging afferent pathways, which would result in uncontrolled widening of MRRFs and unwanted whole limb reflex responses. Numerous experiments in chronic spinal cord injury in humans and animals have shown evidence for whole limb reflex responses to local stimuli (Schmit, McKenna-Cole et al. 2000; Schmit and Benz 2002; Schmit, Benz et al. 2002; Schmit, Hornby et al. 2003; Bennett, Sanelli et al. 2004; Gorassini, Knash et al. 2004). Although limited to the sagittal plane, our study is the first to provide direct quantification of widened MRRFs in motoneurons following spinalization as a result of enhanced muscle afferent transmission. Future studies which address the regulation of MRRF patterns, either through monoaminergic or cortical pathways, could result in better management of whole limb spasms seen following spinal cord injury.

Experimental Methods and Procedures

Surgical Procedures

All procedures were fully approved by Northwestern University Institutional Animal Use and Care Committee. All 23 experiments were done using the decerebrate preparation (for details see Lee and Heckman 1998; Lee and Heckman 1998). Surgical procedures were completed under deep anesthesia (1.5-3% isofluorane in a 1:3 mixture of NO_2 and O_2). Keeping the hindlimb skin as intact as possible, nerves to the medial and lateral gastrocnemius muscles (16 animals), vastus medialus (5 animals), and rectus femoris (5 animals) were identified and a cuff electrode was applied for antidromic stimulation of motoneurons. A laminectomy was done from L_1 to L_7 to expose the spinal cord and the cord was bathed in mineral oil. A pre-collicular decerebration was performed and then the cat was paralyzed with gallamine triethiodide (Sigma-Aldrich). In 10 experiments, the cord was transected at T_{10} prior to the decerebration. Intracellular recording began at least 45 minutes after the decerebration. To diminish movement related cutaneous input, in 1 experiment, keeping musculature intact, the hindlimb was denervated to the pad of the paw using blunt dissection following spinalization. The paw was attached to the robot (Staubli, AG Robotics). For 3 experiments, to determine the contribution of Ia input to the MRRF, the common tendon to MG and LGS was cut distally. The robot was adjusted so that the hindlimb was in the midpoint start position: the ankle at 88°s relative to the tibia, the knee at 130°s, and the hip at 105°s. This position is well within the documented maximum and minimum the passive ranges for the cat hindlimb (Goslow, Stauffer et al. 1973).

Intracellular Recordings

Intracellular recordings of lumbar spinal motoneurons were done using sharp electrodes (3-5 MΩs) filled with 2 M potassium citrate. Single electrode discontinuous voltage clamp (switching frequency 8-10 kHz) was applied using an Axoclamp 2a amplifier. Data with inadequate settling were rejected. To enhance the low frequency gain in the negative feedback loop, an external gain circuit was used which allowed for gains of 100 -300 ηA/mV (for details see Lee and Heckman 2000; Heckman and Lee 2001).

Experimental Protocols and Data Analysis

With the hindlimb held in the starting position, motoneurons (MG, LGS, VM, or RF) were identified by antidromic stimulation. In current clamp mode, spike heights were assessed and cells with spike heights less than 60 mVs were rejected. Holding the cell 5-10 mVs below the estimated resting membrane potential, a slow voltage ramp was applied (30-40 mV/5 s). The voltage onset of the PIC was estimated at the threshold for the negative slope region. The cell was then stepped to the onset of the PIC (5-10 mVs depolarized to the resting membrane potential) and current was measured over 11s. After waiting ~ 30 seconds to avoid warm-up, the step was then repeated while the robot passively flexed and extended the ankle/knee ± 15°s and hip ± 10°s individually and then in combination for a whole limb movement (see Fig. 2). Each movement was repeated 2 times at a speed of ~ 1Hz with a delay of 0.3 to 0.5 seconds between each set of movements. In this way, we were able to measure at the soma the current

generated by both the synaptic input and the PIC. To evaluate the I_n with diminished PICs , we repeated this sequence with the cell held at a steady voltage level of 5-10 mVs hyperpolarized to the resting membrane potential (same voltage from which the initial voltage ramp was initially applied). Current-voltage plots (I-V) were constructed for each cell. Input conductance was calculated as the slope of a line fit through the I-V function over a range of 10 mVs at a voltage 10-15 mVs hyperpolarized to the onset of the PIC. PIC amplitudes were determined by extending the I-V regression line and subtracting the I-V function from it. Modulation of I_N due to joint flexion/extension was calculated by determining the difference between the amplitudes of the peaks and troughs (ΔPT, see Fig. 3). To differentiate between the excitatory and inhibitory contribution to I_N, we calculated the amplitude from a baseline current level (no movements) to the associated peak (IΔPT) and trough (EΔPT). Estimation of change in muscle length for each end range of movement was calculated using a model detailed in (Goslow, Stauffer et al. 1973; Burkholder and Nichols 2004). Data were analyzed using excel and SPSS. For statistics, T-tests were used to evaluate significant differences with the alpha level set at 0.05. Multiple comparisons were made using repeated measures ANOVAs and Bonferroni post hoc analyses were done to determine significant differences between means.

Conclusions

The Interaction of Synaptic Inputs and Dendritic PICs in Motoneurons

Similar to many types of neurons, motoneurons (MNs) contain dendritic voltage sensitive channels (Hausser, Spruston et al. 2000; Reyes 2001). Thus, *in vivo*, integration of excitatory and inhibitory inputs by MNs also involves the activation of voltage sensitive conductances. Recent work in the cortex and spinal cord has shown that neurons may function at least part of the time in the presence of a steady background of both excitatory and inhibitory synaptic inputs or "high conductance state," especially in cells associated with network activity (Steriade 2001; Alaburda and Hounsgaard 2003; Destexhe, Rudolph et al. 2003; Berg, Alaburda et al. 2007). Relevant to cell firing properties, the high conductance states have been shown to diminish or "quench" the role of intrinsic electrical properties of the cell (Alaburda and Hounsgaard 2003) and promote irregular firing. Conversely, low conductance states would enhance the role of intrinsic electrical properties (Alaburda and Hounsgaard 2003; Berg, Alaburda et al. 2007).

Similar amplitudes of tonic excitatory and inhibitory inputs result in a "balanced" operating mode, and in the spinal cord, have been shown to exist in turtle MNs and interneurons (Berg, Alaburda et al. 2007). This study also showed that the maximum

excitatory and inhibitory conductances, estimated from changes in membrane potential, were in phase with each other as well as with the scratch activity.

Our study (Chapter 1) quantified what happens when tonic excitation and inhibition are applied in the presence of active dendrites. We showed that when tonic excitation and inhibition are applied alone, PICs amplify both excitatory and inhibitory conductances in different voltage ranges. The predicted linear or algebraic summation of simultaneous application of both types of inputs would result in a relatively "unbalanced" current voltage relationship that overlaps with repetitive firing voltages. This proved not to be the case. We found that steady excitation and inhibition resulted in a net effective synaptic current (I_N) with less variation as a function of voltage (See Chapter 1, Fig. 2). Thus, when PICs are active, summation of excitatory and inhibitory inputs results in the cell operating in a more balanced mode. Although Berg et al. have demonstrated that MNs operate in this mode during the functional activity of the scratch reflex, it is not yet known how pervasive this mode is in other network activities, e.g. central pattern generators (CPGs).

The experimental design from Chapter 1 best represents what would occur during steady state conditions, e.g. postural activities. Operating in a balanced mode would dampen the potential of large fluctuations in firing gain due to non-linear amplification of excitatory and inhibitory inputs by PICs and promote a smooth maintenance of posture. The relative influence of PICs could be modulated by higher centers by changing the overall "conductance state" of the cell. Since PICs are known to make large

contributions to the $I_{N,}$ it is possible that PICs themselves contribute to the “high conductance state,” but how large a role they play is not known. This may be one reason why CP stimulation had such a strong impact on input conductance in the spinalized condition, when PICs were effectively absent. By interrupting descending drive, this may, at least acutely, contribute to a relatively “low conductance” state making inhibitory interneurons more sensitive to synaptic input and or intrinsic properties. Alternatively, control of motoneuron gain could be achieved by the interaction between active conductances and inhibitory pathways in a reciprocal manner. For example, it is likely that ankle extensor motoneurons need a large PIC to generate sufficient muscle force and reciprocal inhibition could be used to control the PIC. This type of regulation is discussed in the next section.

The Biomechanics of the Limb Can Affect the Intrinsic Properties of MNs

One of the most important findings of the research presented in this thesis is that the position of the limb carries enough sensory information to specifically regulate intrinsic conductances of MNs. Given the powerful effect of the PIC on MN excitability and repetitive firing, precise and timely regulation of the PIC is necessary to prevent unwanted or uncoordinated movement. The presence of PICs largely depends on the relative levels of serotonin (5-HT) and norepinephrine (NE) in the cord (Lee and Heckman 2000). The monoaminergic projections originate largely in the brainstem and have very diffuse projections throughout the cord which do not lend themselves to selective control of motor pools (Proudfit and Clark 1991; Jacobs and Azmitia 1992;

Rekling, Funk et al. 2000). Additionally, 5-HT and NE do not act through fast synaptic transmission, but instead through g-protein coupled receptors which exert their effects through second messenger cascades (Rekling, Funk et al. 2000). Thus the anatomical and pharmacological characteristics of the monoaminergic projections support their role in setting the overall neuromodulatory state of the cord. Given their tendency to excite motoneurons and promote PICs, a state of high neuromodulatory drive would thus promote co-contractions for all muscles around any given joint. This would be detrimental to movements that require reciprocal activation of agonist antagonist pairs.

It would seem then that a focused and fast acting inhibitory pathway would be necessary to regulate the PIC of individual motor pools. Electrical stimulation of reciprocal and recurrent inhibitory pathways had previously been shown to successfully regulate the amplitude of the PIC (Hultborn, Denton et al. 2003; Kuo, Lee et al. 2003). These pathways are focused enough to potentially allow adjustment of the PIC in specific motor pools. Reciprocal inhibition is an attractive candidate from a motor control standpoint, since it provides indirect length information about the antagonist muscle. When the antagonist muscle is maximally stretched, reciprocal inhibition is large. Here it is shown that small changes in joint angle (± 10s) can modulate the amplitude of the PIC on average 50% (for cell example see Chapter 3, Fig.3). This modulation was determined to be mediated primarily through reciprocal inhibition as the correlation between PIC amplitude and joint angle was lost following a transection of the antagonist tendon. It should be emphasized that the PIC must be particularly sensitive

to reciprocal inhibition as changes in input conductance due to inhibition were minimal. This further indicates that most of the interaction between reciprocal inhibition and the PIC occurs in the dendrites. Moreover, cutaneous denervation did not alter the pattern of PIC modulation, and the rotation of joints in which the agonist/antagonist muscles did not cross had no significant effect on the PIC amplitude. In this way, the PIC can be shaped in order to allow reciprocal activation of agonist-antagonist muscle pairs. This would be important for movement transitions, for instance, from late stance to the onset of swing. At the end of stance, the ankle flexors are maximally stretched, inhibiting the active ankle extensors.

Although Ia inhibitory interneurons primarily receive excitatory input from Ia afferents, they also receive excitatory and inhibitory input from several sources including the cortex and polysynaptic afferent pathways (Jankowska 1992). In the rat and the human, reciprocal inhibition can be modulated (Nielsen, Crone et al. 1995; Chen, Chen et al. 2006). In this way, an additional layer of control exists over the regulation of the PIC to meet the needs of the behavior. There is growing evidence of the involvement of PICs and plateau behavior in animal models and human examples of neurological injury as well as derangement of the Ia inhibitory system. Proposed studies regarding this issue are considered below, in the Clinical Implications section.

PICs Increase the Gain of a Motoneuron's Movement Related Receptive Field

During movement, motoneuron output depends on the integration of synaptic inputs from descending and peripheral sources with intrinsic electrical properties. Hindlimb movement would likely stimulate relatively focused pathways such as the Ia afferents and interneurons as well as pathways that carry information from the whole limb. We show that in the decerebrate preparation, in which there is tonic monoaminergic drive, PICs enhanced all movement related synaptic input including that from distal joints by as much as 3 fold (for cell example see Chapter 3, Fig.3) in ankle extensor, knee extensor, and knee extensor/hip flexor motoneurons. These data support recent modeling studies that indicate the location of PIC channels are globally distributed in the mid to proximal dendritic tree (Elbasiouny, Bennett et al. 2005; Anelli, Sanelli et al. 2007; Grande, Bui et al. 2007), and thus do not preferentially amplify specific synaptic inputs. Amplification of all movement related synaptic input would promote consistency in changes in the frequency-current (F-I) gain with respect to multiple joint movements. For example, when monoaminergic drive is relatively strong and PICs are large, F-I gain would increase for all movements and not just to ankle or knee movements. Future experiments are necessary to examine the relationships between the degree of amplification of movement related I_N and the magnitude of the PIC. This could be done by measuring the movement related I_N and varying the amplitude of the PIC by applying depolarizing steps of various sizes. At more depolarized voltages, outward currents are activated which may result in a reduction in ΔPT amplitude and a saturation in the resulting firing gain. Subsequently, a ΔPT- voltage plot could be made to determine the

voltage dependent relationship of a motoneuron's MRRF in order to make firing predictions.

In the majority of cases, the amplification of movement related I_N modulation in the depolarized voltage condition represented an increase in both excitatory and inhibitory inputs. The excitatory component was enhanced by PIC conductances and the inhibitory component was larger than in the hyperpolarized condition due to the suppression of the PIC. The increase in inhibition seen in the depolarized voltage condition was not likely simply a function of driving force. In the spinalized samples, where the PIC amplitudes are minimal, the depolarized voltage condition did not result in a significantly larger increase in the inhibitory component as compared to the hyperpolarized voltage condition.

These data imply that both excitation and inhibition are important in modulating the amplitude of the movement related I_N and this hypothesis was supported by a change in the shape and amplitude of the movement signal when reciprocal inhibition was removed (See Chapter 3, Figure 6). The presence of inhibition thus promotes the matching of the movement trajectory and the movement related I_N. In the absence of Ia inhibition, the movement related I_N has a square shape. The resultant square shape more closely follows the predicted pattern of Ia afferent firing in response to the sagittal plane movement, and suggests the presence of plateau potential. Evidence from Chapter 2 also demonstrated that reciprocal inhibition can significantly modulate PIC amplitude as a function of joint angle.

Besides Ia inhibitory interneurons, MNs also receive inhibitory synaptic inputs from several sources including a subset of the group II interneurons, group Ib interneurons, renshaw cells, cortical and rubrospinal inputs (Baldissera F 1981; Jankowska 1992; Binder and Powers 1999). It is thus likely that during a voluntary or reflexive movement that the movement signal is shaped by other inhibitory inputs depending on the task. Experiments are needed which address the quantification of how different types of inhibition shape the movement related I_N during various tasks and neuromodulatory states. For instance, it could be possible that movements which involve the coordination of muscles throughout the whole limb such as locomotion or flexor-withdrawal reflex maybe more sensitive to polysynaptic inhibitory pathways. Additionally, depending on the task, inhibitory input from specific muscles could be especially important in shaping the movement related I_N. An example of this is the known impact of hip extension on the inhibition of ankle extensors during locomotion (Kriellaars, Brownstone et al. 1994; Hiebert, Whelan et al. 1996; Lebedev and Nicolelis 2006). Current advances in neurorehabilitation involve brain machine interfaces (Lebedev and Nicolelis 2006). Information, like that obtained from these experiments, showing how the MRRF of MNs is shaped, could help to more fully develop algorithms employed by the neural interface.

Tonic Descending Brainstem Inputs to the Cord Influence the MRRF of Spinal Motoneurons

Thus far, we have considered the evidence that PICs primarily function to enhance the amplitude of the movement related I_N modulation, but what are the factors which shape the pattern of the MRRF field? Data presented in Chapter 3 indicates the dominant MRRF pattern can be modulated in part by the relative level of tonic descending inputs to the cord. This is supported by the fact that the overall pattern of the MRRF did not change as a function of the presence or absence of PICs in the intact cord state, but did change when the descending brainstem transmission was interrupted. Specifically, for two of the MN samples, the MRRF pattern shifted to include significantly more hip ΔPT, equaling the ΔPT generated by stretching of agonist and antagonist musculature. In the cord intact state, in which there is tonic monoaminergic drive to the cord, the pattern of each MN sample's MRRF was dominated by Ia pathways. In contrast, in the vastus medialus and triceps surae samples following complete cord transection, pathways carrying multi-segmental information were facilitated. Other studies have also shown a change in pathway facilitation based on the degree of supraspinal input (Eccles and Lundberg 1959; Matthews 1972).

Electrophysiological, pharmacological, and force reflex studies have shown that multiple monosynaptic and polysynaptic pathways co-exist and often share interneuronal pathways (Baldissera F 1981; Jankowska 1992). How do supraspinal centers regulate the various pathways? Since it is unlikely that each spinal pathway would have a separate neurotransmitter systems, it has been suggested that at least some of pathways could be facilitated or inhibited by receptor sub-type expression (Hochman,

Garraway et al. 2001; Jankowska 2001). Alternatively, supraspinal inputs could vary tonic drive to the cord, possibly through inhibitory pathways. When this tonic drive is eliminated, various pathways would be disinhibited. We found that when descending drive was interrupted by acute spinal transection, there was a facilitation of sensory information from the hip onto ankle and uni-articular knee extensor MNs (Chapter 3, Fig. 8). Since polysynaptic pathways work through convergent interneuron pathways, it is possible that following cord transection, MNs such as these received a greater balance of input from convergent pathways as compared to the intact cord state.

Anatomical and electrophysiological data have shown that the monoaminergic centers diffusely innervate the cord and MNs have widespread 5-HT contacts throughout their dendritic tree (Proudfit and Clark 1991; Jacobs and Azmitia 1992; Alvarez, Pearson et al. 1998). Thus the monoaminergic system is a candidate in regulating the overall excitability of the cord, especially MNs. Monoamines are known to suppress high threshold inputs and have mixed effects on group II interneurons (Jankowska, Slawinska et al. 2002). Interruption of monoaminergic pathways could thus result in disinhibition of the high threshold and group II pathways. Since cutaneous denervation did not alter the MRRF following spinalization and muscle paralysis, it is likely that the increase in hip ΔPT is from muscle afferents. Interestingly, in the case of the ankle extensors, hip extension resulted in inhibition. This is in agreement with locomotor studies which show stretch of hip flexors inhibits ankle extensors thus permitting a transition from stance to swing (Kriellaars, Brownstone et al. 1994; Hiebert, Whelan et al. 1996). Future experiments could delineate whether this widening reflects an overlay

of both Ia and polysynaptic pathways or whether Ia pathways are actively suppressed. The fact that ankle and knee ΔPT between the spinalized and the intact hyperpolarized voltage condition were not significantly different suggest that, at least acutely, Ia and Ia inhibitory pathways are still somewhat active. Chronic changes in the Ia system following spinal cord injury are discussed in the Clinical Implications section below.

Intrinsic Electrical Properties of Spinal Motoneurons Optimize Motor Control

The presence of PICs and, equally important, the control of PICs, optimize motor control by providing a built in source of excitation that can be regulated by several mechanisms to match the motor requirement. As described earlier, PICs can exert tremendous changes in motoneuron excitability, promoting the generation of plateau potentials that facilitate self-sustained firing (Heckman, Lee et al. 2003). This would be effective for motor tasks which don't need a continuously updated input signal such as maintenance of posture or driving of networks which control repetitive movements, i.e. CPGs. Indicated by the work here (Chapter 1), the presence of PICs, as a result of steady inputs, results in a more balanced mode of operation which decreases the voltage dependent variability of the net I_N. This would help maintain a "smooth" motor command during steady conditions and prevent fluctuations in firing gain.

Another equally important role of the PIC is to enhance synaptic input to MNs, which in turn increases the cell's firing gain. When neuromodulatory tone is low and PICs are

minimal, the estimated net I_N generated by various descending and peripheral inputs is not sufficient to generate the firing rates required to generate maximal force production (Binder, Heckman et al. 2002; Heckman, Gorassini et al. 2005). We have shown that PICs enhance all sagittal plane movement related synaptic input without altering the MRRF (Chapter 3). In this way, motor commands are conserved, but the modulation of firing rates can be adjusted by the level of PICs. During reciprocal movements in the sagittal plane, excitation and inhibition from the Ia afferent and interneuron pathways would wax and wane out of phase. This would allow the intrinsic electrical properties to exert a significant effect on net I_N because the cell is operating in a relatively "lower conductance" or "unbalanced" state than when steady excitation and inhibition are presented continuously (see Chapter 1).

In addition to the direct effects on excitability, the regulation of PICs also optimizes motor control by allowing a more flexible platform for the execution of movement commands. Descending monoaminergic systems control the amplitude of the PICs (Hounsgaard, Hultborn et al. 1988; Lee and Heckman 2000) allowing the overall level of intrinsic excitability to be set by different neuromodulatory states. Our experiments extend this finding by showing that the effects of the PIC can also be modulated as a function of inhibition to the cell. As a result, specific patterns of motoneuron excitability can be created from a diffuse neuromodulatory background by focused inhibitory systems. As mentioned in Chapter 2 and previously in this discussion, Ia inhibitory interneurons can be modulated and show plasticity. This allows an additional layer of control over the PIC. Furthermore, data from Chapter 2 indicates that in the absence of

reciprocal inhibition, cells showed a warm-up response to a change in joint position. In other words, repeated joint movements resulted in an increase in PIC amplitude, despite joint position. This would result in inappropriate MN excitability and firing (see the section below for possible clinical implications).

Clinical Implications for Spinal Cord Injury and Future Studies

Spinal cord injury results in a disruption of the transmission of supraspinal input, abnormalities in spinal reflex circuitry and processing of sensory information, and changes in intrinsic electrical properties. The relationships between these pathologies and the degree to which they interfere with voluntary movement are unknown. Typically there is an initial period of spinal shock where MN excitability is very low. Chronically, hyperreflexia develops, manifesting as whole limb spasms. Whole limb spasms and reflex responses have been shown to be triggered by stimulation of cutaneous, load, and muscle afferent pathways (Schmit, McKenna-Cole et al. 2000; Schmit and Benz 2002; Schmit, Benz et al. 2002; Gorassini, Knash et al. 2004; Wu, Hornby et al. 2005; Wu, Hornby et al. 2006; Wu and Schmit 2006). In addition to the derangement of reflex circuitry, changes in motoneuron intrinsic excitability, specifically the reemergence and disregulation of PICs may also contribute to spasticity by increasing the intrinsic excitability of MNs (Hultborn 2003, Heckman 2005). In the rat sacral cord model of spinal cord injury, Bennett has shown that the emergence of spasms coincides with the reemergence of PICs (Li and Bennett 2003; Harvey, Li et al. 2006). Studies in animal and human motor units support plateau like firing behaviors following spinal cord injury (Gorassini, Knash et al. 2004; Rank, Li et al. 2007). Additionally, there is evidence of

warm-up or a temporal facilitation of flexion and stretch reflexes in chronic spinal cord injury which could also be related to the disregulation of the PIC (Hornby, Rymer et al. 2003; Schmit, Hornby et al. 2003; Hornby, Kahn et al. 2006). In addition to the abnormal excitation of reflex circuitry and MNs associated with spasticity, there is a reduction or even a reversal of inhibitory pathways, such as reciprocal inhibition (multiple sclerosis: (Crone, Nielsen et al. 1994),spinal cord injury:(Boorman, Lee et al. 1996; Okuma and Lee 1996; Okuma, Mizuno et al. 2002; Crone, Johnsen et al. 2003; Xia and Rymer 2005), stroke: (Okuma and Lee 1996). The loss of reciprocal inhibition, following neurological insult, may be due to a decrease in background activity from supraspinal sources. To what extent due abnormalities in reflex circuitry, intrinsic properties, and descending inputs affect motor control?

Data from this thesis show that reciprocal inhibition is particularly important in modulating the amplitude of the PIC in both static and dynamic conditions (Chapter 2 and 3). Furthermore, in the absence of reciprocal inhibition, there was evidence of warm-up, at least in the static conditions (Chapter 2). It is possible that following spinal cord injury, the reduction or loss of reciprocal inhibition results in a decrease in control of intrinsic MN properties. Future studies should explore whether reciprocal inhibition provided either by electrical stimulation or tendon vibration can diminish wind-up responses of stretch reflexes in subjects who have suffered a spinal cord injury. Alternatively, we could show a negative correlation between the degree of reciprocal inhibition measured by the H-Reflex with the wind-up response.

Recently, Knikou and colleagues have demonstrated that hip position during a sinusoidal movement enhances inhibitory circuits of ankle extensors in humans (2006). Specifically, that hip extension enhances inhibition of the ankle extensors. Interestingly, we found that ankle extensors showed an increase in inhibition to hip extension in the acute spinalized condition as compared to the cord intact condition. Future experiments could explore how inhibition of ankle extensors generated by hip extension affects wind-up. These proposed experiments would address how the modulation of sensory input could be used to diminish undesirable reflex or motor unit activity and could ultimately be adapted for use as therapeutic strategies.

Introduction, Figure 1

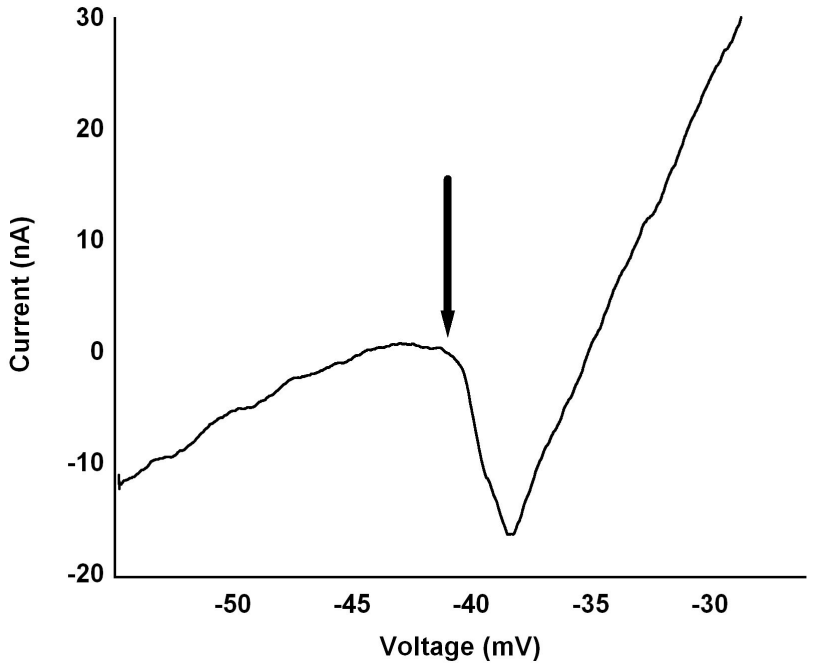

Figure 1: The current-voltage relationship of a spinal motoneuron. The PIC manifests as a negative slope region (arrow indicates onset). As the cell is depolarized further, outward conductances are activated, restoring a positive slope region.

Introduction, Figure 2

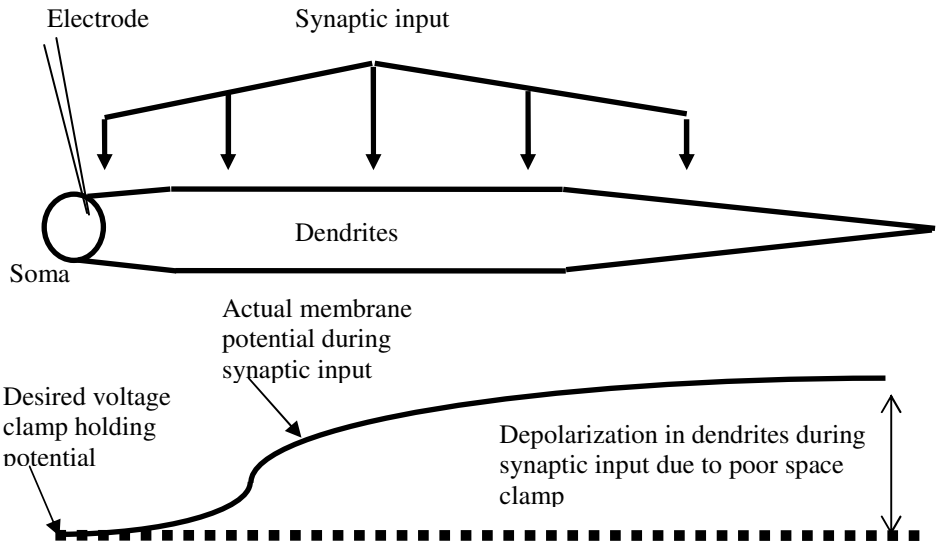

Figure 2: A schematic illustrating the use of *in vivo* voltage clamp recording techniques in the measurement of active conductances and synaptic currents in the dendrites of spinal motoneurons. Due to the extensive dendritic tree of spinal motoneurons, voltage clamp is only effective in somatic and proximal dendritic regions. Steady synaptic input to the dendrites would thus be able to activate voltage sensitive conductances in the dendrites. However, there is some effect of the voltage clamp on dendritic regions as adequate hyperpolarization can be sufficient enough to prevent PIC activation. Adapted from Heckman and Lee 2001,with permission.

Chapter 1, Figure 1: The Relationship Between Excitatory and Inhibitory Synaptic Input and the Current Voltage (I-V) Function. (A) The effect of excitatory and inhibitory synaptic input applied separately and simultaneously on the shape of the PIC during a voltage ramp for one cell in the monoaminergic intact condition. All inputs were applied steadily through the duration of the I-V function. In the absence of additional synaptic input, the PIC appears as a downward deflection in the current profile during a voltage ramp (dotted line) with a voltage onset near the threshold for firing. Synaptic inhibition, via Ia interneuron pathways, causes a reduction in amplitude, but not voltage onset of the PIC (upper thin black trace). In contrast, excitatory synaptic input results in a relatively depolarized PIC activation (lower thin black trace). (**B)** Comparison of effective synaptic current (I_N) generated during excitatory and inhibitory synaptic input (same cell as A). I_N was calculated by subtracting I-V traces made during the application of synaptic input with traces generated during trials with no additional synaptic input (control ramps). The top solid black trace shows the I_N as a result of excitatory synaptic input and PICs. With the activation of the PIC, the excitatory I_N is enhanced two fold (as compared to more hyperpolarized regions) and then saturates at more depolarized levels. The lower solid black trace illustrates the inhibitory I_N, which also shows amplification, but is a result of the PIC deactivation by the Ia reciprocal inhibition. Note that peak excitatory I_N occurs at a more hyperpolarized voltage than the peak inhibitory I_N. We are able to effectively voltage clamp the soma and proximal dendrites of the cell, which allows us to evaluate the interaction between the PIC and synaptic input occurring more distally in the dendrites. The dashed lines associated with both traces predict what the I_N would be if the cell were a perfect sphere and under total

clamp control. In both instances, the current voltage relationship would be linear, undergoing no amplification.

Chapter 1, Figure 1

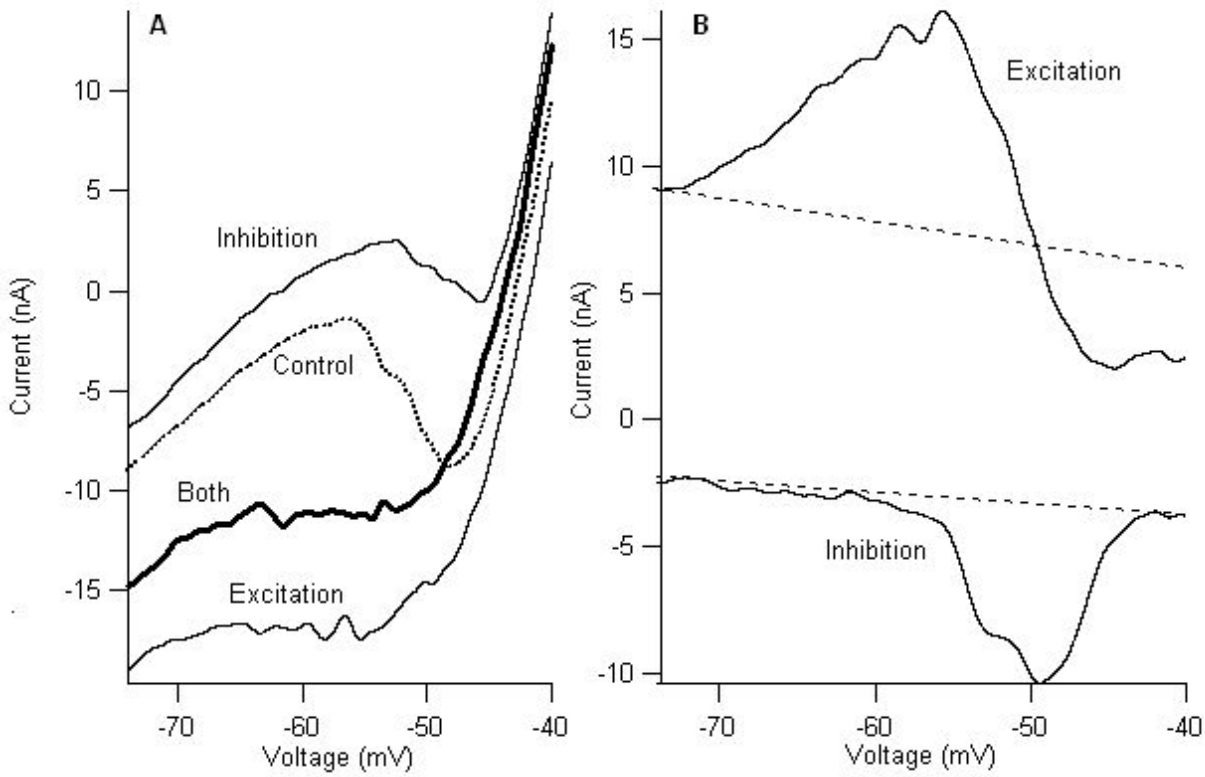

Chapter 1, Figure 2: The Difference in Voltage Onset and Amplitude of Peak Excitation and Inhibition I_n Shape the Pattern of Summation. Each cell illustrated here received excitatory (thin black trace) and inhibitory (line with asterisk) synaptic inputs applied separately and simultaneously (thick black trace). The I_N was calculated by subtracting stimulation trials from control trials and represents the net current measured at the soma resulting from synaptic input. **(A)** In this cell, the excitatory I_N was larger than the inhibitory I_N (18 nA vs. -10 nA). The net change in the actual summation (ΔSum Actual) of excitation and inhibition is due to the difference in voltages where excitation and inhibition I_N's peak in amplitude. Overall, the actual net change in summation was smaller than the predicted net change in summation (ΔSum Predicted). In the peak excitation voltage window, inhibition was stronger than predicted and conversely in the peak inhibitory voltage window, excitation was stronger than predicted. This pattern was consistent in cells where excitation and inhibition were balanced (**B**, ~10 nA each) and where inhibition was larger than excitation (**C**, -18 na versus 10 naA). Note the trend of larger differences in the actual and predicted I_N's with larger values of ΔSum Predicted (compare B and C with A).

Chapter 1, Figure 2

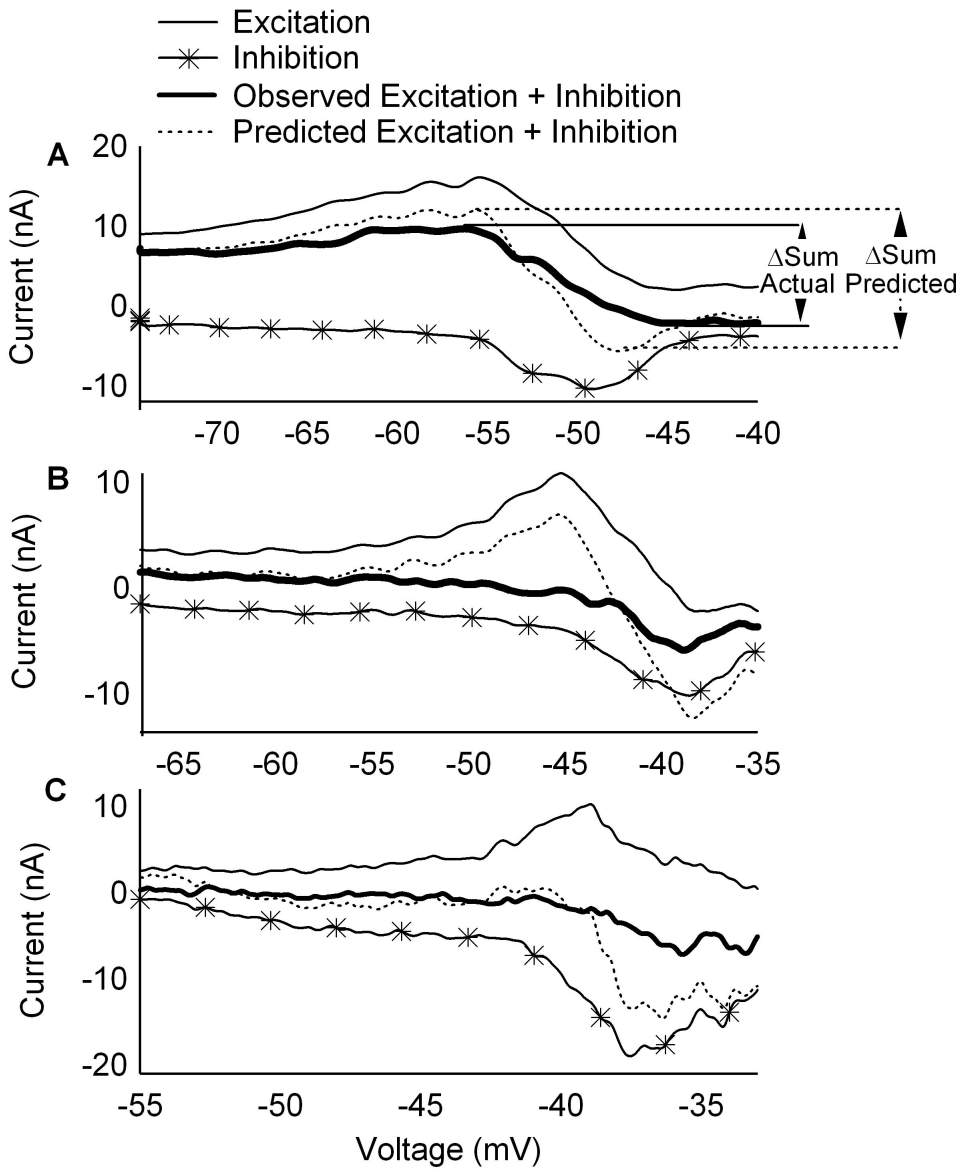

Chapter 1, Figure 3: **Non-linear Summation is Modest in Cells with Active Dendrites.** The actual summation of excitatory and inhibitory I_N's was plotted against the predicted I_N for three voltage windows in the standard monoaminergic state: peak excitation (open squares), peak inhibition (solid squares) and sub-pic (diamonds). The thick line is a hypothetical case of linear summation with a slope of 1 and a y intercept of zero. Scatter of the observed data from this line represent non-linear summation. Although the slopes of the regression lines fit to each data set were less than 1, the confidence intervals for all regression lines overlapped with the hypothetical y=x line. The slopes for each of the lines were not significantly different from one another ($p > .1$, ANCOVA). However, the lines fit to the data in the peak excitatory and peak inhibitory voltage windows did have offsets significantly different than zero; an inhibitory offset during peak excitation (right arrow) and an excitatory offset during peak inhibition (left arrow). These offsets are only 10% of the total range of I_N for each window.

Chapter 1, Figure 3

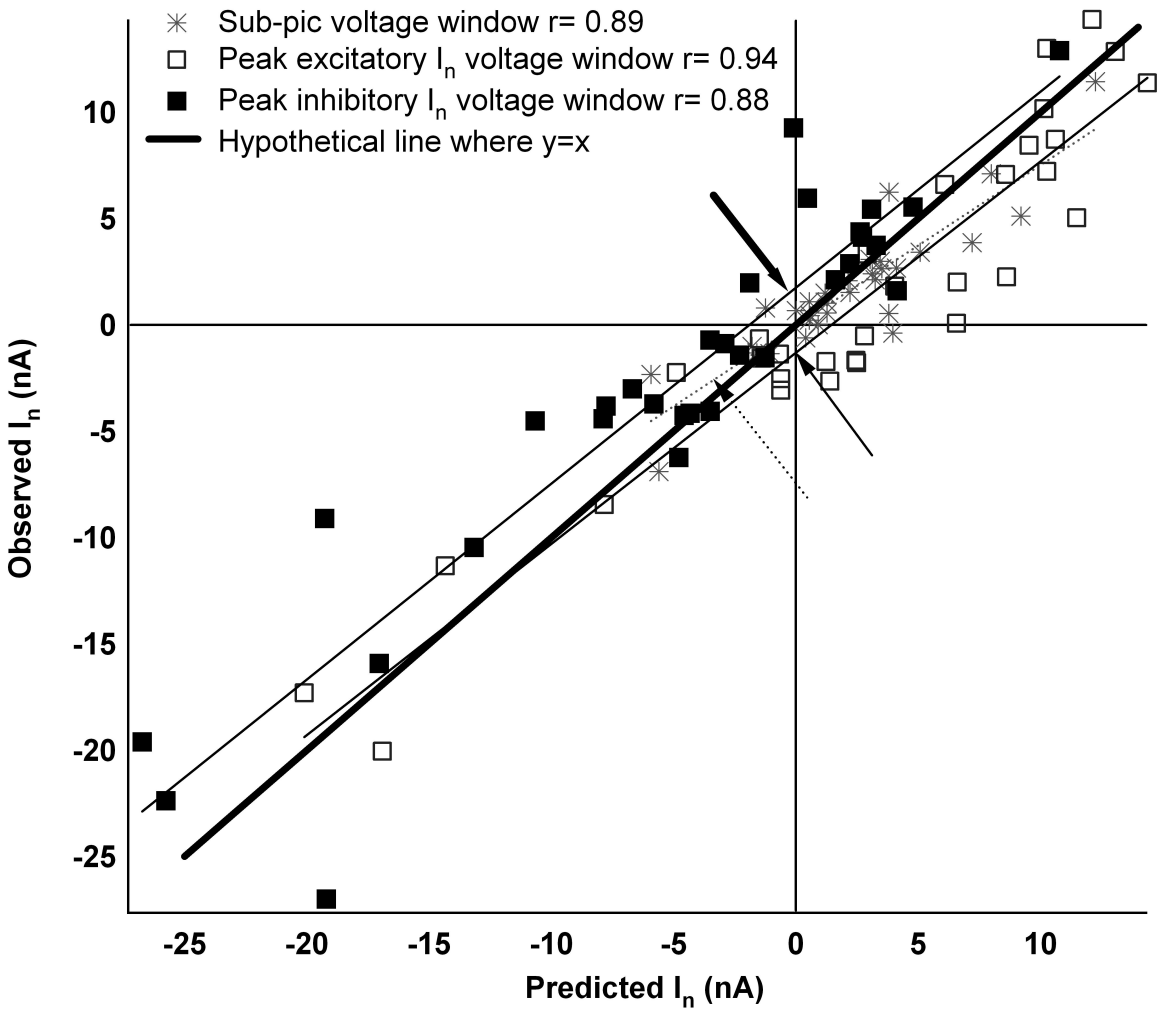

Chapter 1, Figure 4.

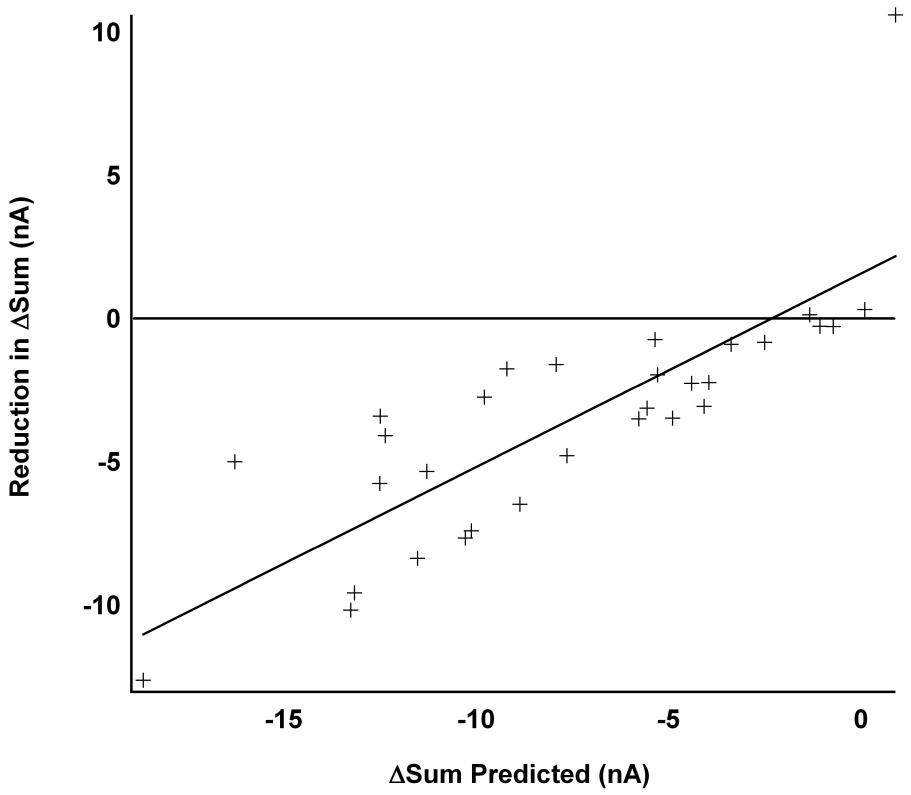

Chapter 1, Figure 4: The Reduction of the ΔSum (ΔSum Predicted- ΔSum Actual) Depends on the Amplitude of the Predicted I_N. As the ΔSum Predicted increases, the reduction in ΔSum Actual also increases ($r = 0.81$, $r^2 = 0.65$; $p < 0.001$). Compare Fig. 2B and C to 2A for specific cell examples. This relationship is functionally relevant in that the larger reduction in ΔSum values where currents of 10 to 15 nA represent 30-50% of a motoneurons firing range.

Chapter 1, Figure 5

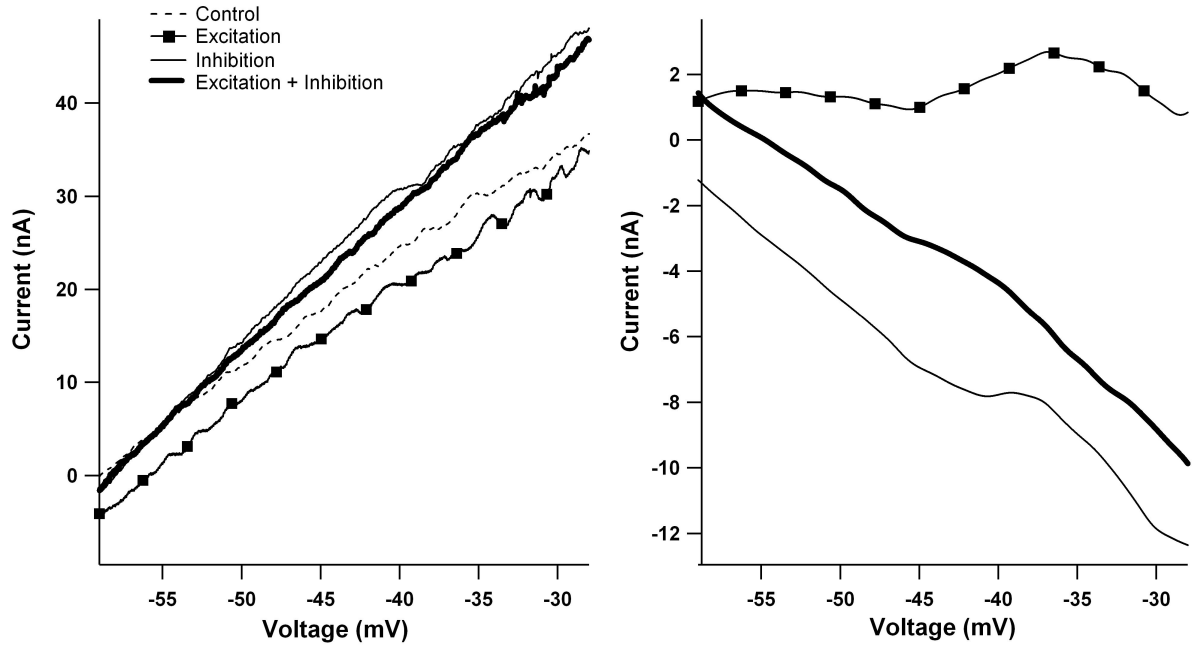

Chapter 1, Figure 5: The Minimal Monoaminergic State Results in Linear I-V Functions. (A) Current voltage plots for one cell during control (dashed line), excitation (line with squares), inhibition (thin black line) and excitation + inhibition (thick black line). Note the absence of any PICs (which would manifest as a negative slope region) even during the excitation trial (compare to Fig. 1a). Inhibition was applied via C. Peroneal nerve stimulation and excitation by tendon vibration. **(B)** Due to the lack of PICs, the I-V relationship of the I_N's also reveal a very linear relationship (same cell as A). Further evidence of decreased PIC activity is that excitation remained relatively small across voltage ranges and on average was not significantly different than the average amplitude of excitatory I_n measured in the standard state's sub-pic voltage region ($p > 0.2$).

Chapter 1, Figure 6

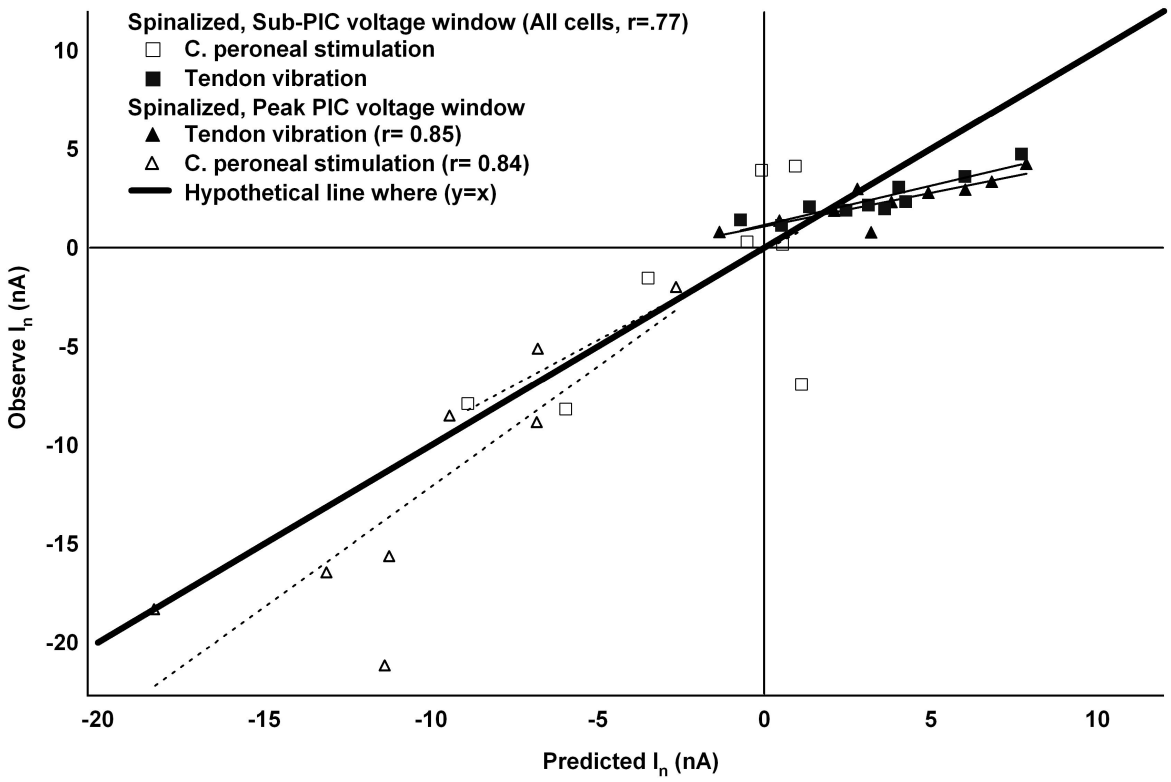

Chapter 1, Figure 6: The Pattern of Summation in the Minimal Monoaminergic State Depends on the Type of Stimulus. In cells where excitation and inhibition was applied via tendon vibration, summation transitioned from supra-linear to sub-linear as the excitatory I_N increased (closed symbols) for both voltage windows. This resulted in a regression line whose confidence intervals did not overlap with a hypothetical y=x line. In contrast, in cases where inhibition was applied via C. Peroneal nerve stimulation (open symbols), summation was approximately linear and the regression line was not significantly different than the regression line for the standard state sub-pic window. These relationships suggest that even in the minimal state dendrites are not completely passive and small activity in voltage sensitive conductances compensated for expected shunting of excitation by inhibition.

Chapter 1, Figure 7: Restoration of Amplification of Excitatory Input when Inhibition is Removed from the Balanced State. When the cell is in a balanced state with both excitation and inhibition (thick middle trace, “Actual sum”), entirely removing inhibition produces a difference current (dotted upper trace) that is equal to the difference between that in the balanced state and that for excitation alone (thin upper trace). The nonlinear summation in the actual sum makes this difference current larger than it would be if linear summation occurred (compared arrows 1 and 2). At the depolarized level with saturation, nonlinear summation reduces the amplitude of the difference current (compare arrows 3 and 4) but the difference current is still greater than excitation alone. The traces in this figure are based on the data for the cell in Fig. 2B. In push-pull mode, the synaptic current (I_N) generated by decreasing inhibition adds to that for increasing excitation. As a consequence, the amplification for the two inputs may also add. The trace defining the push-pull I_N as a function of voltage were calculated by starting with the summed I_N trace where both excitation and inhibition are activated simultaneously, then reducing inhibition by 100% (making it zero) and adding 100% to the excitation (i.e. doubling its amplitude).

Chapter 1, Figure 7

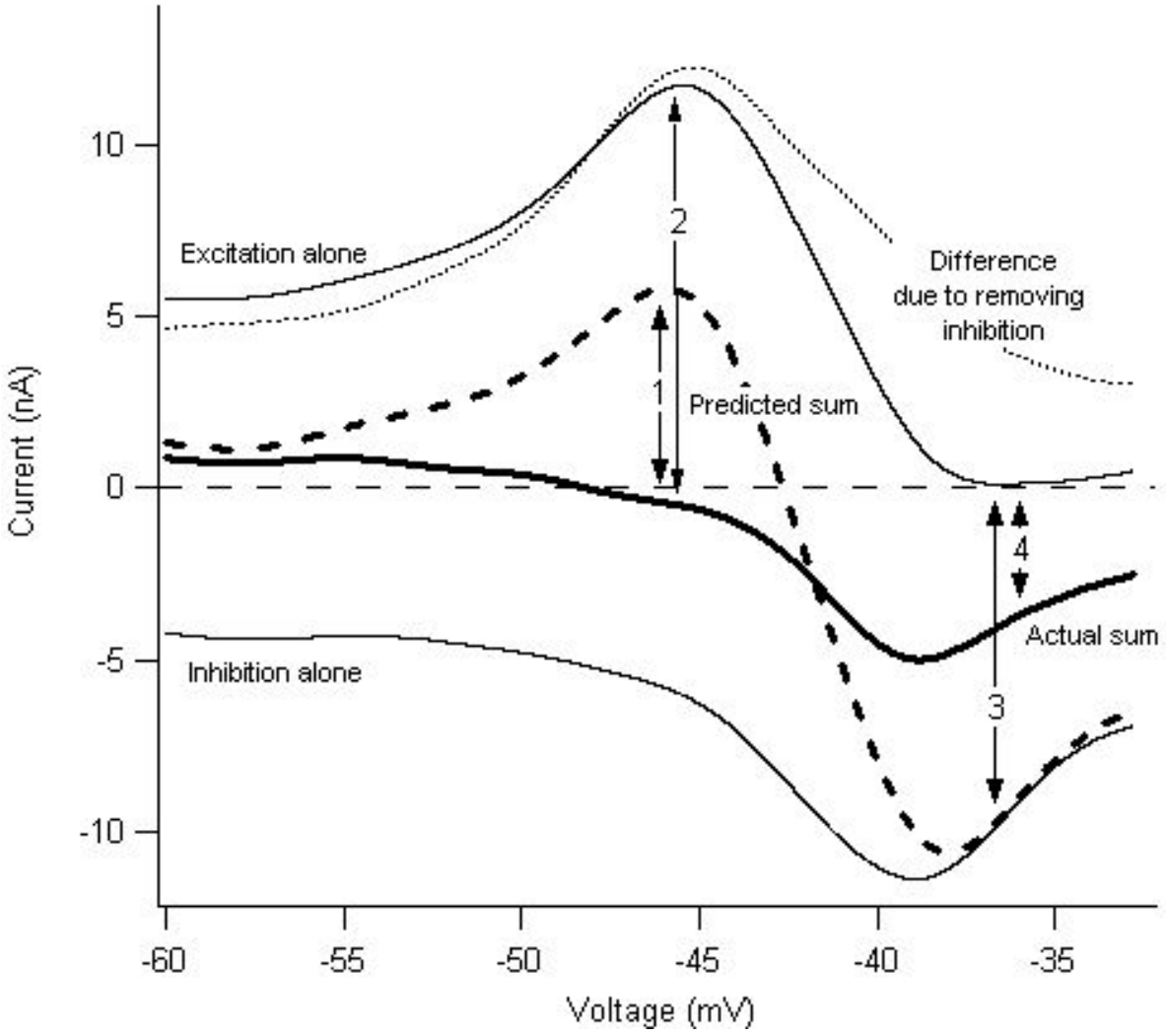

Chapter 2, Figure 1

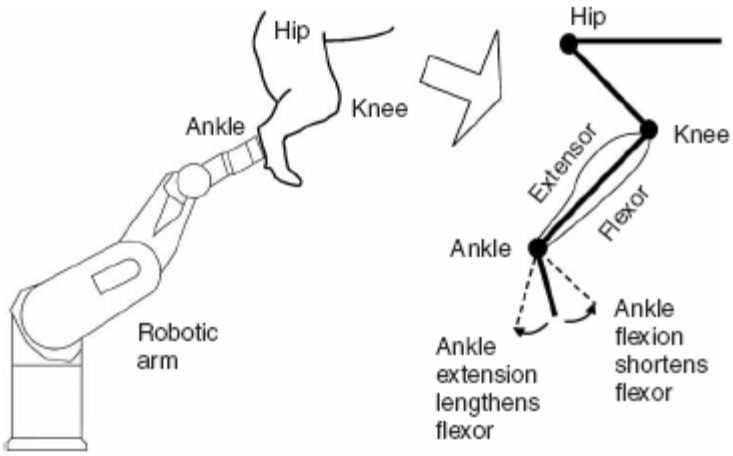

Chapter 2, Figure 1: Schematic showing the hindlimb and the robotic arm. The computer controlled robotic arm passively flexed and extended the ankle, lengthening and shortening the triceps surae and pre-tibial flexor musculature.

Chapter 2, Figure 2.

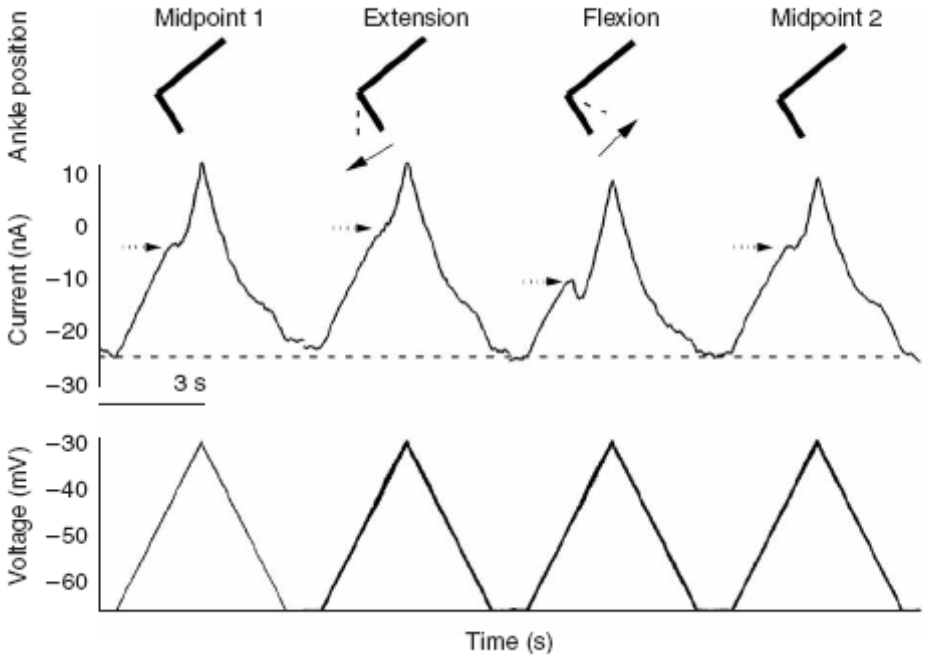

Chapter 2, Figure 2: Sequence of ankle joint positions during the reciprocal inhibition intact condition (upper panel) and resulting current (middle panel) and voltage traces (lower panel) measured in one cell. There was up to 0.5 s wait between trials. The ankle was passively rotated by a computer controlled robot and each movement was completed during the hyperpolarizing phase of each preceding voltage ramp. Each movement was completed within 1–2 seconds. Dashed arrows (middle panel), indicate the occurrence of the PIC which manifests as a downward deflection.

Chapter 2, Figure 3.

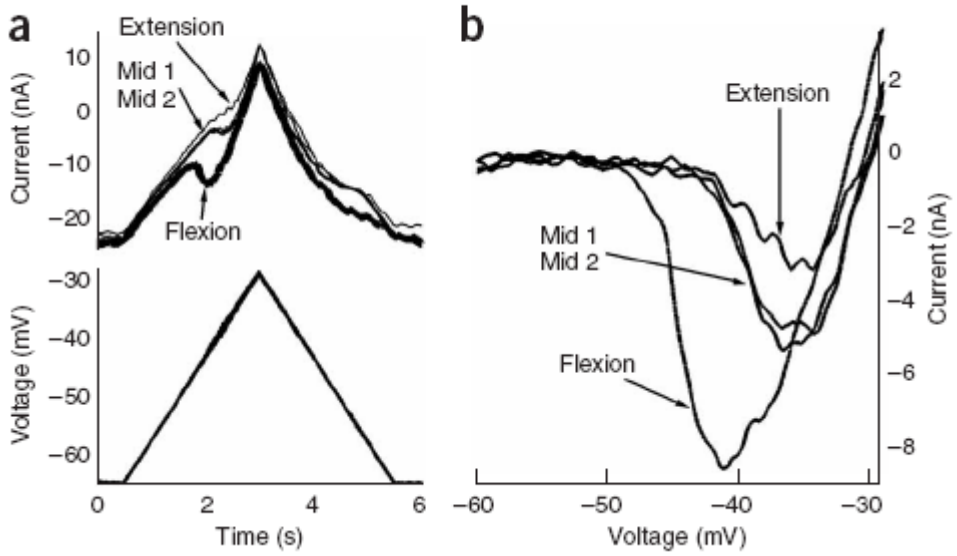

Chapter 2, Figure 3: Modulation of PIC amplitude as a function of ankle joint position in the reciprocal inhibition intact condition. (**a**) Overlaid current (upper panel) and voltage (lower panel) traces from cell in Fig. 2b. (**b**) Relationship between leak subtracted current traces and voltage for each ankle position. PIC amplitude was the greatest during ankle flexion and the least during ankle extension.

Chapter 2, Figure 4.

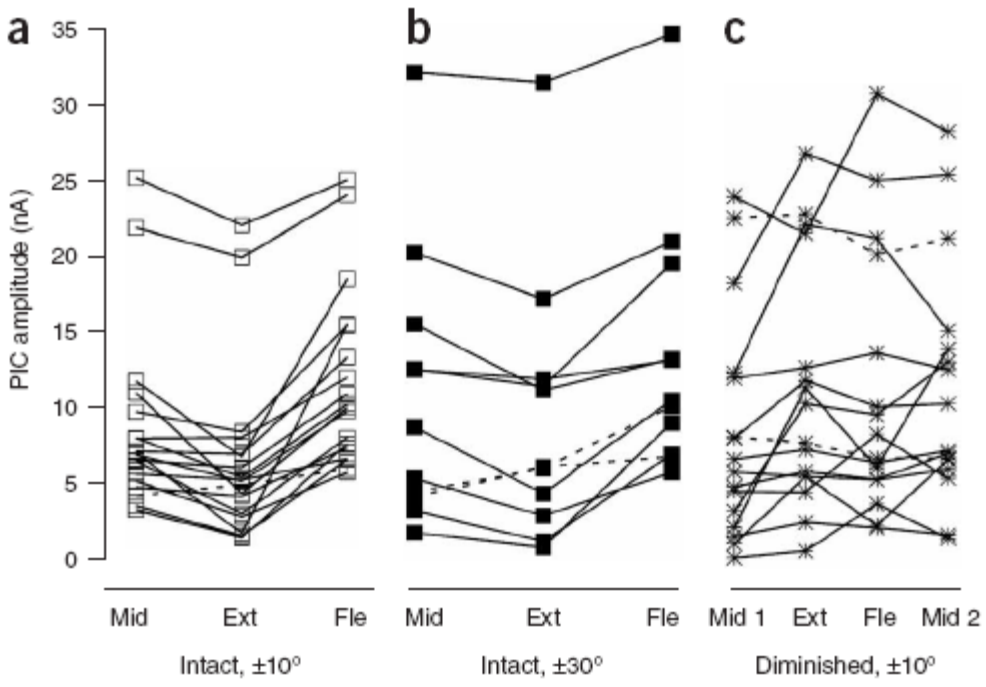

Chapter 2, Figure 4: PIC amplitude as a function of joint position for each cell (lines connecting symbols) for the reciprocal inhibition intact (**a**, **b**) and diminished conditions (**c**). (**a**) Cells from the reciprocal inhibition intact condition ($n = 18$) where the ankle was rotated ± 10 degrees from the midpoint. (**b**) Cells from the reciprocal inhibition intact condition ($n = 11$) in which the ankle was rotated ± 30 degrees from the midpoint. Dashed lines indicate cells in which PIC did not decrease with extension (**a,b**). Note in the ± 30 degree group that although PIC amplitude was modulated in the same way as in the ± 10 degree group there is no apparent scaling of PIC modulation. (**c**) Cells from the reciprocal inhibition diminished condition ($n = 16$). In this group PIC amplitude does not vary as a function of joint angle (see cell example in Fig. 5). Dashed lines indicate cells where the PIC did not increase with repeated activation.

Chapter 2, Figure 5.

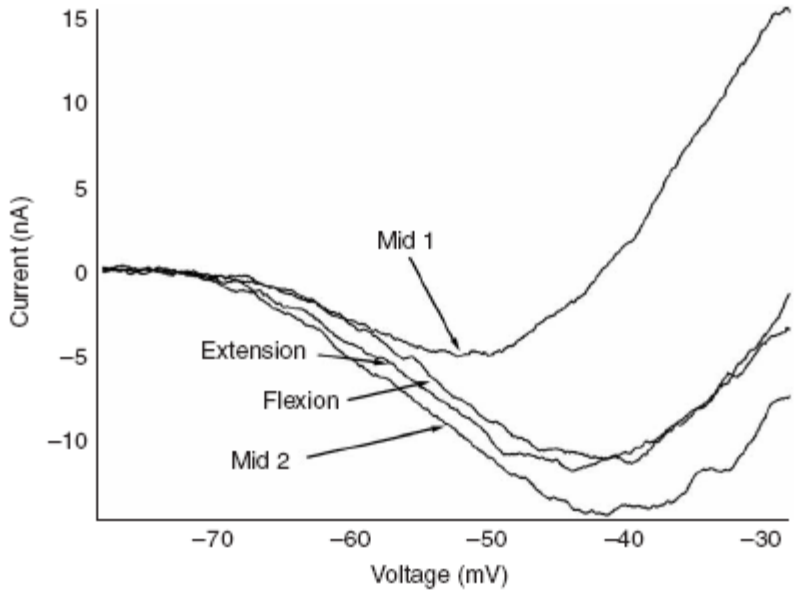

Chapter 2, Figure 5: Leak subtracted current-voltage relationship of one cell from the reciprocal inhibition diminished condition. Note the lack of PIC modulation with ankle position and the increase in PIC amplitude following the first mid trial.

Chapter 2, Supplementary Figure: The dendritic PIC is suppressed by synaptic inhibition but not by synaptic excitation. The basic interaction between the dendritic PIC and synaptic input, as established in our previous studies (Lee, 2003;Kuo, 2003;Lee, 2000), is illustrated in Fig. S1. The dendritic origin of most of the PIC becomes evident when a steady background of synaptic input is applied throughout the ramp voltage command, in this study through changes in ankle position. If the PIC were generated solely in regions where voltage clamp control is good, i.e., the soma and perhaps part of the proximal dendrites, then a steady background of ionotropic excitatory input would simply shift the I-V function downwards along the current axis in proportion to the intensity of the synaptic input (this hypothetical change is illustrated by the lower thin dotted trace in Fig. S1a). Ionotropic inhibition would generate a shift in the opposite direction, coupled with a significant change in slope due to the change in input conductance (Fig. S1a, upper thin dotted trace).

These simple changes do not occur with the real inputs. Instead the PIC is markedly altered by the steady background of both excitation (generated by activation of ionotropic, monosynaptic input from muscle spindle Ia afferents) (Lee, 2000) and inhibition (from electrical stimulation of the common peroneal nerve to antagonist muscles) (Kuo, 2003). These alterations are not due to loss of voltage control at the soma. The actual voltages for each of the above states are overlaid in Fig. S1c. These commands vary by less than 0.5 mV in all of our experiments due to a modification to enhance low frequency feedback gain of the amplifier – see METHODS, Intracellular recordings subsection. Thus the changes in the PIC due to the steady background of synaptic input necessarily take place in regions where voltage clamp control is poor – i.e., in the dendrites (Heckman, 2001).

Subtraction of the leak current (Fig. S1b) reveals marked differences in how the dendritic PIC is influenced by excitation compared to inhibition. The steady background of excitatory synaptic input markedly hyperpolarizes the activation of the PIC. This effect occurs because the excitatory input depolarizes dendritic regions under poor space clamp control, thereby lowering the threshold of the PIC as seen in the clamped somatic region (Lee, 2003;Lee, 2000). Although this shift coupled with the net inward synaptic current makes it appear that the excitation increases the PIC in the raw I-V function in Fig. S1a, leak subtraction (which removes the net offset as well) shows that this is not the case: in Fig. S1c, the PIC amplitude during excitation is similar to control conditions. Because changes in PIC amplitude were not specifically analyzed in our previous studies of excitation, we performed this analysis for 18 cells from recent experiments (including data from Lee, 2003; Kuo, 2003) and from unpublished data. There was no significant difference in peak PIC amplitude with and without the background excitation ($p > 0.9$, paired t-test). Therefore, although ionotropic excitation influences PIC threshold, its amplitude is set by the intensity of the monoaminergic input that stayed approximately constant (Heckman, 2005; Heckman, 2003). In the preparation used in these studies, monoaminergic input level stays approximately constant.

Inhibition has a very different action. As illustrated by the dashed traces in Figs. S1a,b, a background of steady inhibition has little effect on activation voltage for the PIC but markedly decreases PIC amplitude, with a strong source of inhibition completely eliminating the PIC (Kuo, 2003). Thus in the present study, changes in PIC amplitude were attributed primarily to changes in level of inhibition.

Chapter 2, Supplemental Figure.

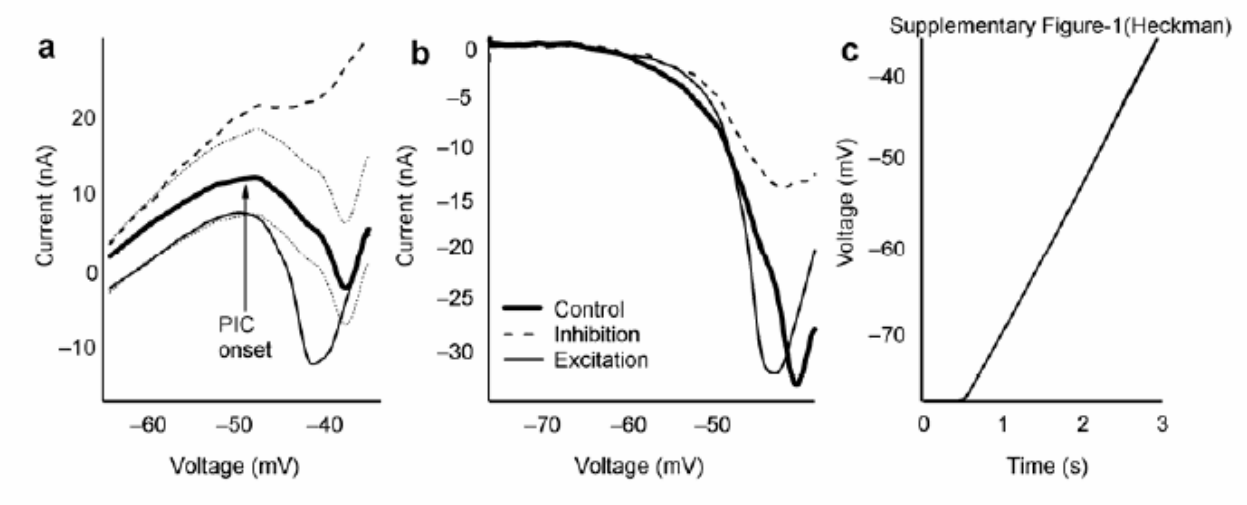

Chapter 2, Table 1.

Table 1 Descriptive statistics of PIC amplitudes for all conditions and ankle joint positions[a]

Condition	Intact	Intact	Reciprocal inhibition diminished	Cutaneous denervation
Degrees	±10	±30	±10	±10
No. of cells	18	11	16	8
Ankle extension:				
Mean ± s.d.	6.5 ± 5.7	10.9 ± 8.4	12.5 ± 7.5	8.1 ± 5.4
Minimum	1.4	2.8	2.6	3.0
Maximum	22.0	31.6	27.2	18.8
Midpoint 1:				
Mean ± s.d.	8.8 ± 5.7	13.2 ± 9.5	10.0 ± 7.0	10.0 ± 5.6
Minimum	3.54	4.07	2.2	3.0
Maximum	23.6	37.15	24.6	18.5
Midpoint 2:				
Mean ± s.d.	8.4 ± 6.3	11.84 ± 7.2	12.7 ± 7.5	8.5 ± 4.7
Minimum	2.3	3.40	3.4	2.6
Maximum	26.6	28.41	28.6	17.3
Average (mid 1, mid 2):				
Mean ± s.d.	8.6 ± 5.9	12.3 ± 8.6	n/a	9.2 ± 4.9
Minimum	3.2	3.7		4.0
Maximum	25.1	32.3		17.9
Ankle flexion:				
Mean ± s.d.	11.7 ± 5.9	14.9 ± 8.0	12.4 ± 8.1	11.5 ± 4.2
Minimum	5.7	7.5	4.0	6.5
Maximum	25.0	34.7	31.0	17.3

[a]PIC amplitudes were measured in nanoamperes.

Chapter 2, Table 2.

Table 2 *P* values for *t*-tests performed on PIC amplitudes

Condition	Intact	Intact	Reciprocal inhibition diminished	Cutaneous denervation
Degrees	±10	±30	±10	±10
Mid 1–mid 2	0.23	0.16	0.0087*	0.164
Average (mid 1, mid 2)–extension	0.0004*	0.05	0.013*	0.026
Average (mid 1, mid 2)–flexion	0.0018*	0.02	0.006*	0.012*
Flexion-extension	<0.0001*	0.0003*	0.87	0.004*

Asterisks indicate significant differences.

Chapter 3, Figure 1.

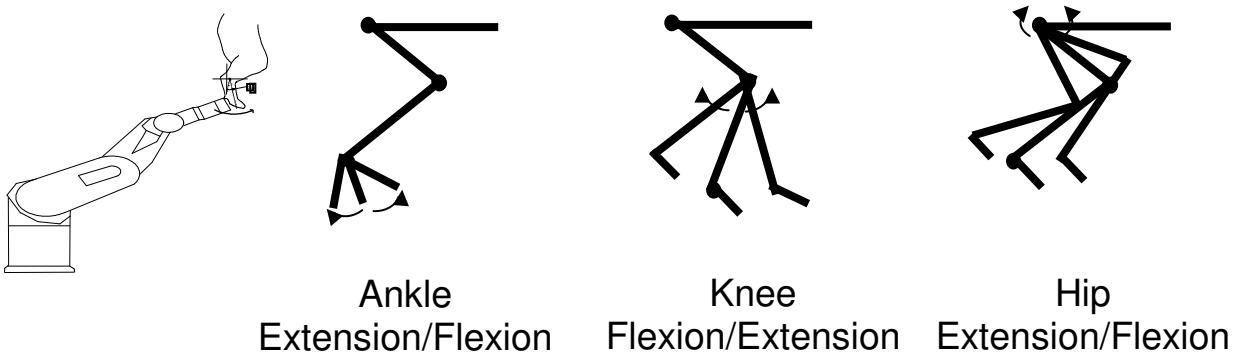

Chapter 3, Figure 1: Schematic of the robot and hindlimb configuration. The plantar surface of the paw is attached to the robot and positioned to allow full range of motion of the ankle. The distance from the center of rotation of the ankle, knee and hip joints to the end point of the robotic arm is calculated to allow precise (± 2 mm) and reliable rotations around each joint. The computer controlled robotic arm flexed and extended the ankle (± 15°), knee (± 15°) and hip (± 10°).

Chapter 3, Figure 2.

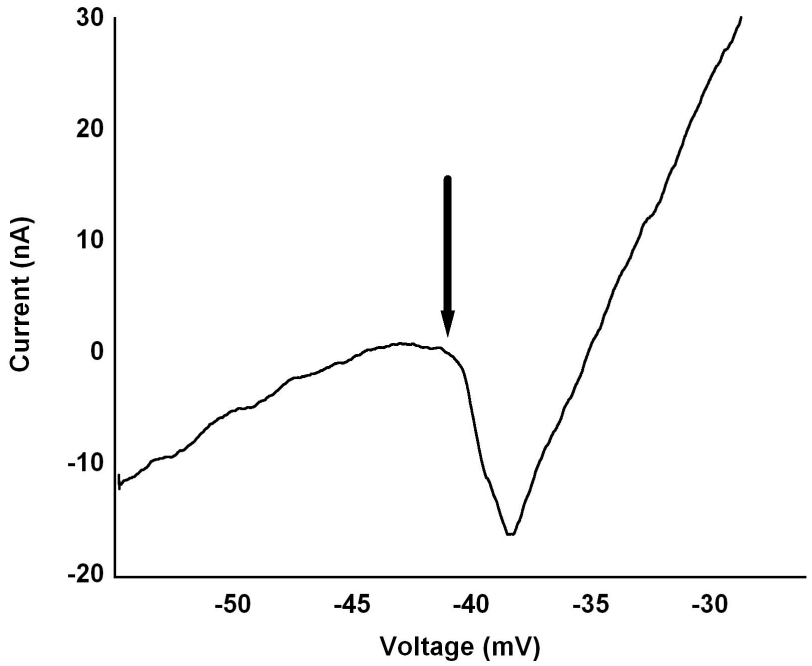

Chapter 3, Figure 2: Current-voltage (I/V) relationship for 1 cell from the cord intact condition. During voltage clamp, the PIC manifests as a downward deflection (arrow) that results in a negative slope region. As the cell is further depolarized, outward conductances are activated which restore the positive slope of the current trace. Since the cell is effectively clamped at the soma, the measured PIC is primarily dendritic. To assess the impact of the PIC on the MRRF, a voltage step to the onset of the PIC is applied. For this cell, a 15 mV step was applied (see Fig.3).

Chapter 3, Figure 3.

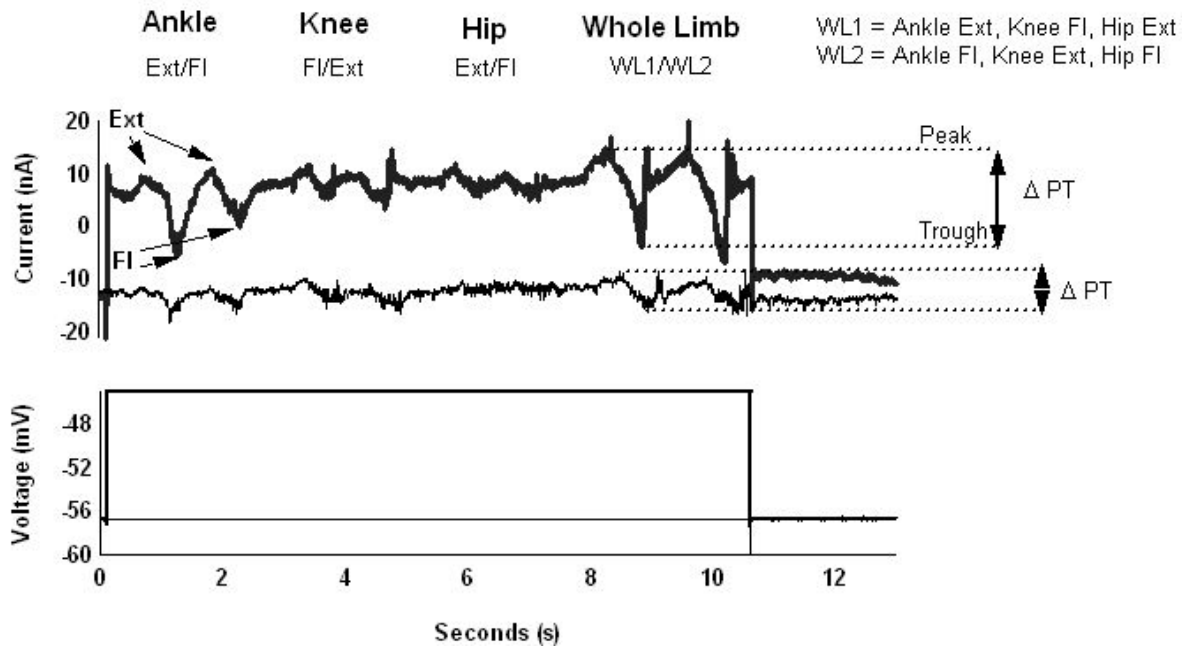

Chapter 3, Figure 3: Intracellular response of an ankle extensor motoneuron to the movement and voltage clamp protocols from the decerebrate, cord intact condition. The movement related I_N was recorded while the ankle, knee, hip were flexed and extended (2 repetitions) individually and then in a combination whole limb movement. To examine the effects of the PIC, the movement was repeated at a voltage where the PIC is activated (bottom panel, dark trace, see Fig. 1 for I/V function of this cell) and hyperpolarized to PIC onset (bottom panel, thin trace). To assess the movement related I_N, for each movement the peak to trough difference in I_N was calculated (ΔPT, see arrows) for each movement repetition and averaged. Note for each movement, the ΔPT is larger in the depolarized condition. As was generally seen in cells from the decerebrate, cord intact condition, the order of ΔPT amplitude in descending amplitude was whole limb, ankle, knee, and hip. This indicates a focused MRRF that is dominated by Ia muscle afferent pathways.

Chapter 3, Figure 4.

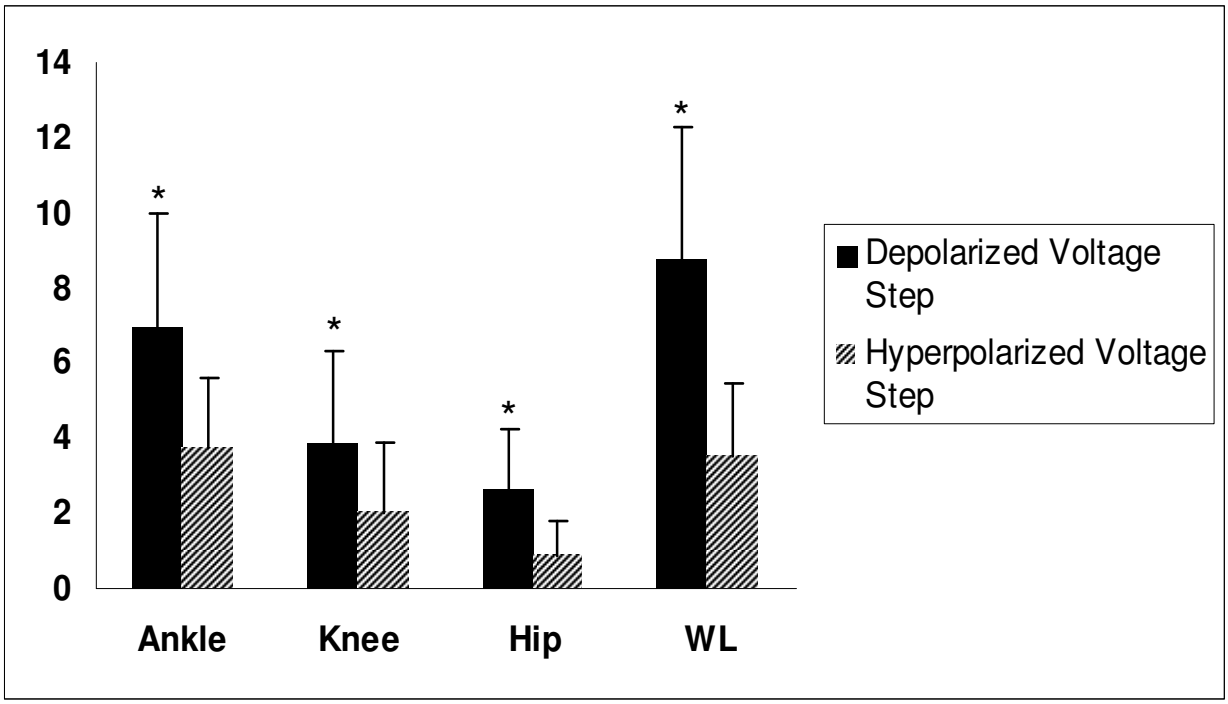

Chapter 3, Figure 4: The mean ΔPT amplitudes and standard deviations (error bars) of ankle extensor motoneurons for the depolarized and hyperpolarized voltage conditions. For each joint movement, the ΔPT was significantly greater in the depolarized voltage condition than in the hyperpolarized voltage condition. PICs thus enhanced all movement related synaptic input.

Chapter 3, Figure 5: The average ΔPT amplitudes for each movement for all MG/LGS, vastus medialus (VM), and rectus femorus (RF) motoneurons in the decerebrate, cord intact condition. **A.** The ΔPT amplitudes for the MG/LGS motoneurons (n = 15). MG/LG are bi-articular muscles, crossing the ankle and knee joints. There primary action is to extend the ankle, but they also have a flexion moment at the knee. In three cells (dashed lines), data were only collected for the single joint movements. As noted in Figure 3, the order of ΔPT amplitude was whole limb, ankle, knee, and hip. **B.** The ΔPT amplitudes for vastus medialus motoneurons (n = 5). Vastus medialus is a uni-articular knee extensor. The order of average ΔPT amplitudes was WL> knee > hip > ankle. **C.** The ΔPT amplitudes for RF cells (n = 6). RF is a bi-articular muscle, which crosses the knee and hip joint. RF primarily extends the knee, but also flexes the hip. The order of the averaged ΔPT amplitudes was WL> knee = hip > ankle. In 3 of the 6 cells, hip ΔPT was larger than knee and in the other 3, knee ΔPT was greater than hip ΔPT. This is not unexpected as RF receives heteronymous Ia input from knee extensors and hip flexors.

Chapter 3, Figure 5.

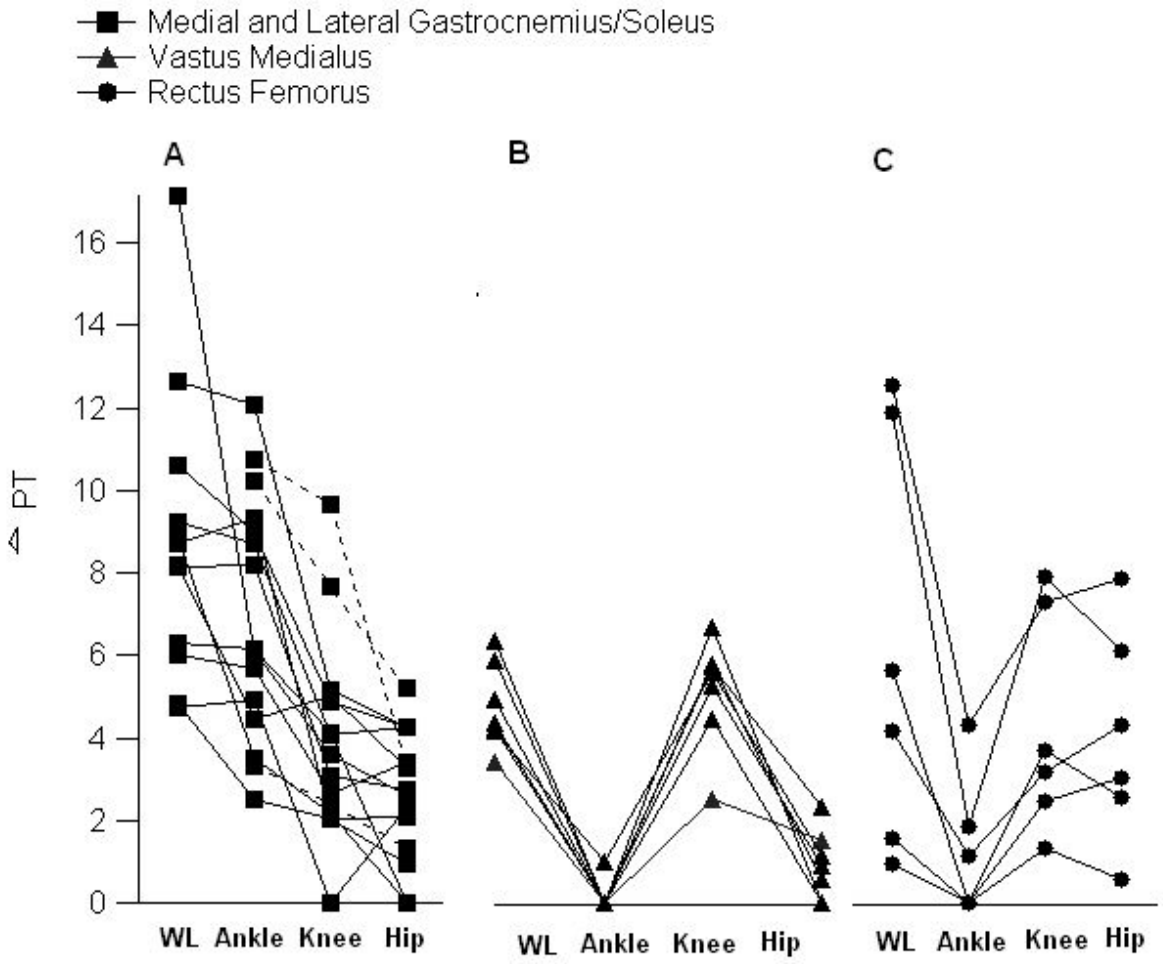

Chapter 3, Figure 6: Reciprocal inhibition is important in shaping the amplitude of the movement related modulations of I_N. **A.** The change in length (cms) of tibialis anterior (solid line) and medial gastrocnemius (hatched line) as the robot extends and flexes the ankle. Muscle length changes were estimated using the muscle model developed by Burkholder and Nichols (2004). **B.** Robot trajectory as the ankle is extended and flexed ± 15°s (arrows). **C**. Current recorded from two separated MG motoneurons during ankle movements with reciprocal inhibition present (tendon intact, black trace) and reciprocal inhibition diminished (tendon cut, gray trace) in the decerebrate preparation. Note that in the tendon intact condition the current trace more closely follows the triangular shape of the robot trajectory and change in muscle length. In the tendon cut sample (n = 9), the change in IΔPT was significantly less than in the tendon intact sample (n = 15) (depolarized voltage condition, student's t-test, $p < 0.03$).

Chapter 3, Figure 6.

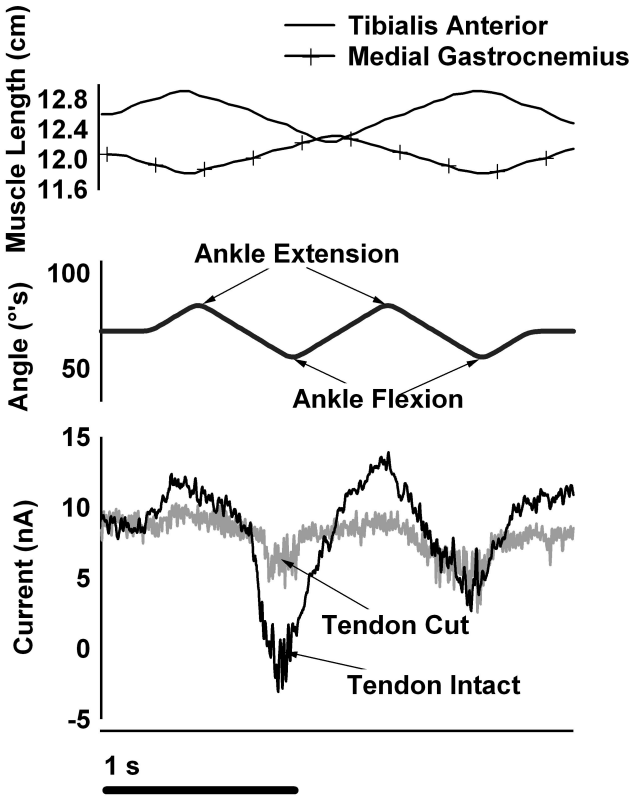

Chapter 3, Figure 7: The ΔPT for each joint movement for all MG/LGS, VM, and RF cells in the decerebrate, spinalized condition. A. The ΔPT for MG/LGS (n = 12). On average, the order of ΔPT amplitude for MG/LGS cells was WL > ankle = hip > knee. This represented an increase in the average hip ΔPT as compared to the cord intact sample (hyperpolarized voltage condition, ANOVA, Bonferroni Post Hoc, p = 0.0001). Note in only 2/12 cells (dashed lines) was hip ΔPT < knee ΔPT. **B.** The ΔPT for VM cells (n = 9). The overall patter of the ΔPT amplitude was WL > knee=hip > ankle. As with the MG/LGS cells, this represented an increase in the hip movement related I_N as compared to the cord intact sample (ANOVA, Bonferroni Post Hoc, p < 0.002). **C.** The ΔPT for RF cells (n = 5). In contrast to the MG/LGS and VM samples, RF pattern of ΔPT amplitudes remained the same as in the intact condition where WL > knee = hip> ankle.

Chapter 3, Figure 7.

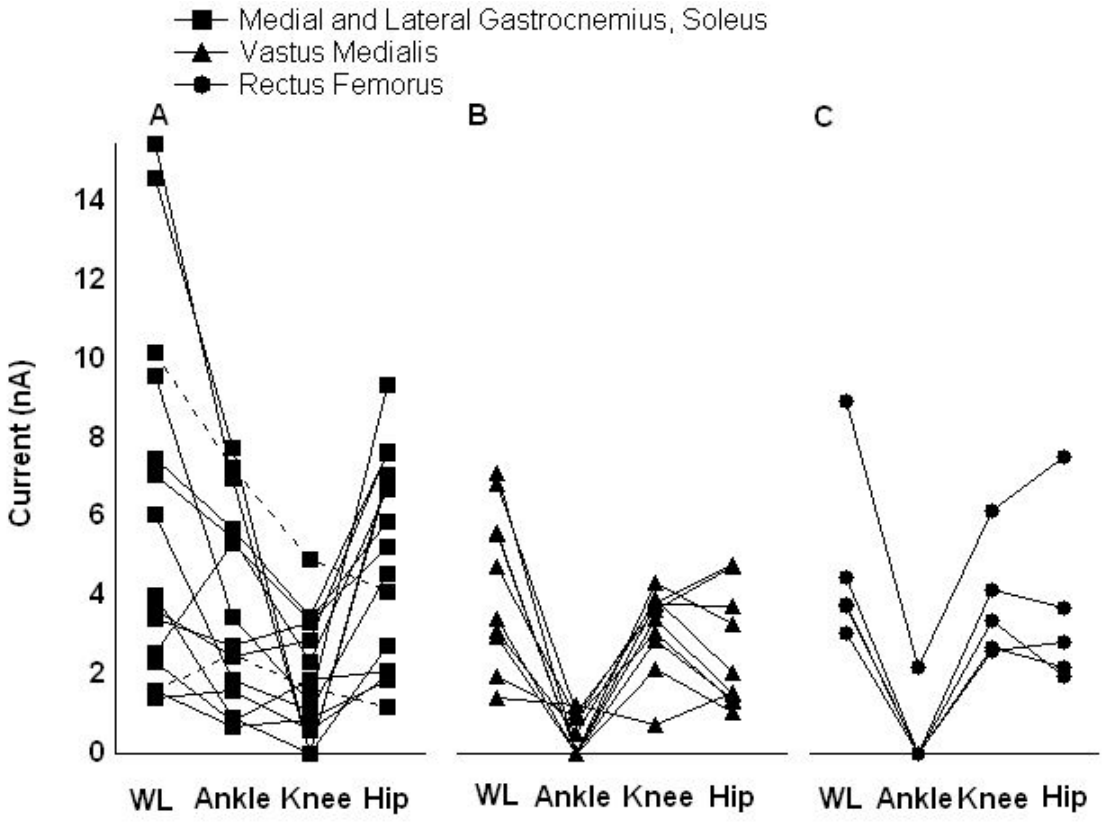

Chapter 3, Figure 8.

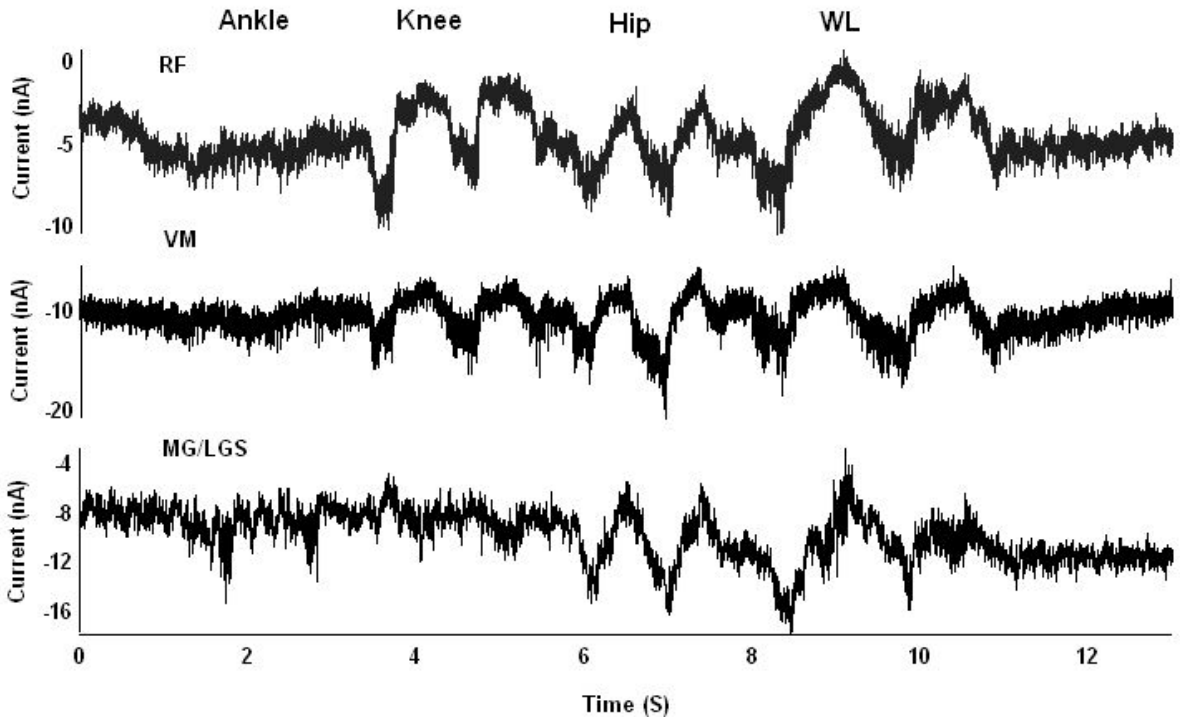

Chapter 3, Figure 8: Spinalization resulted in the widening of the MRRF for MG/LGS and VM cells, but not RF cells. The panels show the current traces of individual cells from the hyperpolarized voltage condition. Similar to the intact cord condition, RF shows strong modulation to hip and knee movements (top panel). In contrast with their MRRF in the intact cord condition, both the VM (middle panel) and MG (bottom panel) show an increased modulation to hip movements. Note in the MG cell example, the hip modulation is equal if not larger than the ankle modulation in I_N.

Chapter 3, Table 1. The mean ΔPT values for each single and multi-joint movement for both the cord intact and acutely spinalized condition. In the spinalized condition, the ΔPT was not significantly different between the depolarized and hyperpolarized condition (paired t-test, $p \geq 0.05$) and the ΔPTs were subsequently averaged together.

Joint Movement	Depolarized Cord Intact (n=15)	Hyperpolarized Cord Intact (n=15)	Spinalized (n=14)
Ankle Ext/FL			
Mean ΔPT ± STD	6.9 nA ± 2.9	3.7 nA ± 1.8	3.7 nA ± 2.5
Min	2.5 nA	1.3 nA	0.8 nA
Max	12.1nA	7.6 nA	7.2 nA
Knee FL/Ext			
Mean ΔPT ± STD	3.9 nA ± 2.4	2.0 nA ± 1.9	2.0 nA ± 1.5
Min	0.0 nA	0.6 nA	0.0 nA
Max	9.7 nA	5.5 nA	4.9 nA
Hip FL/Ext			
Mean ΔPT ± STD	2.6 nA ± 1.5	0.9 nA ± 0.9	5.0 nA ± 2.6
Min	0.0 nA	0.0 nA	1.2 nA
Max	5.2 nA	2.8 nA	7.7 nA
WL1/WL2	(n=12)	(n=12)	
Mean ΔPT ± STD	8.7 nA ± 3.5	3.5 nA ± 1.9	5.3 nA ± 3.9
Min	4.7 nA	1.2 nA	1.0 nA
Max	17.2 nA	6.5 nA	14 nA

Chapter 3, Table 2. The mean IΔPTs and EΔPTs for the cord intact and acutely spinalized conditions.

Joint Movement	IΔPTs Depolarized Cord Intact (n=15)	EΔPTs Depolarized Cord Intact (n=15)	IΔPTs Hyperpolarized Cord Intact (n=15)	EΔPTs Hyperpolarized Cord Intact (n=15)	IΔPTs Spinalized (n = 14)	EΔPTs Spinalized (n = 14)
Ankle Ext/FL						
Mean ΔPT ± STD	2.7 nA ± 2.3	4.8 nA ± 2.1	1.2 nA ± 2.1	2.8 nA ± 1.7	1.8 nA ± 2.1	2.3 nA ± 1.8
Min	0.5	1.1	0.2	1.25	0.0	.4
Max	9.1	8.1	7.2	5.8	7.9	6.0
Knee Fl/Ext						
Mean ΔPT ± STD	1.8 nA ± 1.2	2.0 nA ± 1.2	.2 nA ± .85	1.6 nA ± 1.5	1.3 nA ± 1.7	1.72 nA ± 2.1
Min	.22	.22	0	0.6	0.0	0
Max	3.9	3.9	2.1	5.2	5.2	7.2
Hip						
Mean ΔPT ± STD	1.7 nA ± 0.9	1.2 nA ± 0.9	0.6 nA ± 0.8	0.6 ± 0.7	2.3 nA ± 2.5	4.0 nA ± 2.6
Min	0.7	0.2	0.3	0.2	0.0	.3
Max	3.9	2.8	2.8	1.7	9.9	9.3
WL1/WL2						
Mean ΔPT ± STD	2.8 nA ± 1.8	6.1 ± 2.6	1.6 ± 2.2	1.8 ± 2.5	4.4 nA ± 2.3	5.8 nA ± 3.1
Min	0.9	2.9	0.5	0.9	1.7	.1
Max	6.1	9.3	2.6	4.6	8.7	11.2

References

Alaburda, A. and J. Hounsgaard (2003). "Metabotropic modulation of motoneurons by scratch-like spinal network activity." J Neurosci **23**(25): 8625-9.

Alaburda, A., J. F. Perrier, et al. (2002). "Mechanisms causing plateau potentials in spinal motoneurones." Adv Exp Med Biol **508**: 219-26.

Alvarez, F. e. a. (1998). "Distribution of 5-hydroxytryptamine immunoreactive boutons on alpha motoneurons in the lumbar spinal cord of adult cats." J Comp Neurol **393**: 69-83.

Alvarez, F. J., J. C. Pearson, et al. (1998). "Distribution of 5-hydroxytryptamine-immunoreactive boutons on alpha-motoneurons in the lumbar spinal cord of adult cats." J Comp Neurol **393**(1): 69-83.

Alzheimer, C., P. C. Schwindt, et al. (1993). "Postnatal development of a persistent Na+ current in pyramidal neurons from rat sensorimotor cortex." J Neurophysiol **69**(1): 290-2.

Anelli, R., L. Sanelli, et al. (2007). "Expression of L-type calcium channel alpha(1)-1.2 and alpha(1)-1.3 subunits on rat sacral motoneurons following chronic spinal cord injury." Neuroscience **145**(2): 751-63.

Aston-Jones, G., S. Chen, et al. (2001). "A neural circuit for circadian regulation of arousal." Nat Neurosci **4**(7): 732-8.

Aston-Jones, G., J. Rajkowski, et al. (2000). "Locus coeruleus and regulation of behavioral flexibility and attention." Prog Brain Res **126**: 165-82.

Baldissera, Hultborn, et al. (1981). Integration in spinal neuronal systems. Handbook of Physiology. B. VB. Bethesda, American Physiological Society**:** 509-595.

Baldissera F, H. H., and Illert M (1981). Integration in spinal neuronal systems. Handbook of Physiology. B. VB. Bethesda, American Physiological Society**:** 509-595.

Bannatyne, B. A., S. A. Edgley, et al. (2006). "Differential projections of excitatory and inhibitory dorsal horn interneurons relaying information from group II muscle afferents in the cat spinal cord." J Neurosci **26**(11): 2871-80.

Barrett, J. N. and W. E. Crill (1971). "Specific membrane resistivity of dye-injected cat motoneurons." Brain Res **28**(3): 556-61.

Barrett, J. N. and W. E. Crill (1974). "Influence of dendritic location and membrane properties on the effectiveness of synapses on cat motoneurones." J Physiol **239**(2): 325-45.

Barrett, J. N. and W. E. Crill (1974). "Specific membrane properties of cat motoneurones." J Physiol **239**(2): 301-24.

Bennett, D. J., H. Hultborn, et al. (1998). "Short-term plasticity in hindlimb motoneurons of decerebrate cats." J Neurophysiol **80**(4): 2038-45.

Bennett, D. J., H. Hultborn, et al. (1998). "Synaptic activation of plateaus in hindlimb motoneurons of decerebrate cats." J Neurophysiol **80**(4): 2023-37.

Bennett, D. J., Y. Li, et al. (2001). "Plateau potentials in sacrocaudal motoneurons of chronic spinal rats, recorded in vitro." J Neurophysiol **86**(4): 1955-71.

Bennett, D. J., L. Sanelli, et al. (2004). "Spastic long-lasting reflexes in the awake rat after sacral spinal cord injury." J Neurophysiol **91**(5): 2247-58.

Berg, R. W., A. Alaburda, et al. (2007). "Balanced inhibition and excitation drive spike activity in spinal half-centers." Science **315**(5810): 390-3.

Binder, M. D. (1996). The physiological control of motoneuron activity. Handbook of Physiology. L. Rowell and J. Sheperd. New York, Oxford University Press**:** 3-53.

Binder, M. D., C. J. Heckman, et al. (1993). "How different afferent inputs control motoneuron discharge and the output of the motoneuron pool." Curr Opin Neurobiol **3**(6): 1028-34.

Binder, M. D., C. J. Heckman, et al. (2002). "Relative strengths and distributions of different sources of synaptic input to the motoneurone pool: implications for motor unit recruitment." Adv Exp Med Biol **508**: 207-12.

Binder, M. D. and R. K. Powers (1999). "Synaptic integration in spinal motoneurones." J Physiol Paris **93**(1-2): 71-9.

Binder, M. D., F. R. Robinson, et al. (1998). "Distribution of effective synaptic currents in cat triceps surae motoneurons. VI. Contralateral pyramidal tract." J Neurophysiol **80**(1): 241-8.

Bjorklund, A. and G. Skagerberg (1982). Descending monoaminergic projections to the spinal cord. Brainstem Control of Spinal Mechanisms. S. B and B. A. Amsterdam, Elsevier Biomedical Press**:** 55-88.

Boorman, G. I., R. G. Lee, et al. (1996). "Impaired "natural reciprocal inhibition" in patients with spasticity due to incomplete spinal cord injury." Electroencephalogr Clin Neurophysiol **101**(2): 84-92.

Bowery, N. G., B. Bettler, et al. (2002). "International Union of Pharmacology. XXXIII. Mammalian gamma-aminobutyric acid(B) receptors: structure and function." Pharmacol Rev **54**(2): 247-64.

Brannstrom, T. (1993). "Quantitative synaptology of functionally different types of cat medial gastrocnemius alpha-motoneurons." J Comp Neurol **330**(3): 439-54.

Brock, L. G., J. S. Coombs, et al. (1952). "The recording of potentials from motoneurones with an intracellular electrode." J Physiol **117**(4): 431-60.

Brock, L. G., J. S. Coombs, et al. (1953). "Intracellular recording from antidromically activated motoneurones." J Physiol **122**(3): 429-61.

Brown, A. G. and R. E. Fyffe (1978). "The morphology of group Ia afferent fibre collaterals in the spinal cord of the cat." J Physiol **274**: 111-27.

Brown, A. G. and R. E. Fyffe (1981). "Direct observations on the contacts made between Ia afferent fibres and alpha-motoneurones in the cat's lumbosacral spinal cord." J Physiol **313**: 121-40.

Brown, A. M., P. C. Schwindt, et al. (1994). "Different voltage dependence of transient and persistent Na+ currents is compatible with modal-gating hypothesis for sodium channels." J Neurophysiol **71**(6): 2562-5.

Brownstone, R. M., J. P. Gossard, et al. (1994). "Voltage-dependent excitation of motoneurones from spinal locomotor centres in the cat." Exp Brain Res **102**(1): 34-44.

Burke, R. E., L. Fedina, et al. (1971). "Spatial synaptic distribution of recurrent and group Ia inhibitory systems in cat spinal motoneurones." J Physiol **214**(2): 305-26.

Burke, R. E. and L. L. Glenn (1996). "Horseradish peroxidase study of the spatial and electrotonic distribution of group Ia synapses on type-identified ankle extensor motoneurons in the cat." J Comp Neurol **372**(3): 465-85.

Burke, R. E., P. L. Strick, et al. (1977). "Anatomy of medial gastrocnemius and soleus motor nuclei in cat spinal cord." J Neurophysiol **40**(3): 667-80.

Burke, R. E., B. Walmsley, et al. (1979). "HRP anatomy of group Ia afferent contacts on alpha motoneurones." Brain Res **160**(2): 347-52.

Burkholder, T. J. and T. R. Nichols (2004). "Three-dimensional model of the feline hindlimb." J Morphol **261**(1): 118-29.

Cao, C. Q., R. H. Evans, et al. (1995). "A comparison of the effects of selective metabotropic glutamate receptor agonists on synaptically evoked whole cell currents of rat spinal ventral horn neurones in vitro." Br J Pharmacol **115**(8): 1469-74.

Cao, J., D. O'Donnell, et al. (1998). "Cloning and characterization of a cDNA encoding a novel subtype of rat thyrotropin-releasing hormone receptor." J Biol Chem **273**(48): 32281-7.

Carlin, K. P., Z. Jiang, et al. (2000). "Characterization of calcium currents in functionally mature mouse spinal motoneurons." Eur J Neurosci **12**(5): 1624-34.

Carlin, K. P., K. E. Jones, et al. (2000). "Dendritic L-type calcium currents in mouse spinal motoneurons: implications for bistability." Eur J Neurosci **12**(5): 1635-46.

Chance, F. S., L. F. Abbott, et al. (2002). "Gain modulation from background synaptic input." Neuron **35**(4): 773-82.

Chau, C., H. Barbeau, et al. (1998). "Effects of intrathecal alpha1- and alpha2-noradrenergic agonists and norepinephrine on locomotion in chronic spinal cats." J Neurophysiol **79**(6): 2941-63.

Chen, D., R. D. Theiss, et al. (2001). "Spinal interneurons that receive input from muscle afferents are differentially modulated by dorsolateral descending systems." J Neurophysiol **85**(2): 1005-8.

Chen, D. F., M. Bianchetti, et al. (1987). "The adrenergic agonist tizanidine has differential effects on flexor reflexes of intact and spinalized rat." Neuroscience **23**(2): 641-7.

Chen, X. Y., L. Chen, et al. (2006). "Operant conditioning of reciprocal inhibition in rat soleus muscle." J Neurophysiol **96**(4): 2144-50.

Chen, Y., X. Y. Chen, et al. (2005). "The interaction of a new motor skill and an old one: H-reflex conditioning and locomotion in rats." J Neurosci **25**(29): 6898-906.

Cleland, C. L. and W. Z. Rymer (1990). "Neural mechanisms underlying the clasp-knife reflex in the cat. I. Characteristics of the reflex." J Neurophysiol **64**(4): 1303-18.

Cleland, C. L. and W. Z. Rymer (1993). "Functional properties of spinal interneurons activated by muscular free nerve endings and their potential contributions to the clasp-knife reflex." J Neurophysiol **69**(4): 1181-91.

Clements, J. D., P. G. Nelson, et al. (1986). "Intracellular tetraethylammonium ions enhance group Ia excitatory post-synaptic potentials evoked in cat motoneurones." J Physiol **377**: 267-82.

Collins, D. F., D. Burke, et al. (2001). "Large involuntary forces consistent with plateau-like behavior of human motoneurons." J Neurosci **21**(11): 4059-65.

Collins, D. F., D. Burke, et al. (2002). "Sustained contractions produced by plateau-like behaviour in human motoneurones." J Physiol **538**(Pt 1): 289-301.

Collo, G., R. A. North, et al. (1996). "Cloning OF P2X5 and P2X6 receptors and the distribution and properties of an extended family of ATP-gated ion channels." J Neurosci **16**(8): 2495-507.

Conn, P. J. and J. P. Pin (1997). "Pharmacology and functions of metabotropic glutamate receptors." Annu Rev Pharmacol Toxicol **37**: 205-37.

Conway, B. A., H. Hultborn, et al. (1988). "Plateau potentials in alpha-motoneurones induced by intravenous injection of L-dopa and clonidine in the spinal cat." J Physiol **405**: 369-84.

Coombs, J. S., J. C. Eccles, et al. (1955). "The electrical properties of the motoneurone membrane." J Physiol **130**(2): 291-325.

Crill, W. E. (1996). "Persistent sodium current in mammalian central neurons." Annu Rev Physiol **58**: 349-62.

Crone, C., H. Hultborn, et al. (1987). "Reciprocal Ia inhibition between ankle flexors and extensors in man." J Physiol **389**: 163-85.

Crone, C., L. L. Johnsen, et al. (2003). "Appearance of reciprocal facilitation of ankle extensors from ankle flexors in patients with stroke or spinal cord injury." Brain **126**(Pt 2): 495-507.

Crone, C., J. Nielsen, et al. (1994). "Disynaptic reciprocal inhibition of ankle extensors in spastic patients." Brain **117 (Pt 5)**: 1161-8.

Cullheim, S., J. W. Fleshman, et al. (1987). "Membrane area and dendritic structure in type-identified triceps surae alpha motoneurons." J Comp Neurol **255**(1): 68-81.

Cullheim, S., J. W. Fleshman, et al. (1987). "Three-dimensional architecture of dendritic trees in type-identified alpha-motoneurons." J Comp Neurol **255**(1): 82-96.

Curtis, D. R. and G. Lacey (1994). "GABA-B receptor-mediated spinal inhibition." Neuroreport **5**(5): 540-2.

Curtis, D. R. and G. Lacey (1998). "Prolonged GABA(B) receptor-mediated synaptic inhibition in the cat spinal cord: an in vivo study." Exp Brain Res **121**(3): 319-33.

Cushing, S., T. Bui, et al. (2005). "Effect of nonlinear summation of synaptic currents on the input-output properties of spinal motoneurons." J Neurophysiol **94**(5): 3465-78.

Del Negro, C. A. and S. H. Chandler (1998). "Regulation of intrinsic and synaptic properties of neonatal rat trigeminal motoneurons by metabotropic glutamate receptors." J Neurosci **18**(22): 9216-26.

Delgado-Lezama, R., J. F. Perrier, et al. (1999). "Local facilitation of plateau potentials in dendrites of turtle motoneurones by synaptic activation of metabotropic receptors." J Physiol **515 (Pt 1)**: 203-7.

Delgado-Lezama, R., J. F. Perrier, et al. (1997). "Metabotropic synaptic regulation of intrinsic response properties of turtle spinal motoneurones." J Physiol **504 (Pt 1)**: 97-102.

Derjean, D., S. Bertrand, et al. (2005). "Plateau potentials and membrane oscillations in parasympathetic preganglionic neurones and intermediolateral neurones in the rat lumbosacral spinal cord." J Physiol **563**(Pt 2): 583-96.

Destexhe, A., M. Rudolph, et al. (2003). "The high-conductance state of neocortical neurons in vivo." Nat Rev Neurosci **4**(9): 739-51.

Eccles, J. C., R. M. Eccles, et al. (1957). "The convergence of monosynaptic excitatory afferents on to many different species of alpha motoneurones." J Physiol **137**(1): 22-50.

Eccles, J. C., R. M. Eccles, et al. (1957). "Synaptic actions on motoneurones in relation to the two components of the group I muscle afferent volley." J Physiol **136**(3): 527-46.

Eccles, R. M. and A. Lundberg (1958). "Integrative pattern of Ia synaptic actions on motoneurones of hip and knee muscles." J Physiol **144**(2): 271-98.

Eccles, R. M. and A. Lundberg (1959). "Supraspinal control of interneurones mediating spinal reflexes." J Physiol **147**: 565-84.

Edgley, S., E. Jankowska, et al. (1986). "The heteronymous monosynaptic actions of triceps surae group Ia afferents on hip and knee extensor motoneurones in the cat." Exp Brain Res **61**(2): 443-6.

Edgley, S. A. and E. Jankowska (1987). "An interneuronal relay for group I and II muscle afferents in the midlumbar segments of the cat spinal cord." J Physiol **389**: 647-74.

Elbasiouny, S. M., D. J. Bennett, et al. (2005). "Simulation of dendritic CaV1.3 channels in cat lumbar motoneurons: spatial distribution." J Neurophysiol **94**(6): 3961-74.

Elbasiouny, S. M., D. J. Bennett, et al. (2006). "Simulation of Ca2+ persistent inward currents in spinal motoneurones: mode of activation and integration of synaptic inputs." J Physiol **570**(Pt 2): 355-74.

Fedirchuk, B. and Y. Dai (2004). "Monoamines increase the excitability of spinal neurones in the neonatal rat by hyperpolarizing the threshold for action potential production." J Physiol **557**(Pt 2): 355-61.

Frick, A. and D. Johnston (2005). "Plasticity of dendritic excitability." J Neurobiol **64**(1): 100-15.

Furuyama, T., H. Kiyama, et al. (1993). "Region-specific expression of subunits of ionotropic glutamate receptors (AMPA-type, KA-type and NMDA receptors) in the rat spinal cord with special reference to nociception." Brain Res Mol Brain Res **18**(1-2): 141-51.

Fyffe (2001). Spinal Motoneurons:Synaptic Inputs and Receptor Organization. Motor Neurobiology of the Spinal Cord. T. C. Cope. London, CRC Press.

Fyffe, R. E. (1991). "Spatial distribution of recurrent inhibitory synapses on spinal motoneurons in the cat." J Neurophysiol **65**(5): 1134-49.

Gladden, M. H., D. J. Maxwell, et al. (2000). "Coupling between serotoninergic and noradrenergic neurones and gamma-motoneurones in the cat." J Physiol **527 Pt 2**: 213-23.

Goldin, A. L. (2001). "Resurgence of sodium channel research." Annu Rev Physiol **63**: 871-94.

Gorassini, M., J. F. Yang, et al. (2002). "Intrinsic activation of human motoneurons: possible contribution to motor unit excitation." J Neurophysiol **87**(4): 1850-8.

Gorassini, M. A., M. E. Knash, et al. (2004). "Role of motoneurons in the generation of muscle spasms after spinal cord injury." Brain.

Gorassini, M. A., M. E. Knash, et al. (2004). "Role of motoneurons in the generation of muscle spasms after spinal cord injury." Brain **127**(Pt 10): 2247-58.

Goslow, G. E., Jr., E. K. Stauffer, et al. (1973). "The cat step cycle; responses of muscle spindles and tendon organs to passive stretch within the locomotor range." Brain Res **60**(1): 35-54.

Grande, G., T. V. Bui, et al. (2007). "Estimates of the location of L-type Ca2+ channels in motoneurons of different sizes: a computational study." J Neurophysiol **97**(6): 4023-35.

Gulledge, A. T., B. M. Kampa, et al. (2005). "Synaptic integration in dendritic trees." J Neurobiol **64**(1): 75-90.

Gutman, A. (1991). "Bistability of Dendrites." Int j Neural Sys 1 **1**: 291-304.

Haider, B., A. Duque, et al. (2006). "Neocortical network activity in vivo is generated through a dynamic balance of excitation and inhibition." J Neurosci **26**(17): 4535-45.

Hammar, I. and E. Jankowska (2003). "Modulatory effects of alpha1-,alpha2-, and beta -receptor agonists on feline spinal interneurons with monosynaptic input from group I muscle afferents." J Neurosci **23**(1): 332-8.

Harris-Warrick, R. M. (2002). "Voltage-sensitive ion channels in rhythmic motor systems." Curr Opin Neurobiol **12**(6): 646-51.

Harvey, P. J., Y. Li, et al. (2006). "Persistent sodium currents and repetitive firing in motoneurons of the sacrocaudal spinal cord of adult rats." J Neurophysiol **96**(3): 1141-57.

Hausser, M., N. Spruston, et al. (2000). "Diversity and dynamics of dendritic signaling." Science **290**(5492): 739-44.

Heckman, C. J. (2003). "Active conductances in motoneuron dendrites enhance movement capabilities." Exerc Sport Sci Rev **31**(2): 96-101.

Heckman, C. J. and M. D. Binder (1988). "Analysis of effective synaptic currents generated by homonymous Ia afferent fibers in motoneurons of the cat." J Neurophysiol **60**(6): 1946-66.

Heckman, C. J., M. A. Gorassini, et al. (2005). "Persistent inward currents in motoneuron dendrites: implications for motor output." Muscle Nerve **31**(2): 135-56.

Heckman, C. J. and R. H. Lee (2001). Advances in Measuring Active Dendritic Currents in Spinal Motoneurons *in Vivo*. Motor Neurobiology of the Spinal Cord. T. C. Cope. Boca Raton, CRC Press**:** 89-106.

Heckman, C. J., R. H. Lee, et al. (2003). "Hyperexcitable dendrites in motoneurons and their neuromodulatory control during motor behavior." Trends Neurosci **26**(12): 688-95.

Heckman, C. J., J. F. Miller, et al. (1994). "Reduction in postsynaptic inhibition during maintained electrical stimulation of different nerves in the cat hindlimb." J Neurophysiol **71**(6): 2281-93.

Henneman, E. and L. M. Mendell (1981). Functional organization of the motoneuron pool and its inputs. Handbook of Physiology,The Nervous System, Motor Control, American Physiological Society. **1, part 1:** 423-507.

Hiebert, G. W., P. J. Whelan, et al. (1996). "Contribution of hind limb flexor muscle afferents to the timing of phase transitions in the cat step cycle." J Neurophysiol **75**(3): 1126-37.

Hille, B. (2001). Ion Channels of Excitable Membranes. Sunderland, Sinauer Associates.

Hochman, S., S. Garraway, et al. (2001). 5-HT Receptors and the Neuromodulatory Control of Spinal Receptors. Motor Neurobiology of the Spinal Cord. T. C. Cope. Boca Raton, CRC Press**:** 47-88.

Hollmann, M., M. Hartley, et al. (1991). "Ca2+ permeability of KA-AMPA--gated glutamate receptor channels depends on subunit composition." Science **252**(5007): 851-3.

Holmqvist, B. and A. Lundberg (1961). "Differential supraspinal control of synaptic actions evoked by volleys in the flexion reflex afferents in alpha motoneurones." Acta Physiol Scand Suppl **186**: 1-15.

Hornby, T. G., J. H. Kahn, et al. (2006). "Temporal facilitation of spastic stretch reflexes following human spinal cord injury." J Physiol **571**(Pt 3): 593-604.

Hornby, T. G., J. C. McDonagh, et al. (2002). "Effects of excitatory modulation on intrinsic properties of turtle motoneurons." J Neurophysiol **88**(1): 86-97.

Hornby, T. G., W. Z. Rymer, et al. (2003). "Windup of flexion reflexes in chronic human spinal cord injury: a marker for neuronal plateau potentials?" J Neurophysiol **89**(1): 416-26.

Houk, J. and E. Henneman (1967). "Responses of Golgi tendon organs to active contractions of the soleus muscle of the cat." J Neurophysiol **30**(3): 466-81.

Hounsgaard, J., H. Hultborn, et al. (1988). "Bistability of alpha-motoneurones in the decerebrate cat and in the acute spinal cat after intravenous 5-hydroxytryptophan." J Physiol **405**: 345-67.

Hounsgaard, J. and O. Kiehn (1985). "Ca++ dependent bistability induced by serotonin in spinal motoneurons." Exp Brain Res **57**(2): 422-5.

Hounsgaard, J. and O. Kiehn (1989). "Serotonin-induced bistability of turtle motoneurones caused by a nifedipine-sensitive calcium plateau potential." J Physiol **414**: 265-82.

Hounsgaard, J. and O. Kiehn (1993). "Calcium spikes and calcium plateaux evoked by differential polarization in dendrites of turtle motoneurones in vitro." J Physiol **468**: 245-59.

Hultborn, H., R. B. Brownstone, et al. (2004). "Key mechanisms for setting the input-output gain across the motoneuron pool." Prog Brain Res **143**: 77-95.

Hultborn, H., M. E. Denton, et al. (2003). "Variable amplification of synaptic input to cat spinal motoneurones by dendritic persistent inward current." J Physiol **552**(Pt 3): 945-52.

Hyngstrom, A. S., M. D. Johnson, et al. (2007). "Intrinsic electrical properties of spinal motoneurons vary with joint angle." Nat Neurosci **10**(3): 363-9.

Ishida, M., T. Saitoh, et al. (1993). "A novel metabotropic glutamate receptor agonist: marked depression of monosynaptic excitation in the newborn rat isolated spinal cord." Br J Pharmacol **109**(4): 1169-77.

Jacobs, B. L. and E. C. Azmitia (1992). "Structure and function of the brain serotonin system." Physiol Rev **72**(1): 165-229.

Jacobs, B. L. and C. A. Fornal (1993). "5-HT and motor control: a hypothesis." Trends Neurosci **16**(9): 346-52.

Jacobs, B. L., F. J. Martin-Cora, et al. (2002). "Activity of medullary serotonergic neurons in freely moving animals." Brain Res Brain Res Rev **40**(1-3): 45-52.

Jankowska, E. (1992). "Interneuronal relay in spinal pathways from proprioceptors." Prog Neurobiol **38**(4): 335-78.

Jankowska, E. (2001). "Spinal interneuronal systems: identification, multifunctional character and reconfigurations in mammals." J Physiol **533**(Pt 1): 31-40.

Jankowska, E. and I. Hammar (2002). "Spinal interneurones; how can studies in animals contribute to the understanding of spinal interneuronal systems in man?" Brain Res Brain Res Rev **40**(1-3): 19-28.

Jankowska, E., I. Hammar, et al. (2000). "Effects of monoamines on interneurons in four spinal reflex pathways from group I and/or group II muscle afferents." Eur J Neurosci **12**(2): 701-14.

Jankowska, E., J. S. Riddell, et al. (1993). "Gating of transmission to motoneurones by stimuli applied in the locus coeruleus and raphe nuclei of the cat." J Physiol **461**: 705-22.

Jankowska, E., U. Slawinska, et al. (2002). "On organization of a neuronal network in pathways from group II muscle afferents in feline lumbar spinal segments." J Physiol **542**(Pt 1): 301-14.

Jones, S. M. and R. H. Lee (2006). "Fast amplification of dynamic synaptic inputs in spinal motoneurons in vivo." J Neurophysiol **96**(5): 2200-6.

Kernell, D. (2006). The motoneurone and its muscle fibers. Oxford, Oxford University Press.

Kernell, D. and B. Zwaagstra (1989). "Size and remoteness: two relatively independent parameters of dendrites, as studied for spinal motoneurones of the cat." J Physiol **413**: 233-54.

Krawitz, S., B. Fedirchuk, et al. (2001). "State-dependent hyperpolarization of voltage threshold enhances motoneurone excitability during fictive locomotion in the cat." J Physiol **532**(Pt 1): 271-81.

Kriellaars, D. J., R. M. Brownstone, et al. (1994). "Mechanical entrainment of fictive locomotion in the decerebrate cat." J Neurophysiol **71**(6): 2074-86.

Kuo, J. J., R. H. Lee, et al. (2003). "Active dendritic integration of inhibitory synaptic inputs in vivo." J Neurophysiol **90**(6): 3617-24.

Kurihara, T., H. Suzuki, et al. (1993). "Muscarinic excitatory and inhibitory mechanisms involved in afferent fibre-evoked depolarization of motoneurones in the neonatal rat spinal cord." Br J Pharmacol **110**(1): 61-70.

LaBella, L. A. and D. A. McCrea (1990). "Evidence for restricted central convergence of cutaneous afferents on an excitatory reflex pathway to medial gastrocnemius motoneurons." J Neurophysiol **64**(2): 403-12.

Lafleur, J., D. Zytnicki, et al. (1992). "Depolarization of Ib afferent axons in the cat spinal cord during homonymous muscle contraction." J Physiol **445**: 345-54.

Lafleur, J., D. Zytnicki, et al. (1993). "Declining inhibition in ipsi- and contralateral lumbar motoneurons during contractions of an ankle extensor muscle in the cat." J Neurophysiol **70**(5): 1797-804.

Lebedev, M. A. and M. A. Nicolelis (2006). "Brain-machine interfaces: past, present and future." Trends Neurosci **29**(9): 536-46.

Lee, R. H. and C. J. Heckman (1996). "Influence of voltage-sensitive dendritic conductances on bistable firing and effective synaptic current in cat spinal motoneurons in vivo." J Neurophysiol **76**(3): 2107-10.

Lee, R. H. and C. J. Heckman (1998). "Bistability in spinal motoneurons in vivo: systematic variations in persistent inward currents." J Neurophysiol **80**(2): 583-93.

Lee, R. H. and C. J. Heckman (1998). "Bistability in spinal motoneurons in vivo: systematic variations in rhythmic firing patterns." J Neurophysiol **80**(2): 572-82.

Lee, R. H. and C. J. Heckman (1999). "Enhancement of bistability in spinal motoneurons in vivo by the noradrenergic alpha1 agonist methoxamine." J Neurophysiol **81**(5): 2164-74.

Lee, R. H. and C. J. Heckman (1999). "Paradoxical effect of QX-314 on persistent inward currents and bistable behavior in spinal motoneurons in vivo." J Neurophysiol **82**(5): 2518-27.

Lee, R. H. and C. J. Heckman (2000). "Adjustable amplification of synaptic input in the dendrites of spinal motoneurons in vivo." J Neurosci **20**(17): 6734-40.

Lee, R. H., J. J. Kuo, et al. (2003). "Influence of active dendritic currents on input-output processing in spinal motoneurons in vivo." J Neurophysiol **89**(1): 27-39.

Li, Y. and D. J. Bennett (2003). "Persistent sodium and calcium currents cause plateau potentials in motoneurons of chronic spinal rats." J Neurophysiol **90**(2): 857-69.

Li, Y., X. Li, et al. (2004). "Effects of baclofen on spinal reflexes and persistent inward currents in motoneurons of chronic spinal rats with spasticity." J Neurophysiol **92**(5): 2694-703.

Lundberg, A., K. Malmgren, et al. (1987). "Reflex pathways from group II muscle afferents. 1. Distribution and linkage of reflex actions to alpha-motoneurones." Exp Brain Res **65**(2): 271-81.

Machacek, D. W., S. M. Garraway, et al. (2001). "Serotonin 5-HT(2) receptor activation induces a long-lasting amplification of spinal reflex actions in the rat." J Physiol **537**(Pt 1): 201-7.

Magee, J. C. and D. Johnston (2005). "Plasticity of dendritic function." Curr Opin Neurobiol **15**(3): 334-42.

Manuel, M., C. Meunier, et al. (2005). "How much afterhyperpolarization conductance is recruited by an action potential? A dynamic-clamp study in cat lumbar motoneurons." J Neurosci **25**(39): 8917-23.

Manuel, M., C. Meunier, et al. (2006). "The afterhyperpolarization conductance exerts the same control over the gain and variability of motoneurone firing in anaesthetized cats." J Physiol **576**(Pt 3): 873-86.

Marder, E. and D. Bucher (2007). "Understanding circuit dynamics using the stomatogastric nervous system of lobsters and crabs." Annu Rev Physiol **69**: 291-316.

Matthews, P. B. C. (1972). Mammalian Muscle Receptors and their Central Actions. London, Edward Arnold LTD.

Maurice, N., T. Tkatch, et al. (2001). "D1/D5 dopamine receptor activation differentially modulates rapidly inactivating and persistent sodium currents in prefrontal cortex pyramidal neurons." J Neurosci **21**(7): 2268-77.

Mayer, M. L., G. L. Westbrook, et al. (1984). "Voltage-dependent block by Mg2+ of NMDA responses in spinal cord neurones." Nature **309**(5965): 261-3.

Migliore, M. and G. M. Shepherd (2002). "Emerging rules for the distributions of active dendritic conductances." Nat Rev Neurosci **3**(5): 362-70.

Miller, J. F., K. D. Paul, et al. (1995). "Effect of reversible dorsal cold block on the persistence of inhibition generated by spinal reflexes." Exp Brain Res **107**(2): 205-14.

Miller, J. F., K. D. Paul, et al. (1996). "Restoration of extensor excitability in the acute spinal cat by the 5-HT2 agonist DOI." J Neurophysiol **75**(2): 620-8.

Miller, J. F., K. D. Paul, et al. (1995). "5-HT1B/1D agonist CGS-12066B attenuates clasp knife reflex in the cat." J Neurophysiol **74**(1): 453-6.

Mitchell, J. J. and K. J. Anderson (1991). "Quantitative autoradiographic analysis of excitatory amino acid receptors in the cat spinal cord." Neurosci Lett **124**(2): 269-72.

Moritz, A. T., G. Newkirk, et al. (2007). "Facilitation of somatic calcium channels can evoke prolonged tail currents in rat hypoglossal motoneurons." J Neurophysiol **98**(2): 1042-7.

Nichols, T. R. (1999). "Receptor mechanisms underlying heterogenic reflexes among the triceps surae muscles of the cat." J Neurophysiol **81**(2): 467-78.

Nichols, T. R., T. C. Cope, et al. (1999). "Rapid spinal mechanisms of motor coordination." Exerc Sport Sci Rev **27**: 255-84.

Nielsen, J., C. Crone, et al. (1995). "Central control of reciprocal inhibition during fictive dorsiflexion in man." Exp Brain Res **104**(1): 99-106.

Okuma, Y. and R. G. Lee (1996). "Reciprocal inhibition in hemiplegia: correlation with clinical features and recovery." Can J Neurol Sci **23**(1): 15-23.

Okuma, Y., Y. Mizuno, et al. (2002). "Reciprocal Ia inhibition in patients with asymmetric spinal spasticity." Clin Neurophysiol **113**(2): 292-7.

Ornung, G., O. P. Ottersen, et al. (1998). "Distribution of glutamate-, glycine- and GABA-immunoreactive nerve terminals on dendrites in the cat spinal motor nucleus." Exp Brain Res **118**(4): 517-32.

Perrier, J. F., A. Alaburda, et al. (2003). "5-HT1A receptors increase excitability of spinal motoneurons by inhibiting a TASK-1-like K+ current in the adult turtle." J Physiol **548**(Pt 2): 485-92.

Perrier, J. F. and J. Hounsgaard (2003). "5-HT2 receptors promote plateau potentials in turtle spinal motoneurons by facilitating an L-type calcium current." J Neurophysiol **89**(2): 954-9.

Perrier, J. F. and M. C. Tresch (2005). "Recruitment of motor neuronal persistent inward currents shapes withdrawal reflexes in the frog." J Physiol **562**(Pt 2): 507-20.

Pilowsky, P. M., D. de Castro, et al. (1990). "Serotonin immunoreactive boutons make synapses with feline phrenic motoneurons." J Neurosci **10**(4): 1091-8.

Pin, J. P. and F. Acher (2002). "The metabotropic glutamate receptors: structure, activation mechanism and pharmacology." Curr Drug Targets CNS Neurol Disord **1**(3): 297-317.

Powers, R. K. and M. D. Binder (1995). "Effective synaptic current and motoneuron firing rate modulation." J Neurophysiol **74**(2): 793-801.

Powers, R. K. and M. D. Binder (2000). "Summation of effective synaptic currents and firing rate modulation in cat spinal motoneurons." J Neurophysiol **83**(1): 483-500.

Powers, R. K. and M. D. Binder (2001). "Input-output functions of mammalian motoneurons." Rev Physiol Biochem Pharmacol **143**: 137-263.

Powers, R. K., F. R. Robinson, et al. (1993). "Distribution of rubrospinal synaptic input to cat triceps surae motoneurons." J Neurophysiol **70**(4): 1460-8.

Prather, J. F., R. K. Powers, et al. (2001). "Amplification and linear summation of synaptic effects on motoneuron firing rate." J Neurophysiol(85): 45-53.

Proudfit, H. K. and F. M. Clark (1991). "The projections of locus coeruleus neurons to the spinal cord." Prog Brain Res **88**: 123-41.

Prut, Y. and S. I. Perlmutter (2003). "Firing properties of spinal interneurons during voluntary movement. I. State-dependent regularity of firing." J Neurosci **23**(29): 9600-10.

Raman, I. M. and B. P. Bean (1997). "Resurgent sodium current and action potential formation in dissociated cerebellar Purkinje neurons." J Neurosci **17**(12): 4517-26.

Rank, M. M., X. Li, et al. (2007). "Role of endogenous release of norepinephrine in muscle spasms after chronic spinal cord injury." J Neurophysiol **97**(5): 3166-80.

Rekling, J. C., G. D. Funk, et al. (2000). "Synaptic control of motoneuronal excitability." Physiol Rev **80**(2): 767-852.

Reppert, S. M., D. R. Weaver, et al. (1991). "Molecular cloning and characterization of a rat A1-adenosine receptor that is widely expressed in brain and spinal cord." Mol Endocrinol **5**(8): 1037-48.

Rexed, B. (1952). "The cytoarchitectonic organization of the spinal cord in the cat." J Comp Neurol **96**(3): 414-95.

Reyes, A. (2001). "Influence of dendritic conductances on the input-output properties of neurons." Annual Reviews of Neuroscience **24**: 653-675.

Riddell, J. S. and M. Hadian (2000). "Field potentials generated by group II muscle afferents in the lower-lumbar segments of the feline spinal cord." J Physiol **522 Pt 1**: 97-108.

Roby-Brami, A. and B. Bussel (1987). "Long-latency spinal reflex in man after flexor reflex afferent stimulation." Brain **110 (Pt 3)**: 707-25.

Rose, P. K., S. A. Keirstead, et al. (1985). "A quantitative analysis of the geometry of cat motoneurons innervating neck and shoulder muscles." J Comp Neurol **239**(1): 89-107.

Rose, P. K. and F. J. Richmond (1981). "White-matter dendrites in the upper cervical spinal cord of the adult cat: a light and electron microscopic study." J Comp Neurol **199**(2): 191-203.

Rudomin, P. (2002). "Central control of information transmission through the intraspinal arborizations of sensory fibers examined 100 years after Ramon y Cajal." Prog Brain Res **136**: 409-21.

Safronov, B. V. (1999). "Spatial distribution of NA+ and K+ channels in spinal dorsal horn neurones: role of the soma, axon and dendrites in spike generation." Prog Neurobiol **59**(3): 217-41.

Safronov, B. V., M. Wolff, et al. (1997). "Functional distribution of three types of Na+ channel on soma and processes of dorsal horn neurones of rat spinal cord." J Physiol **503 (Pt 2)**: 371-85.

Salinas, E. and T. J. Sejnowski (2000). "Impact of correlated synaptic input on output firing rate and variability in simple neuronal models." J Neurosci **20**(16): 6193-209.

Schmit, B. D. and E. N. Benz (2002). "Extensor reflexes in human spinal cord injury: activation by hip proprioceptors." Exp Brain Res **145**(4): 520-7.

Schmit, B. D., E. N. Benz, et al. (2002). "Afferent mechanisms for the reflex response to imposed ankle movement in chronic spinal cord injury." Exp Brain Res **145**(1): 40-9.

Schmit, B. D., T. G. Hornby, et al. (2003). "Absence of local sign withdrawal in chronic human spinal cord injury." J Neurophysiol **90**(5): 3232-41.

Schmit, B. D., A. McKenna-Cole, et al. (2000). "Flexor reflexes in chronic spinal cord injury triggered by imposed ankle rotation." Muscle Nerve **23**(5): 793-803.

Schwindt, P. C. and W. Crill (1980). "Properties of a persistent inward current in normal and TEA injected motoneurons." J Neurophysiol **43**: 1700-1725.

Shadlen, M. N. and W. T. Newsome (1998). "The variable discharge of cortical neurons: implications for connectivity, computation, and information coding." J Neurosci **18**(10): 3870-96.

Shefchyk, S. J. and L. M. Jordan (1985). "Motoneuron input-resistance changes during fictive locomotion produced by stimulation of the mesencephalic locomotor region." J Neurophysiol **54**(5): 1101-8.

Sherrington, C. S. (1898). "Decerebrate Rigidity, and Reflex Coordination of Movements." J Physiol **22**(4): 319-32.

Sherrington, C. S. (1906). The Integrative Action of the Nervous System. New Haven, Yale University Press.

Stephens, J. A., R. M. Reinking, et al. (1975). "Tendon organs of cat medial gastrocnemius: responses to active and passive forces as a function of muscle length." J Neurophysiol **38**(5): 1217-31.

Steriade, M. (2001). "Impact of network activities on neuronal properties in corticothalamic systems." J Neurophysiol **86**(1): 1-39.

Stuart, G. and B. Sakmann (1995). "Amplification of EPSPs by axosomatic sodium channels in neocortical pyramidal neurons." Neuron **15**(5): 1065-76.

Stuart, G. J. and S. J. Redman (1992). "The role of GABAA and GABAB receptors in presynaptic inhibition of Ia EPSPs in cat spinal motoneurones." J Physiol **447**: 675-92.

Svirskis, G. and J. Hounsgaard (1997). "Depolarization-induced facilitation of a plateau-generating current in ventral horn neurons in the turtle spinal cord." J Neurophysiol **78**(3): 1740-2.

Svirskis, G. and J. Hounsgaard (1998). "Transmitter regulation of plateau properties in turtle motoneurons." J Neurophysiol **79**(1): 45-50.

Tolle, T. R., A. Berthele, et al. (1993). "The differential expression of 16 NMDA and non-NMDA receptor subunits in the rat spinal cord and in periaqueductal gray." J Neurosci **13**(12): 5009-28.

Tremblay, L. E. and P. J. Bedard (1986). "Effect of clonidine on motoneuron excitability in spinalized rats." Neuropharmacology **25**(1): 41-6.

Wargon, I., J. C. Lamy, et al. (2006). "The disynaptic group I inhibition between wrist flexor and extensor muscles revisited in humans." Exp Brain Res **168**(1-2): 203-17.

Woodbury, J. W. and H. D. Patton (1952). "Electrical activity of single spinal cord elements." Cold Spring Harb Symp Quant Biol **17**: 185-8.

Wu, M., T. G. Hornby, et al. (2005). "Extensor spasms triggered by imposed knee extension in chronic human spinal cord injury." Exp Brain Res **162**(2): 239-49.

Wu, M., T. G. Hornby, et al. (2006). "Flexor reflex responses triggered by imposed knee extension in chronic human spinal cord injury." Exp Brain Res **168**(4): 566-76.

Wu, M. and B. D. Schmit (2006). "Spastic reflexes triggered by ankle load release in human spinal cord injury." J Neurophysiol **96**(6): 2941-50.

Xia, R. and W. Z. Rymer (2005). "Reflex reciprocal facilitation of antagonist muscles in spinal cord injury." Spinal Cord **43**(1): 14-21.

Zhang, M., N. Sukiasyan, et al. (2006). "Localization of L-type calcium channel Ca(V)1.3 in cat lumbar spinal cord--with emphasis on motoneurons." Neurosci Lett **407**(1): 42-7.